

Invited Review

The Compact Steep-Spectrum and Gigahertz Peaked-Spectrum Radio Sources

CHRISTOPHER P. O'DEA

Space Telescope Science Institute, 3700 San Martin Drive, Baltimore, MD 21218; odea@stsci.edu

Received 1997 October 8; accepted 1998 January 20

ABSTRACT. I review the radio to X-ray properties of gigahertz peaked-spectrum (GPS) and compact steep-spectrum (CSS) sources, the current hypotheses for their origin, and their use to constrain the evolution of powerful radio galaxies. The GPS and CSS sources are compact, powerful radio sources with well-defined peaks in their radio spectra (near 1 GHz in the GPS and near 100 MHz in the CSS). The GPS sources are entirely contained within the extent of the narrow-line region (≤ 1 kpc), while the CSS sources are contained entirely within the host galaxy (≤ 15 kpc). The peaks in the spectra are probably due to synchrotron self-absorption, though free-free absorption through an inhomogeneous screen may also play a role. The turnover frequency varies with linear size l as $\nu_m \propto l^{-0.65}$, suggesting a simple physical relationship between these parameters. The radio morphologies are strikingly like those of the large-scale classical doubles, though some sources can have very distorted morphologies suggestive of interactions. Radio polarization tends to be low, and in some cases the Faraday rotation measures can be extremely large. The IR properties are consistent with stellar populations and active galactic nucleus (AGN) bolometric luminosity similar to that of the 3CR classical doubles. The optical host galaxy properties (absolute magnitude, Hubble diagram, evidence for interaction) are consistent with those of the 3CR classical doubles. CSS sources at all redshifts exhibit high surface brightness optical light (most likely emission-line gas) that is aligned with the radio axis. The optical emission-line properties suggest (1) interaction of the radio source with the emission-line gas and (2) the presence of dust toward the emission-line regions. X-ray observations of high-redshift GPS quasars and a couple of GPS galaxies suggest the presence of significant columns of gas toward the nuclei. Searches for cold gas in the host galaxies have revealed large amounts of molecular gas and smaller amounts of atomic gas in several sources, though probably not enough to confine the radio sources. The main competing models for the GPS and CSS sources are that (1) they are frustrated by interaction with dense gas in their environments and (2) they are young and evolving radio sources that will become large-scale sources. Combining the bright GPS and CSS samples with the 3CR results in a sample spanning a range in source size of 10^5 that can be used to study source evolution. The number density versus linear size relation is consistent with a picture in which the sources expand with constant velocity and the radio power drops with linear size l according to $P \propto l^{-0.5}$. This strong evolution suggests that at least some of the GPS and CSS sources evolve to become lower luminosity FR 1 radio sources. The GPS and CSS sources are important probes of their host galaxies and will provide critical clues to the origin and evolution of powerful radio sources.

1. INTRODUCTION

The gigahertz peaked-spectrum (GPS) and compact steep-spectrum (CSS) radio sources make up significant fractions of the bright (centimeter-wavelength–selected) radio source population ($\sim 10\%$ and $\sim 30\%$, respectively) but are not well understood. The GPS sources are powerful ($\log P_{1.4} \geq 25$ W Hz $^{-1}$), compact (≤ 1 kpc), and have a convex radio spectrum that peaks between about 500 MHz and 10 GHz (observer's frame). Any population of sources that peaks above 10 GHz would be strongly underrepresented in the present centimeter-wavelength–selected samples. The CSS sources are just as powerful, are larger (between 1 and 20 kpc in size), and have convex spectra that tend to peak at lower frequencies (< 500 MHz)

where the practical lower limit in measuring the spectral turnover frequency of ~ 30 MHz is given by the ionospheric cutoff at about 10 MHz and the difficulty of making low-frequency measurements (including source confusion). As we shall see below, there is a great deal of overlap in the properties of CSS and GPS sources and the definition given above is somewhat arbitrary, though it is a useful working definition.

Previous general discussions and reviews of the CSS sources have been presented by Saikia (1988), Fanti et al. (1990b), Fanti & Fanti (1994), Dallacasa, Fanti, & Fanti (1993), Fanti & Spencer (1995), and for GPS sources by O'Dea, Baum, & Stanghellini (1991). Other useful references are the proceedings of the Dwingeloo and Leiden Workshops on Compact Steep-Spectrum and GHz Peaked-Spectrum Radio Sources (Fanti et

al. 1990a; Snellen et al. 1996d). We adopt a Hubble constant of $H_0 = 75 \text{ km s}^{-1} \text{ Mpc}^{-1}$ and $q_0 = 0.0$.

GPS and CSS sources are important for two reasons. First, because of their bright and relatively symmetric radio structure on these scales, they probe the narrow-line region (NLR) and interstellar medium (ISM) of the host galaxy via, e.g., Faraday rotation/depolarization and H I absorption, as well as through their interaction with the emission-line gas. On the other hand, in the large-scale sources, the radio emission extends beyond these scales and is not able to serve as a probe. In addition, the core-jet nuclear radio structure of the larger sources does not generally provide a useful probe of the small scales because of its asymmetry and peculiar geometry. Second, the GPS and CSS sources may be the younger stages of powerful large-scale radio sources—giving us insight into radio source genesis and evolution. In this paper, I review the radio, infrared, optical, and X-ray properties, and the current hypotheses for their origin and evolution.

1.1. The Early History of the Study of CSS and GPS Sources

The existence of GPS and CSS sources has been known since the early days of extragalactic radio astronomy. Examples from the 3C sample of compact ($\leq 1''$) radio sources with steep spectra that turn over at frequencies around 100 MHz were discovered in the early 1960s (Conway, Kellermann, & Long 1963; Allen et al. 1962). These were explained as being due to synchrotron self-absorption in sources of angular size $\leq 0''.1$ (Williams 1963; Slish 1963). In 1963, Bolton, Gardener, & Mackey reported the discovery of 1934–G3, the archetype GPS source. The spectrum of 1934–G3 was discussed in detail by Kellermann (1966a) in terms of synchrotron self-absorption, free-free absorption, and a signal from an extraterrestrial civilization.

The study of GPS and CSS sources began in earnest in the early 1980s. Evidence accumulated that the CSS sources made up a significant fraction ($\sim 30\%$) of sources selected at 2.7 or 5.0 GHz (Kapahi 1981; Peacock & Wall 1982; and cf. Gopal-Krishna, Steppe, & Witzel 1980; Gopal-Krishna, Preuss, & Schilizzi 1980). Phillips & Mutel (1982) called attention to the symmetric compact double structures in GPS sources, and Gopal-Krishna, Patnaik, & Steppe (1983) published the first large list of GPS sources.

1.2. Definitions and Samples

We use the term *compact steep spectrum* instead of steep spectrum core (SSC) to describe the CSS sources, since they are not just cores but are full-fledged radio sources complete with jets and lobes on small scales.

Currently, our understanding of these sources is based on samples selected from (rather bright) flux density–limited samples. Similar samples of CSS sources drawn from the 3C and Peacock & Wall (1982, hereafter PW) samples have been con-

structed by Fanti et al. (1990b), Spencer et al. (1989), and Sanghera et al. (1995). The selection criteria for the Fanti et al. sample are (1) projected linear sizes less than 20 kpc, (2) flux density at 178 MHz of at least 10 Jy^1 (the flux densities are extrapolated for the sources that turn over before 178 MHz), (3) $|b| > 10^\circ$ and $\delta > 10^\circ$, and (4) log power at 178 MHz of at least 26.75 W Hz^{-1} . The selection frequency of the 3C sample, 178 MHz, favors sources whose spectra peak around 178 MHz or lower. The PW sample is selected at 2.7 GHz and contains sources with spectral peaks at higher frequencies than the 3C selected objects. However, the PW criterion that the spectral index² between 2.7 and 5 GHz be steeper than -0.5 selects sources that peak below 2.7 GHz and in practice below about 1 GHz (Fanti et al. 1990b). Thus, although it is often stated that the GPS sources are a subset of the CSS sources, there are very few sources with turnover frequencies above 1 GHz in the existing well-studied CSS samples.

The published lists of GPS sources are heterogeneous but are predominantly based on surveys at 5 GHz (S4 and 1 Jy—see, e.g., Pauliny-Toth et al. 1978; Kühn et al. 1981a, 1981b).

The high selection frequency allows sources with higher frequency spectral peaks than in the existing CSS samples to be included. However, sources with spectral peaks much above 5 GHz are underrepresented in these samples, since the flux density is declining at 5 GHz in these sources.

Lists of GPS sources have been published by Gopal-Krishna and collaborators (Gopal-Krishna et al. 1983; Spoelstra, Patnaik, & Gopal-Krishna 1985; Gopal-Krishna & Spoelstra 1993), Cersosimo et al. (1994), O'Dea et al. (1991), Stanghellini et al. (1990c, 1996), and King et al. (1996). A combined list of GPS and CSS sources has been collated by Dallacasa & Stanghellini (1990). Lists of GPS sources selected to have lower flux densities than the other major lists are presented by Snellen et al. (1995), Marecki et al. (1996), and Fanti, Vigotti, & Di Paolo (1996). Stanghellini's sample is well defined: (1) flux density at 5 GHz above 1 Jy, (2) turnover frequency between 0.4 and 6 GHz, (3) spectral index above the peak of steeper than -0.5 , (4) $\delta > -25^\circ$ and $|b| > 10^\circ$. The most comprehensive list of GPS sources so far is that of O'Dea et al. (1991).

The selection effects in the list and the possible redshift evolution of the radio spectral peaks are discussed by de Vries et al. (1997a). The Fanti et al. (1990b) CSS sample and Stanghellini et al. (1990c, 1996) GPS sample are given in Table 1. Future lists of GPS and CSS sources are likely to be generated from follow-ups to surveys now in progress, e.g., the VLA 20 cm surveys NVSS and FIRST, and the WSRT survey WENSS. Selection of sources from VLBI surveys on the basis of compact symmetric object (CSO) morphology (see, e.g., Wilkinson et al. 1994; Taylor et al. 1994; Readhead et al. 1996b; Taylor

¹ $1 \text{ Jy} = 10^{-23} \text{ ergs s}^{-1} \text{ cm}^{-2} \text{ Hz}^{-1}$.

² We define spectral index α such that $S \propto \nu^\alpha$.

TABLE 1
 COMBINED CSS AND GPS COMPLETE SAMPLES

Source (1)	Catalog (2)	Sample (3)	ID (4)	Mag (5)	z (6)	$S_{5\text{ GHz}}$ (Jy) (7)	θ (arcsec) (8)	ν_m (MHz) (9)	$P_{5\text{ GHz}}$ (W Hz^{-1}) (10)	Size (kpc) (11)	$\nu_m(1+z)$ (MHz) (12)
0019-000	...	G	G	21.1	0.305	1.1	0.06	700	26.4	0.240	914
0108+388	...	G	G	22.0	0.669	1.26	0.006	4000	27.3	0.037	6676
0127+233	3C 43	C	Q	20.0	1.459	1.1	2.60	20	28.0	21.054	49
0134+329	3C 48	C	Q	16.1	0.367	5.3	0.50	80	27.3	2.255	109
0138+138	3C 49	C	G	22.0	0.621	0.9	0.92	120	27.0	5.529	195
0221+276	3C 67	C	G	18.0	0.309	0.9	2.5	50	26.3	10.100	65
0223+341	4C 34.07	C	S	21.3	1.0	1.3	1.1	250	27.6	8.004	500
0237-233	...	G	Q	16.6	2.223	3.34	0.018	1000	29.0	0.158	3223
0248+430	...	G	Q	15.5	1.316	1.24	0.06	5000	27.9	0.474	11580
0316+161	4C 16.09	CG	G	22.0	1.0	2.89	0.30	800	28.1	2.183	1600
0319+121	OE 131	C	Q	19.0	2.662	1.10	0.02	400	28.5	0.180	1465
0345+337	3C 93.1	C	G	19.0	0.244	0.8	0.25	60	26.0	0.858	75
0404+769	4C 76.03	C	G	22.0	0.5985	2.82	0.15	600	27.4	0.886	959
0428+205	OF 247	CG	G	20.0	0.219	2.38	0.250	1100	26.4	0.793	1341
0429+415	3C 119	C	G	20.0	1.023	3.5	0.08	150	28.1	0.587	303
0457+024	...	G	Q	19.4	2.384	1.57	...	2100	28.7	0.000	7106
0500+019	...	G	Q	20.2	0.583	1.89	0.015	1800	27.2	0.087	2849
0518+165	3C 138	C	Q	18.8	0.760	4.1	0.60	100	27.8	3.942	176
0538+498	3C 147	C	Q	17.8	0.545	8.2	0.55	150	27.9	3.101	232
0710+439	...	G	G	20.7	0.518	1.68	0.025	1900	27.1	0.137	2884
0738+313	...	G	Q	16.1	0.630	3.62	0.010	5300	27.6	0.061	8639
0740+380	3C 186	C	Q	17.6	1.063	0.3	2.2	40	27.2	16.330	83
0742+103	...	G	EF	21.9	1.0	3.46	0.010	2700	28.1	0.073	5400
0743-006	...	G	Q	17.5	0.994	2.05	0.005	5800	27.8	0.036	11565
0758+143	3C 190	C	Q	20.3	1.197	0.9	4.1	40	27.8	31.538	88
0941-080	...	G	G	19.0	0.228	1.11	0.05	500	26.1	0.163	614
1005+077	3C 237	C	G	21.0	0.877	2.0	1.3	50	27.8	9.033	94
1019+222	3C 241	C	G	22.0	1.617	0.4	0.84	40	27.8	6.960	105
1031+567	...	G	Q	20.3	0.459	1.28	0.040	1300	26.9	0.206	1897
1117+146	4C 14.41	G	G	20.0	0.362	1.00	0.08	500	26.5	0.358	681
1127-145	...	G	Q	16.9	1.187	3.82	0.003	1000	28.3	0.023	2187
1143-245	...	G	Q	18.5	1.950	1.40	0.006	2200	28.4	0.052	6490
1153+317	4C 31.38	C	Q	19.0	1.557	1.0	0.9	100	28.0	7.397	256
1203+645	3C 268.3	C	G	19.0	0.371	1.1	1.36	80	26.6	6.175	110
1225+368	ON 343	C	Q	21.7	1.974	0.77	0.060	1200	28.5	0.516	3569
1245-197	...	G	Q	20.5	1.280	2.34	0.500	500	28.2	3.918	1140
1250+568	3C 277.1	C	Q	17.9	0.321	1.0	1.67	100	26.4	6.918	132
1323+321	4C 32.44	CG	G	19.0	0.369	2.39	0.06	500	26.9	0.272	684
1328+254	3C 287	C	Q	17.7	1.055	3.2	0.048	50	28.1	0.355	103
1328+307	3C 286	C	Q	17.2	0.849	7.4	3.2	80	28.2	21.966	148
1345+125	4C 12.50	G	G	17.0	0.122	3.05	0.080	400	26.0	0.160	449
1358+624	4C 62.22	CG	G	19.9	0.429	1.80	0.07	500	26.9	0.347	714
1404+286	OQ 208	G	G	14.0	0.077	2.69	0.007	4200	25.5	0.009	4523
1413+349	OQ 323	C	EF	22.0	1.0	1.02	0.06	1000	27.5	0.437	2000
1416+067	3C 298	C	Q	16.8	1.439	1.5	1.49	80	28.3	12.026	195
1442+101	OQ 172	CG	Q	17.8	3.535	1.20	0.02	900	29.3	0.185	4081
1443+77	3C 303.1	C	G	19.0	0.267	0.5	1.7	100	26.0	6.219	127
1447+77	3C 305.1	C	G	21.0	1.132	0.5	2.34	90	27.5	17.709	192
1458+718	3C 309.1	C	Q	16.8	0.905	3.5	2.11	40	28.0	14.831	76
1517+204	3C 318	C	G	20.3	0.752	0.8	1.05	40	27.2	6.868	70
1518+047	...	G	S	22.6	1.296	1.09	0.135	800	28.1	1.061	1837
1600+335	OS 300	CG	EF	23.2	1.0	2.67	0.06	2400	28.0	0.437	4800
1607+268	CTD 93	CG	G	20.7	0.473	1.73	0.05	1100	27.1	0.262	1620
1634+628	3C 343	C	Q	20.6	0.988	1.48	0.20	250	27.7	1.449	497
1637+626	3C 343.1	C	G	20.8	0.750	1.2	0.24	250	27.4	1.568	438
1819+39	4C 39.56	C	G	19.0	0.4	1.0	0.44	100	26.6	2.091	140
1829+29	4C 29.56	C	Q	20.0	0.842	1.1	3.1	100	27.3	21.212	184
2008-068	...	G	G	21.1	1.0	1.34	0.030	1400	27.8	0.218	2800

TABLE 1
(Continued)

Source (1)	Catalog (2)	Sample (3)	ID (4)	Mag (5)	z (6)	$S_{5\text{ GHz}}$ (Jy) (7)	θ (arcsec) (8)	ν_m (MHz) (9)	$P_{5\text{ GHz}}$ (W Hz ⁻¹) (10)	Size (kpc) (11)	$\nu_m(1+z)$ (MHz) (12)
2126-158	G	Q	17.3	3.270	1.17	0.008	4100	28.9	0.073	17507
2128+048	G	G	23.4	0.990	2.02	0.030	700	27.9	0.218	1393
2134+004	G	Q	16.8	1.936	8.50	0.002	4300	29.2	0.017	12625
2210+016	G	S	21.7	1.0	1.05	0.055	500	27.6	0.400	1000
2248+71	3C 454.1	C	G	22.0	1.841	0.3	1.6	40	27.9	13.600	114
2249+185	3C 454	C	Q	18.5	1.758	0.8	0.66	40	28.1	5.562	110
2252+129	3C 455	C	Q	19.7	0.543	0.8	3.3	40	26.9	18.570	62
2342+821	CG	Q	20.5	0.735	1.28	0.18	500	27.4	1.166	868
2352+495	G	G	18.4	0.237	1.49	0.050	700	26.3	0.168	866

NOTES.—Master list of Fanti et al. CSS and Stanghellini et al. GPS source samples. Col. (1), B1950 IAU name. Col. (2), catalog name. Col. (3), membership in CSS (C) or GPS (G) sample. Col. (4), ID: (Q) quasar, (G) galaxy, (S) stellar, or (EF) empty field. Col. (5), optical magnitude. Col. (6), heliocentric redshift; we adopt $z = 1.0$ for sources with unknown redshift. Col. (7), flux density at 5 GHz. Col. (8), angular size. Col. (9), observed frequency of spectral turnover. Col. (10), log of power at 5 GHz. Col. (11), linear size. Col. (12), rest-frame turnover frequency.

et al. 1996c) is very successful in identifying GPS galaxies because of the strong correlation between GPS-type radio spectra and CSO or compact double (CD) morphology in radio galaxies.

The statistics of occurrence of GPS and CSS sources in several flux density-limited samples is given in Table 2. The CSS and GPS sources make up about 30% and 10%, respectively, of the sources selected at frequencies around 5 GHz. This is a significant fraction of the powerful radio sources!

In the rest of this paper, I use the Stanghellini et al. GPS sample and the Fanti et al. CSS sample when I discuss the global properties of GPS and CSS sources. The Fanti and Stanghellini samples contain a few sources that overlap (0316+161, 0428+205, 1323+321, 1358+624, 1442+101, 1600+335, 1607+268, 2342+821), and these are of course only counted once in the combined sample. I have removed a few sources that no longer fit the original sample criteria (3C 216, 3C 299, 3C 346, 3C 380, and 2230+110; see § 3.1). The resulting combined sample contains 67 sources (Table 1).

TABLE 2
GPS/CSS DEMOGRAPHICS

Subsample	Parent Sample	Selection Frequency	Fraction (%)	Reference
CSS	S4	5 GHz	29	1
CSS	PW	2.7 GHz	31	2
CSS	3CR	178 MHz	12	2
GPS	S4	5 GHz	8.5	3
GPS	1 Jy	5 GHz	10	3

NOTES.—The frequency of occurrence of the GPS and CSS sources in different flux density-limited samples. The identification of GPS sources is not straightforward, since it requires sufficient spectral data that a peak in the spectrum can be identified. Thus, the GPS statistics are probably lower limits.

REFERENCES.—(1) Kapahi 1981; (2) Peacock & Wall 1982; (3) this work.

2. RADIO SPECTRA

The turnover in the radio spectrum is a defining characteristic of the GPS and CSS sources. It contains information on the source size, its physical properties, and its environment.

2.1. Spectral Shape and Implications for Lifetimes

The shapes of the radio spectra are one of the chief identifying characteristics of the GPS and CSS sources (see Fig. 1 and Fanti et al. 1985, 1989; Schilizzi et al. 1990; Steppe, Salter, & Saikia 1990; O'Dea et al. 1990b; Kameno et al. 1995; Steppe et al. 1995; Stanghellini et al. 1996, 1998b; de Vries et al. 1997a). These sources have simple peaked spectra with steep spectral indices at high frequencies. O'Dea et al. (1990b, 1991) noted that the spectra of GPS sources can be quite narrow with values for the full width to half the peak flux density of around 1–1.5 decades of frequency. The GPS source with the most inverted spectrum is 0108+388 (Baum et al. 1990), which has a value of $\alpha \geq 2$ and approaches the canonical value of 2.5 for a simple homogeneous synchrotron source. However, the fact that none of the GPS or CSS sources have spectra as inverted as 2.5 suggests that there is inhomogeneity in the radio structure (this is of course confirmed by the radio imaging [§ 3], which shows cores, jets, hot spots, and lobes in these objects).

The distribution of spectral index above the peak is shown in Figure 2. This plot combines the data for the Fanti et al. (1990b) sample of CSSs and the Stanghellini et al. (1998b) sample of GPSs (*shaded*). The lower limit at about -0.5 is imposed by the selection criteria.³ There is a broad distribution

³ Note that there is some small inconsistency, since the updated values of spectral index used here are not the same as those originally used to define these samples.

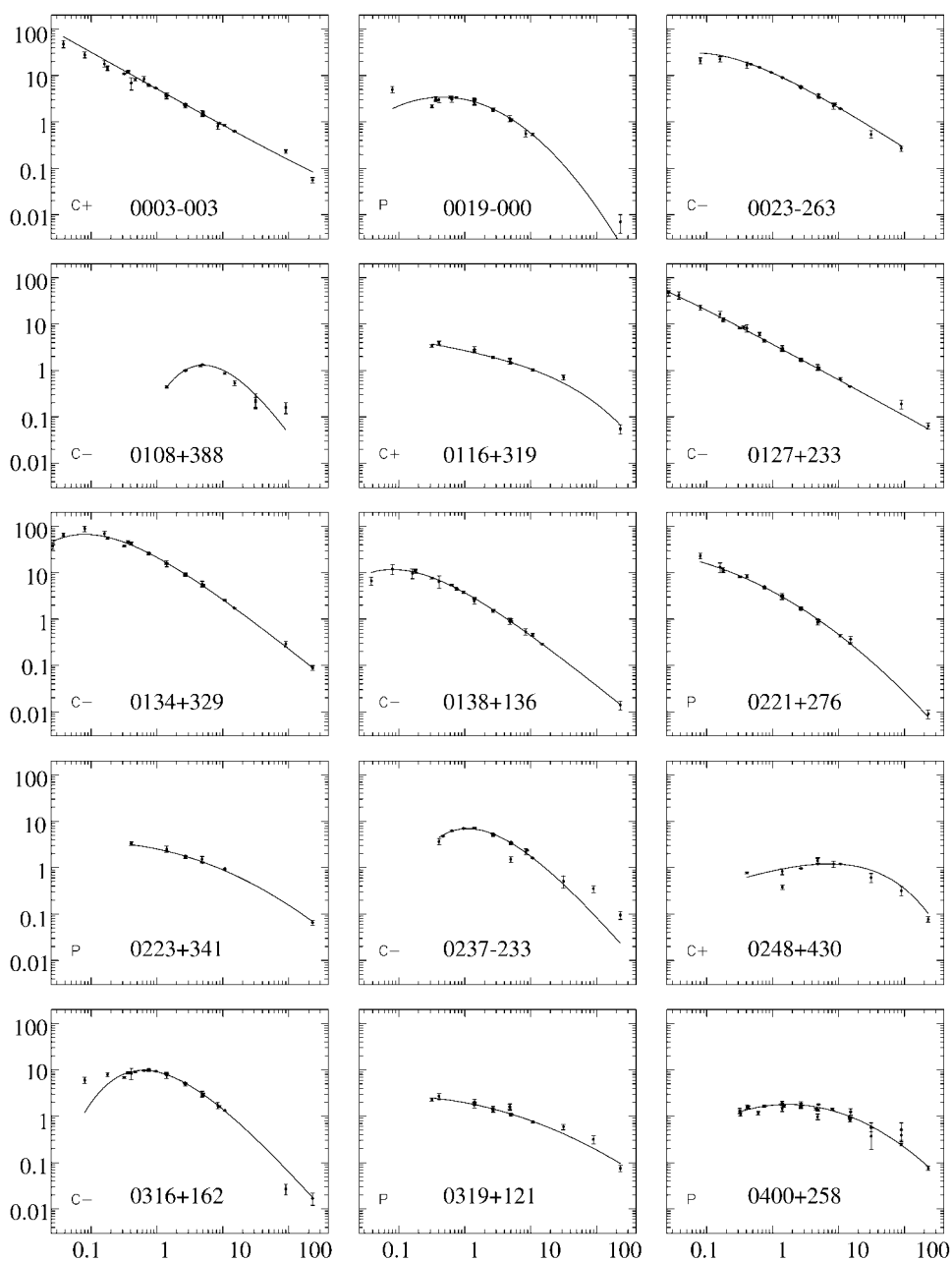


FIG. 1.—Radio spectra of GPS and CSS radio sources (S. Jeyakumar 1997, private communication; see also Steppe et al. 1995). Vertical axis is flux density in Jy, and horizontal axis is frequency in GHz.

from -0.5 to -1 with a few sources around -1.1 to -1.3 .⁴ The GPS and CSS sources have similar distributions. There is a slight suggestion that the GPS sources have flatter spectra than the CSSs, but this may be mainly a result of the fact that the spectral indices are measured closer to the spectral peak in the GPSs than in the CSSs. de Vries et al. (1997a) have de-

⁴ Curiously, the spectra can be as steep as those of the high-redshift ultrastep-spectrum sources (see, e.g., Röttgering et al. 1994).

termined an “average” radio spectrum for a sample of 72 GPS radio sources. The average spectral indices below and above the spectral peak are 0.56 and -0.77 , respectively. The average value of $\alpha \approx -0.77$ is also typical for the large-scale powerful sources (see, e.g., Kellermann 1966b), suggesting that relativistic electron acceleration and energy loss mechanisms preserve the same average spectral index over most of the lifetime of the source.

If the turnover is due to synchrotron self-absorption, then

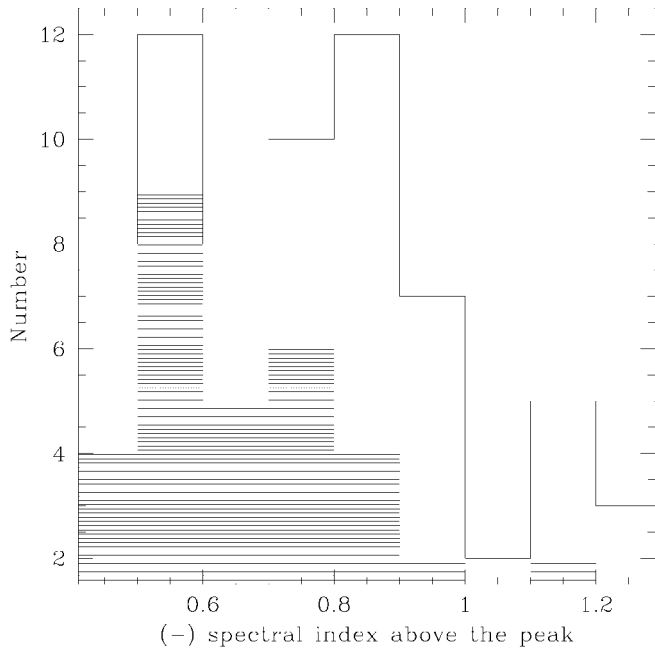


FIG. 2.—Histogram of spectral index above the spectral peak. The sources are the Fanti et al. CSS sample and the Stanghellini et al. GPS sample (*shaded*).

from equation (2) the generally narrow spectrum implies that there is a limited range of spatial scales that contribute to the bulk of the radio luminosity; i.e., there is a cutoff in both the largest and smallest scales (see also Phinney 1985). This is consistent with the lack of large-scale structure in these sources.

The spectra tend to be fairly straight (constant spectral index) at high frequencies with few sources showing either steepening from radiation losses, or flattening due to a compact component (though there are examples of both phenomena). This has consequences for the inferred “spectral age” of the radiating electrons. Two possible explanations for the lack of an observed break are that the spectral break is either (1) still at higher frequencies (≈ 100 GHz) or (2) hidden below the spectral peak. As pointed out by Kardashev (1962), continuous resupply will limit the change in spectral index at the break frequency to 0.5 instead of an exponential drop. Thus, if the jets supply sufficient energy to the extended radio structure that Kardashev’s condition is met, it is possible that the break is below the spectral peak for the sources with a high-frequency spectral index steeper than -1 . For sources with flatter spectra the implied initial spectrum $\alpha \approx -0.5$ may be too flat to be consistent with the extended optically thin emission, and these sources may have their break at high frequency. Because of both continuing resupply and adiabatic losses, which will have opposite effects on the spectrum, the interpretation of the spectral age is uncertain. The electron lifetime is given by

$$t \approx 2.6 \times 10^4 \frac{B^{1/2}}{B^2 + B_R^2} [(1+z)\nu_b]^{-1/2} \text{ yr}, \quad (1)$$

where B is the magnetic field in G, $B_R \approx 4(1+z)^2 \times 10^{-6}$ G is the equivalent magnetic field of the microwave background, and ν_b is the break frequency in Hz (van der Laan & Perola 1969). For a high value of break frequency $\nu_b = 100$ GHz, for a GPS source ($B = 10^{-3}$ G) and a CSS source ($B = 10^{-4}$ G), the electron lifetimes are $t \approx 2 \times 10^3$ yr and $t \approx 7 \times 10^4$ yr, respectively. However, for a low value of the break frequency $\nu_b = 100$ MHz, the ages are $t \approx 7 \times 10^4$ yr and $t \approx 2 \times 10^6$ yr, respectively. Given the uncertainties, the range of spectral indices is consistent with a range of electron lifetimes among these sources, with some sources having possibly quite short electron lifetimes. The correspondence between electron lifetime and source age is not yet clear—though these results could be consistent with a range of ages for the GPS and CSS sources, with some of them, especially the GPS sources with flatter spectra, being quite young ($\lesssim 10^4$ yr). Katz-Stone & Rudnick (1997) have presented a “spectral tomography” analysis of two CSS sources, 3C 67 and 3C 190. They find complex spectral structure in these two sources and suggest that the sources could be young if the initial injection spectrum is as steep as $\alpha \approx -0.8$. It is clear that images of spectral index are necessary to fully address the questions of electron age and source lifetime.

2.2. Redshift Dependence of the Turnover Frequency

The distribution of the observed turnover frequency for the complete samples is shown in Figure 3a adapted from O’Dea & Baum (1997). There is a strong peak below 200 MHz, a shoulder that extends down to about 1 GHz, then a fairly flat distribution out to about 5 GHz. The distribution of rest-frame turnover frequency extends out to 15 GHz (Fig. 3b). This suggests the existence of a previously unknown population of sources that peak at high frequencies (see also de Vries et al. 1997a; Edge et al. 1996). There could be a population of low-redshift sources with turnovers at high frequency, but they would be missing from our samples because the surveys only go out to 5 GHz. If a local population of sources with turnovers at high frequency does exist, they might contribute to spurious measurements of the cosmic microwave background anisotropy (Crawford et al. 1996). Surveys at high frequency, ≥ 10 GHz, will be needed to search for this population of sources (see, e.g., Cooray et al. 1998).

de Vries et al. (1997a) noted that the GPS sources with high turnover frequencies are found preferentially at high redshift (see also Menon 1983). This can be seen for the combined sample of CSS/GPS sources in the plot of intrinsic turnover frequency versus redshift (Fig. 4).⁵ The tendency for the high-redshift (and thus more powerful) quasars to have a higher value of the intrinsic turnover frequency suggests that the

⁵ Note that this sample does not show as strong a correlation between turnover frequency and redshift as Menon’s (1983) sample of quasars. However, an exact comparison with Menon is not possible, since he used different selection criteria to construct his sample.

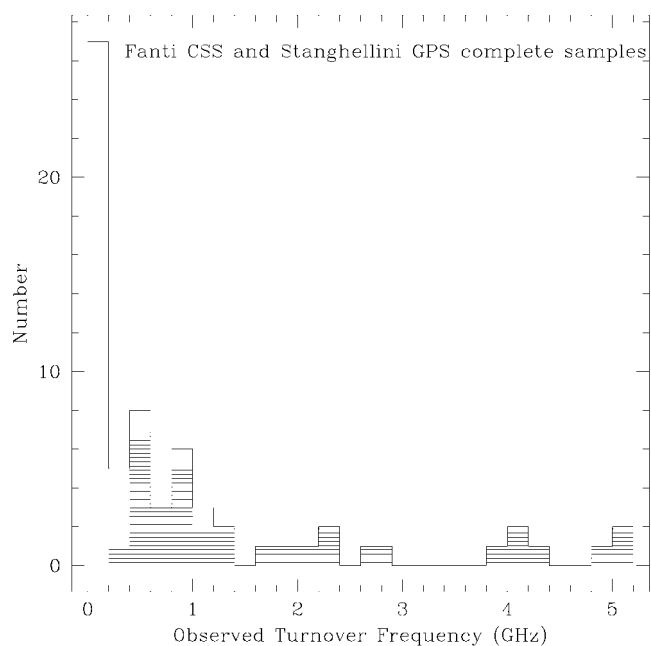


FIG. 3a

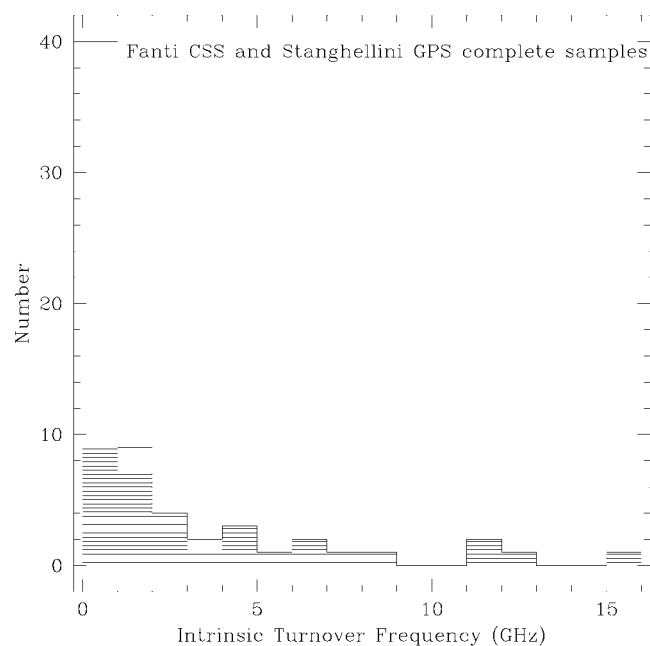


FIG. 3b

FIG. 3.—(a) Histogram of observed turnover frequency (GHz) for the Fanti et al. CSS sample and the Stanghellini et al. GPS sample (shaded). (b) Same as (a), with turnover frequency given in the source rest frame. Adapted from O’Dea & Baum (1997).

sources are more compact at high redshifts. This may reflect the higher density environments expected at high redshift.

2.3. What Causes the Turnover in GPS Sources?

The interpretation of the turnover and its possible evolution depends on the assumed mechanism for the turnover. In the

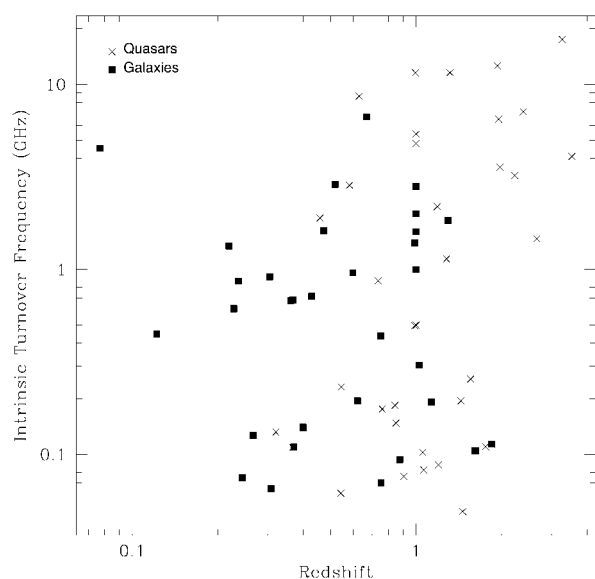


FIG. 4.—Intrinsic turnover frequency vs. redshift for the Fanti et al. CSS sample and the Stanghellini et al. GPS sample. Galaxies are represented by solid squares, and quasars by crosses. Adapted from O’Dea & Baum (1997).

GPS sources, the two major possibilities that have been discussed so far in the literature are synchrotron self-absorption (Kellermann 1966a; Hodges, Mutel, & Phillips 1984; Mutel, Hodges, & Phillips 1985; O’Dea et al. 1991; Readhead et al. 1996b) and free-free absorption (Kellermann 1966a; O’Dea et al. 1991; Bicknell, Dopita, & O’Dea 1996). Absorption by induced Compton scattering has also been suggested as a possibility by Kuncic, Bicknell, & Dopita (1998). Table 3 gives some parameters of GPS radio sources. If we assume that the sources are near minimum pressure (which is close to equipartition; see, e.g., Burns, Owen, & Rudnick 1979), then we can compare the values of the magnetic field estimated via minimum pressure and synchrotron self-absorption. This is subject to several caveats, since (1) we do not know whether the sources are in minimum pressure,⁶ (2) the parameters derived from synchrotron self-absorption are dependent on high powers of the input parameters, thus magnifying the effect of any errors in the source observables, and (3) there are no other independent measures of the magnetic field strength. Given these uncertainties, we note that the estimates of the magnetic field are in rough agreement. Thus, the data are *consistent* with the hypothesis that the turnover is due to synchrotron self-absorption.

If the turnover in the spectrum is due to synchrotron self-

⁶ Güijosa & Daly (1996) suggest that the agreement between the Doppler factors estimated assuming an inverse Compton origin for the X-rays and that obtained by assuming that the sources are in equipartition (i.e., the “equipartition Doppler factor”; Readhead 1994, Singal & Gopal-Krishna 1985) indicates that the sources are close to equipartition.

TABLE 3
DERIVED GPS SOURCE PARAMETERS

Source	Component	T_B	P_{\min} (dyn cm ⁻²)	$B_{\min P}$ (G)	B_{SSA} (G)	References
1518+047	N1	7.7×10^{11}	1.3×10^{-5}	1.2×10^{-2}	8.1×10^{-5}	1
	N2	3.2×10^{11}	8.7×10^{-6}	9.7×10^{-3}	4.7×10^{-4}	1
	S1	2.6×10^{11}	4.7×10^{-5}	2.2×10^{-2}	1.4×10^{-3}	1
	S2	3.1×10^{11}	6.8×10^{-5}	2.7×10^{-2}	9.6×10^{-4}	1
1607+268	N1	1.0×10^{12}	2.2×10^{-5}	1.5×10^{-2}	8.0×10^{-5}	1
	N2	1.2×10^{11}	4.8×10^{-5}	7.2×10^{-3}	6.0×10^{-3}	1
	S1	2.2×10^{11}	7.7×10^{-6}	9.1×10^{-3}	1.7×10^{-3}	1
	S2	2.6×10^{10}	2.5×10^{-6}	5.1×10^{-3}	1.2×10^{-1}	1
2050+364	S3	7.2×10^{11}	2.9×10^{-5}	1.8×10^{-2}	1.6×10^{-4}	1
	W1	4.2×10^{11}	5.6×10^{-5}	2.4×10^{-2}	9.2×10^{-4}	1
	E1	3.7×10^{11}	1.4×10^{-5}	1.2×10^{-2}	5.4×10^{-4}	1
	E2	8.4×10^{11}	2.9×10^{-5}	1.8×10^{-2}	1.0×10^{-4}	1
2352+495	E3	4.0×10^{11}	1.7×10^{-5}	1.3×10^{-2}	4.4×10^{-4}	1
	N HS	9.3×10^{10}	2.7×10^{-5}	1.7×10^{-2}	3.7×10^{-2}	2
	S HS	4.0×10^{10}	5.7×10^{-6}	7.8×10^{-3}	5.3×10^{-2}	2
	N lobe	3.5×10^{10}	1.2×10^{-6}	3.7×10^{-3}	3.7×10^{-2}	2
Cocoon	S lobe	8.3×10^{10}	8.0×10^{-7}	2.9×10^{-3}	3.7×10^{-3}	2
	Cocoon	1.3×10^{10}	7.8×10^{-8}	9.2×10^{-4}	$\leq 9.0 \times 10^{-2}$	2

NOTES.—The B_{SSA} in the 2352+495 cocoon is an upper limit, since the turnover frequency is also an upper limit.

REFERENCES.—(1) Mutel et al. 1985; (2) Readhead et al. 1996b.

absorption, then the turnover frequency in a homogeneous, self-absorbed, incoherent synchrotron radio source with a power-law electron energy distribution is given by

$$\nu_{\max} \sim 8B^{1/5} S_m^{2/5} \theta^{-4/5} (1+z)^{1/5} \text{ GHz}, \quad (2)$$

where the magnetic field B is in G, the flux density at the peak S_m is in Jy, z is the redshift, and the angular size θ is in milliarcseconds (see, e.g., Kellermann & Pauliny-Toth 1981).

Given the evidence for (1) high densities in the optical emission-line clouds (§ 8), (2) strong depolarization of the radio source (§ 4), and (3) strong confinement of the radio sources, it seems plausible that the densities may be high enough that free-free absorption may play a role in these sources (van Breugel, Heckman, & Miley 1984a; O'Dea et al. 1991). The emission measure for free-free absorption is as follows (see, e.g., Osterbrock 1977):

$$n_e^2 L \approx 3.05 \times 10^6 \tau \left(\frac{T}{10^4 \text{ K}} \right)^{1.35} \left(\frac{\nu}{1 \text{ GHz}} \right)^{2.1} \text{ cm}^{-6} \text{ pc}, \quad (3)$$

where τ is the optical depth at frequency ν in GHz, and T is the temperature in K. For a free-free absorption optical depth of unity at 1 GHz, the emission measure is then $n_e^2 L \approx 3.05 \times 10^6 \text{ cm}^{-6} \text{ pc}$, giving an electron density of $n_e \approx 2 \times 10^3 \text{ cm}^{-3}$ for a path length of 1 pc.

Readhead et al. (1996b) argue against free-free absorption by a simple uniform screen causing the turnover in 2352+495. However, as discussed by Bicknell et al. (1997), the optical depth in a free-free absorption screen will vary with radius if

produced in a shock around the radio source in a medium whose density declines with radius. If free-free absorption is important in determining the spectral turnovers in GPS sources, then the turnovers due to synchrotron self-absorption must occur at lower frequencies ν_m and with higher flux density at the turnover S_m than observed. Since the magnetic field depends on these observables as $B \propto \nu_m^5 S_m^{-2}$, the true magnetic field would be less than estimated using the observed turnover and attributing it to synchrotron self-absorption.

At this point both synchrotron self-absorption and free-free absorption are consistent with the observations. I believe that Occam's razor currently favors synchrotron self-absorption; however, additional observations are needed to establish which is the dominant effect.

2.4. Turnover Frequency versus Largest Linear Size

The relationship between the turnover frequency and the projected linear size of the radio source constrains (1) the mechanism for the turnover—e.g., free-free or synchrotron self absorption—and (2) models for the source evolution. Sources should follow trajectories on the ν_m - l plane just as they do on the power-size plane (see § 6).

Fanti et al. (1990b) found an anticorrelation between linear size and turnover frequency for the CSS sources. This result is even stronger in the combined sample of CSS and GPS sources discussed by O'Dea & Baum (Fig. 5). This figure shows the following: (1) The properties of the GPS sources (*upper left*) and the CSS sources (*lower right*) are not bimodal but contiguous. There is a continuous distribution of sources across

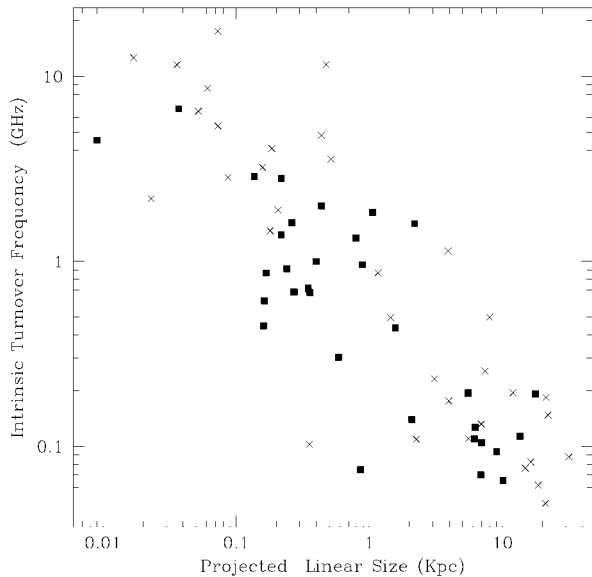


FIG. 5.—The intrinsic turnover frequency vs. linear size for the Fanti et al. CSS sample and the Stanghellini et al. GPS sample. The quasars are represented by crosses, and the galaxies by solid squares. Adapted from O’Dea & Baum (1997).

the ν_m - l plane. This suggests that the GPS and CSS sources are simply scaled versions of each other. (2) The correlation is the same for the galaxies and quasars. (3) There is a simple linear relationship on the log-log plot. O’Dea & Baum (1997) find

$$\log \nu_m \approx -0.21(\pm 0.05) - 0.65(\pm 0.05) \log l, \quad (4)$$

or $\nu_m \propto l^{-0.65}$. The fact that a simple physical relationship exists suggests that the physical properties of the GPS and CSS sources are related and that the mechanism for the turnover depends simply on the source size.

Note, however, that if the GPS sources evolve in luminosity as they age (§ 12), the sources in the upper left part of the plane may dim sufficiently that they leave the current flux density—selected samples before they reach the lower right part of the plane. Thus, Figure 5 does not necessarily imply that sources evolve along the locus of points of the observed correlation. O’Dea & Baum show that assuming the turnover is due to synchrotron self-absorption, the evolution model of Beigelman (1996) produces plausible evolution on the ν_m - l plane. Bicknell et al. (1997) show that the assumption of free-free absorption can also reproduce similar evolutionary tracks on the ν_m - l plane.

3. RADIO MORPHOLOGY

Because the radio sources are on the arcsecond scale or smaller, the development of a clear picture of the radio properties awaited the ability to image these sources with high fidelity at subarcsecond resolution (the VLA, MERLIN, the

EVN and global VLBI networks, and finally the VLBA). Examples of GPS and CSS radio morphology are shown in Figure 6, and statistics are given in Table 4. Pioneering VLBI work on the GPS sources (see, e.g., Phillips & Mutel 1980, 1981, 1982; Phillips & Shaffer 1983; Mutel, Phillips, & Skuppin 1981; Hodges et al. 1984; Jones 1984; Mutel et al. 1985; Pearson & Readhead 1984, 1988) revealed simple, relatively symmetric structure in the radio sources associated with galaxies. These structures were dubbed “compact doubles” by Phillips & Mutel (1982). Deeper images have revealed additional details in the structure of the GPS radio galaxies (see, e.g., Conway et al. 1990a, 1990b, 1992, 1994; Wilkinson et al. 1994; Readhead et al. 1996a, 1996b; Dallacasa et al. 1995; Stanghellini et al. 1996, 1997b; Polatidis et al. 1995; Thakkar et al. 1995; Taylor et al. 1994). The new observations revealed multiple components in the sources, including in some cases the “core” of the radio source. In a growing number of sources, e.g., 0710+439 and 2352+495 (Wilkinson et al. 1994; Readhead et al. 1996b), it seems that the radio structure is “triple” with radio jets and lobes on both sides of a core. These sources with two-sided radio structures have been called compact triples by Conway et al. (1990a, 1990b) and CSOs by Wilkinson et al. (1994) and Readhead et al. (1996b). The term “symmetric” is used by Readhead et al. to mean “two-sided,” i.e., there is emission on both sides of the core, rather than implying exact symmetry between the two sides. Although many of the GPS radio galaxies are two-sided, in many cases the morphologies, arm ratios, and flux density ratios are not especially symmetric. This asymmetry may be due to strong interactions of the radio source with the ambient medium.

From Table 4, it is clear that nearly all GPS *galaxies* have either compact double (CD) or triple (CSO) morphology. The current data suggest that the GPS *quasars* can have a mixture of morphologies, including compact sources, triples, and core-jet (Hodges et al. 1984; Hummel et al. 1988; Spangler, Mutel, & Benson 1983; Gurvits et al. 1992, 1994; Dallacasa et al. 1995; Stanghellini et al. 1996, 1997b).

A large body of data on the radio structures of the CSS sources has been accumulated (Pearson, Perley, & Readhead 1985; van Breugel et al. 1984b, 1992; Fanti et al. 1985, 1989; Simon et al. 1990; Wilkinson et al. 1984a, 1984b, 1991b; Spencer et al. 1989, 1991; Zhang et al. 1991, 1994; Mantovani et al. 1994; Akujor, Spencer, & Wilkinson 1990; Akujor, Spencer, & Saikia 1991a; Akujor et al. 1991b, 1993; Akujor & Garrington 1995; Nan et al. 1991a, 1991b, 1992; Sanghera et al. 1995; Cotton et al. 1997a, 1997b). The CSS galaxies tend to be (sometimes asymmetric) doubles and triples, while the quasars tend to be triple with a single bright jet (Spencer et al. 1989; Fanti et al. 1990b; Sanghera et al. 1995). Based on early low-fidelity images, the quasars were often thought to be core-jets, but recent observations have shown that they are mostly triples (Sanghera et al. 1995). A similar situation may hold for the GPS quasars. The CSS quasars tend to have brighter jets

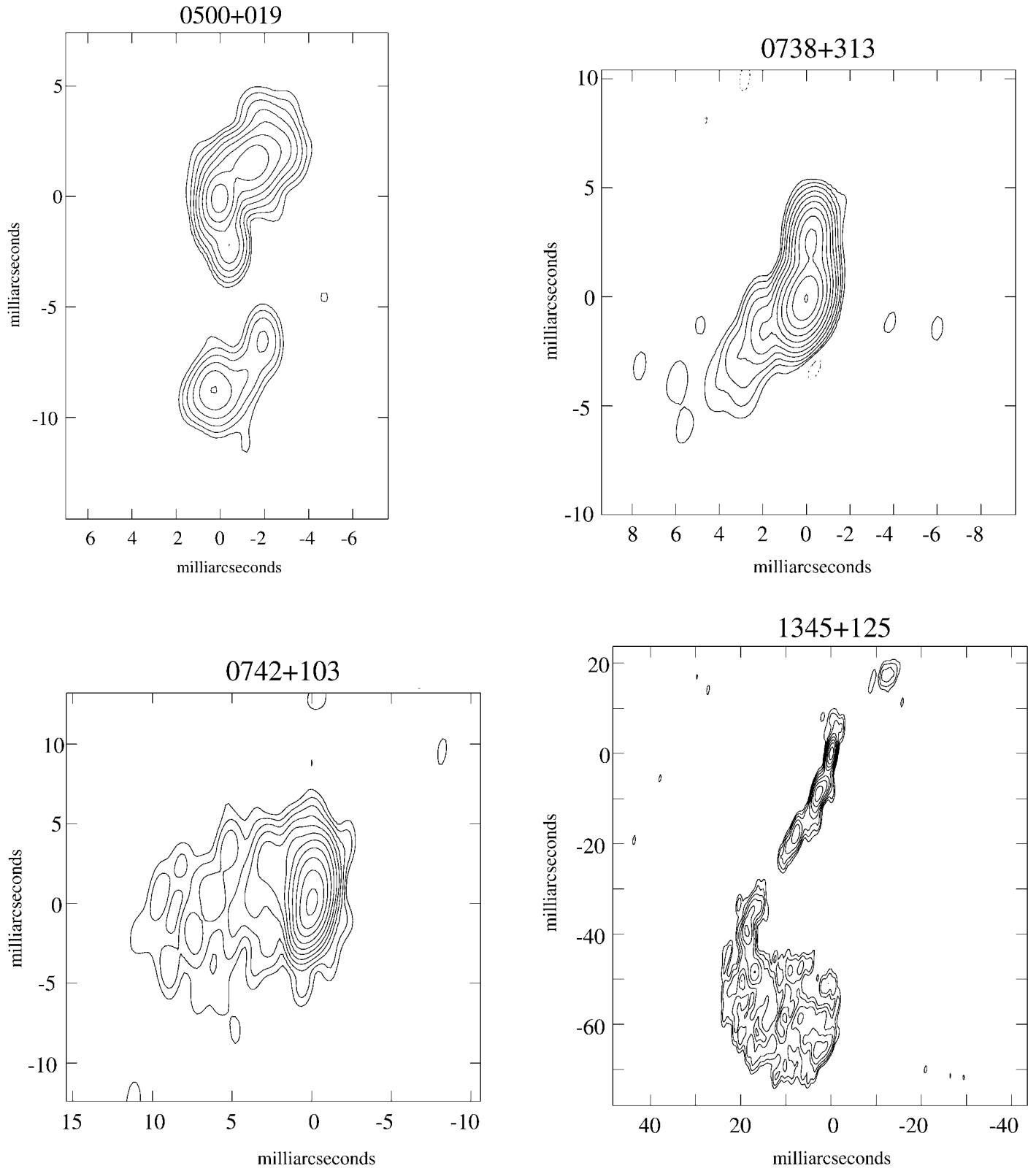


FIG. 6.—Radio images of GPS and CSS sources from C. Stanghellini (1997, private communication; see also Stanghellini et al. 1997b)

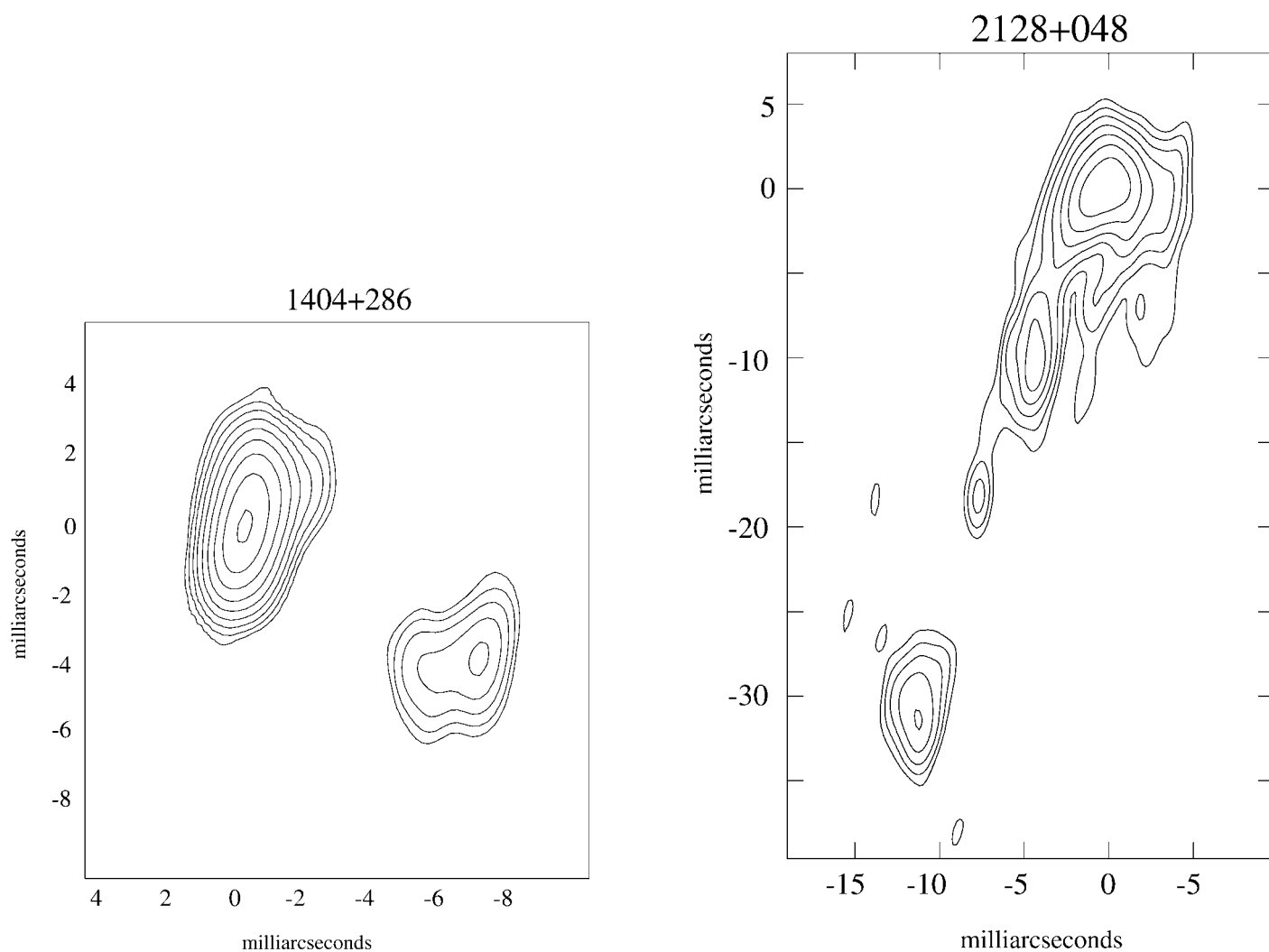


FIG. 6.—Continued

 TABLE 4
 IDENTIFICATION VERSUS RADIO MORPHOLOGY

Subsample	Total	CD+CSO	Compact	Linear/Core-Jet	Complex
GPS galaxies (total)	28	23 (82%)	1 (4%)	3 (11%)	1 (4%)
GPS quasars (total)	27	8 (30%)	8 (30%)	7 (26%)	4 (15%)
GPS galaxies (Stanghellini)	21	19 (90%)	0 (0%)	1 (5%)	1 (5%)
GPS quasars (Stanghellini)	14	5 (36%)	1 (7%)	6 (43%)	2 (14%)
CSS galaxies	23	21 (91%)	0 (0%)	0 (0%)	2 (23%)
CSS quasars	20	17 (85%)	0 (0%)	1 (20%)	2 (10%)
Combined galaxies	36	32 (89%)	0 (0%)	1 (3%)	3 (8%)
Combined quasars	32	20 (62%)	1 (3%)	7 (32%)	4 (12%)

NOTES.—Radio morphology as a function of optical identification for the sources for which there are radio images. The GPS (total) sample includes the master list of GPS sources maintained by the author, which is a very heterogeneous list. The GPS (Stanghellini) subsample is the Stanghellini complete sample. The empty fields are included with the galaxies and the stellar objects are included with the quasars. Compact sources includes those that are only slightly resolved by the existing data and for which no definite classification can be made. The combined sample is the Stanghellini GPS plus the Fanti CSS with overlap consolidated.

and brighter cores than the galaxies (Fanti et al. 1990b; Spencer et al. 1991; Sanghera et al. 1995).

Some CSS sources exhibit very distorted morphology (e.g., 3C 287 (quasar), Fanti et al. 1989; 3C 119 (galaxy? see Eracleous & Halpern 1994)—Fanti et al. 1986; Nan Rendong et al. 1991a, 1991b). The distorted morphologies have led to the suggestion that the sources are interacting with dense clouds in their environment (see, e.g., van Breugel, Miley, & Heckman 1984b; Wilkinson et al. 1984a, 1984b). Direct evidence for interactions between kiloparsec-scale radio jets and ambient gas has been found in some objects (e.g., 3C 305, Heckman et al. 1982; 4C 26.42, van Breugel et al. 1984a; 3C 303.1, Gelderman & Whittle 1994; PKS 2322–123, O’Dea, Baum, & Gallimore 1994a). However, in most cases the interaction is merely inferred from the distorted morphology (see, e.g., van Breugel et al. 1984b; Akujor et al. 1991a; Wilkinson et al. 1984a, 1984b, 1991b). In 3C 147 (Zhang et al. 1991) the distorted morphology has also been attributed to the existence of more than one “engine.”

The existence of two-sided GPS/CSS radio sources has two important implications. (1) These structures are in sharp contrast to the one-sided “core-jet” structures usually found in powerful compact radio sources (and thought to be due to relativistically boosted jets). (2) There is a continuity in morphology between the GPS and CSS sources and the large-scale radio sources.

3.1. Extended Emission

An important question is whether the CSS and GPS sources are “complete” and compact sources in their own right, or whether they are just the inner parts of much more extended sources as are the “steep-spectrum cores” in 3C 236 and 3C 293 (Schilizzi et al. 1988; Bridle, Fomalont, & Cornwell 1981). Several of the sources in the Fanti et al. 3C + PW sample are now known to have larger scale structure (3C 216, Barthel, Pearson, & Readhead 1988, van Breugel et al. 1992; Taylor, Ge, & O’Dea 1995; 3C 299, van Breugel et al. 1992; 3C 346, van Breugel et al. 1992, Dey & van Breugel 1994, ; Cotton et al. 1995; 3C 380, van Breugel et al. 1992, Wilkinson et al. 1991a). 3C 299 is a very asymmetric double, and 3C 346, 3C 380, and 3C 216 are probably large doubles that are projected with their radio axes at a small angle to the line of sight.⁷ However, the majority of the 3C+PW CSS sample do not show any evidence for very extended emission up to limits of $\approx 3\%$ of the compact emission (van Breugel et al. 1992).

Baum et al. (1990) reported the discovery of extended emission around the CSO 0108+388. Stanghellini et al. (1990a, 1990b) reported extended emission associated with the candidate GPS sources 0201+113 and 1045+019. The spectrum of 1045+019 is not well determined and its identification as a GPS source requires confirmation. However, 0108+388 and

0201+113 both have GPS-type spectra (Baum et al. 1990; O’Dea et al. 1990b). Thus, these first results suggested that 3/14 or 21% of GPS sources had extended emission. Stanghellini et al. (1998b) have searched for extended emission associated with the Stanghellini complete sample to limits of about 0.1% of the compact emission and found extended emission around two additional sources, 0738+313 (see also Murphy, Browne, & Perley 1993) and 2134+004. In addition, two other sources show secondary emission whose association with the source is still uncertain, 0248+430 and 0941–080. Thus, the Stanghellini complete sample contains 3–5 sources out of 33 with extended emission for a fraction of 9%–15%; if we combine the Stanghellini et al. (1990c) and Stanghellini et al. (1998b) searches, we have 4/42–7/42 or 9%–17% with extended emission. In all cases, the extended emission is diffuse and very faint. Thus, extended structure associated with GPS sources is not common, and the vast majority of GPS sources appear to be truly compact and isolated.

Baum et al. (1990) suggested two scenarios to explain the fraction of GPS sources with extended emission (cf. § 11). (1) “Smothered” sources: If the parsec-scale jet in a large-scale radio source is smothered and the jet propagation is halted on the scales of tens of parsecs, then the source would have both the still existing large-scale structure and the confined parsec-scale source that would have a GPS. The smothering could be produced by a large influx of dense gas acquired in galactic cannibalism (Baum et al. 1990) or by a distortion of the central torus causing the jet to ram into the dense torus gas (Gopal-Krishna 1995). Since the extended emission is no longer being resupplied by the jet, the extended structure would become faint and diffuse on the shorter of the radiative and adiabatic loss timescales. (2) Recurrent sources: If radio sources are recurrent and the new phase of activity (which is initially a GPS source) begins while the extended relic of the previous cycle of activity is still present, this would also give the appearance of a GPS core surrounded by faint extended emission.

4. RADIO POLARIZATION

Rudnick & Jones (1982) first pointed out that the GPS sources tend to have low centimeter-wavelength polarization. Further observations (Pearson & Readhead 1988; Rusk 1988; O’Dea et al. 1990b; Aller, Aller, & Hughes 1992; Stanghellini et al. 1998b) have firmly established that GPS sources have very low integrated polarization ($\sim 0.2\%$ at 6 cm). At present, there are not many high-frequency ($\nu \gtrsim 8.4$ GHz) measurements, so the frequency dependence of the polarization is not known. High-frequency polarization measurements of the GPS sources would be very useful. The low integrated polarizations could be due to (1) cancellation of polarization due to vector averaging of polarizations with different orientations in different components, (2) a very tangled magnetic field, and (3) large Faraday depths in or around the radio source. Cawthorne et al. (1993a, 1993b) have obtained polarization VLBI mea-

⁷ These four sources are removed from the statistical analysis in this paper.

measurements of several GPS sources from the Pearson-Readhead sample. They find that the galaxies 0108+388, 0153+744, 2021+614, and 2352+495 (even the bright core component) are unpolarized; however, the quasar 0711+356 is 2.5% polarized. Stanghellini et al. (1998a) report 15 GHz VLBI observations, which reveal that OQ 208 and 0500+019 are unpolarized. The lack of high polarization in individual components in the sources argues against (1) as an explanation. Cawthorne et al. (1993a) also favor high Faraday depths as the explanation for the low polarization in the GPS galaxies.

The fractional polarizations of the CSS sources tend to be higher than those of the GPS sources ($\sim 1\%$ – 3% at 6 cm) and higher still ($\sim 6\%$ – 7%) at higher frequencies (van Breugel et al. 1984a, 1992; Saikia, Singal, & Cornwell 1987; Mantovani et al. 1994; Sanghera et al. 1995; Akujor & Garrington 1995). Some sources show a polarization asymmetry where the polarization tends to be higher on the side with the jet in the quasars and the side farthest from the nucleus in the galaxies (Mantovani et al. 1994; Akujor & Garrington 1995; Lüdke et al. 1996), consistent with the Laing-Garrington effect (Laing 1988; Garrington et al. 1988).

The fact that the polarization increases with increasing frequency (in the CSS sources) suggests that large Faraday depths are responsible for the depolarization between 15 and 5 GHz rather than magnetic field geometry.

There is some evidence that the CSS quasars are more highly polarized than the galaxies at 6 cm (Saikia et al. 1987; Sanghera et al. 1995). However, Akujor & Garrington (1995) find that quasars and galaxies have a similar distribution of fractional polarization at 3.6 cm. These conflicting results may mean that the final answer is not yet in, or it may mean that the galaxies depolarize more than the quasars. In this case, at higher frequencies, when the sources are more Faraday thin, the differences in polarization should become smaller.

4.1. Faraday Rotation Measures

Faraday rotation measures (RMs) where available are given in Table 5. There are many sources in the complete samples without measured RMs. Note that it is often difficult to measure reliable RMs in GPS sources for the following reasons. (1) The polarization is so low that it is often difficult to detect polarization at multiple wavelengths. (2) The existing observations tend to straddle the peak of the spectrum, so that (assuming the turnover is due to synchrotron self-absorption) the wavelength dependence of the polarization is contaminated by the effects of synchrotron opacity. Polarization measurements at high frequencies above the spectral peak are needed to determine if GPS sources generally have high RMs.

Saikia, Swarup, & Kodali (1985) suggested that the RMs of CSS sources tend to be slightly higher than those of large-scale 3CR sources. Since then, examples of GPS/CSS sources with extreme values of RM ($\geq 1000 \text{ rad m}^{-2}$ in the source rest frame) have been found (Kato et al. 1987; Aizu et al. 1990; Taylor,

Inoue, & Tabara 1992; Inoue et al. 1995). Note, however, that there are also GPS/CSS sources with *small* measured values of RM. Lüdke et al. (1996) show that the CSS and large FR 2 sources display a trend of increasing Faraday dispersion with decreasing source size. Table 5 lists 11 sources with rest-frame RM $\geq 1000 \text{ rad m}^{-2}$. Figure 7 shows that (1) GPS and CSS sources have similar RMs; (2) there is a large range of RMs, possibly divided into three groups, small (RM ≤ 100), intermediate (RM ~ 200), and large (RM ≥ 1000); and (3) there is an upper envelope to the RM (defined mainly by the quasars) that decreases with increasing projected linear size (consistent with Lüdke et al.). Curiously, the quasars have a broader range in RM than the galaxies; the sources with the smallest and largest values are quasars.

Currently, there are two classes of extragalactic radio sources that are found to have high RMs: GPS/CSS sources and radio galaxies at the centers of cluster cooling flows (Perley 1990; Taylor et al. 1992; Ge & Owen 1994). The high RMs in the cooling flow radio galaxies are thought to be produced in the intracluster medium (ICM) surrounding the radio galaxy. The inflowing cluster gas may compress, amplify, and radially align the intracluster magnetic field (Soker & Sarazin 1990), resulting in large Faraday depths. This raises the question of whether the GPS/CSS sources with high RMs are also in cooling flow clusters or whether the high RMs are produced in some other way, e.g., via interactions between the radio jet and the ambient medium.

The possible relationship between GPS/CSS sources and cooling flows should be investigated. At present, there is only mixed anecdotal evidence. O’Dea et al. (1994a) noted that PKS 2322–123, which is in the center of a large cooling flow in Abell 2597, is similar to many CSS sources and could be considered to be a low-redshift example of a CSS source. Forbes et al. (1990) argue that 3C 309.1 has a massive cooling flow based on pressures in the optical emission-line nebula. On the other hand, O’Dea et al. (1996b) used *ROSAT* observations to rule out a cooling flow greater than $3 M_{\odot} \text{ yr}^{-1}$ in the GPS galaxies 1345+125 and 2352+495 (see § 9).

Recent VLBA polarimetry observations have clarified the location of the high RMs in the CSS quasars OQ 172 (Taylor et al. 1996b; cf. Udomprasert et al. 1997) and 3C 138 (Cotton et al. 1997a). OQ 172 has a very large rest-frame RM $\geq 2 \times 10^4 \text{ rad m}^{-2}$ measured in its integrated polarization. Taylor et al. find that the high RM is confined to the nuclear region of the quasar, and that over a scale of about 50 pc (projected) the RM in the jet drops below 100 m^{-2} . Similar results (i.e., very high RM near the core, much lower farther out) are found for 3C 138 (Cotton et al. 1997a). This suggests that the high RM is produced in the nuclear environment of the quasar and not in a cluster cooling flow. Thus, the high-RM phenomenon depends sensitively on the source structure and resolution.

What conditions in the ambient medium would produce RMs

TABLE 5
FARADAY ROTATION MEASURES

IAU Name (1)	Catalog Name (2)	Class (3)	RM (rad m ⁻²) (4)	RM (1+z) ² (rad m ⁻²) (5)	Reference (6)
0127+23	3C 43	CSS	-65	-393	1
0134+32	3C 48	CSS	-67	-126	2
0221+27	3C 67	CSS	-64	-110	1
0237-233	OD -263	GPS	19	195	3
0248+430		GPS	44	236	3
0319+121		GPS	-15	-202	1
0429+41	3C 119	CSS	1728	3400	4
0457+024		GPS	258	2954	5
0500+019	OG 003	GPS	-7	-18	1
0518+16	3C 138	CSS	-2	-22	1
0538+49	3C 147	CSS	-1510	-3150	4
0552+398		GPS	-658	4446	6
0658+38	3C 173	CSS	-11	-46	1
0738+313		GPS	-813	-2160	5
0802+10	3C 191	CSS	89	778	1
0941-08		GPS	35	53	1
1005+07	3C 237	CSS	141	497	1
1019+22	3C 241	CSS	18	123	1
1117+146	4C 14.41	GPS	-112	208	1
1127-145		GPS	33	158	1
1143-245		GPS	146	1270	5
1203+64	3C 268.3	CSS	86	161	1
1245-197		GPS	942	4875	7
1354-17	OP -190.4	GPS	-29	-499	1
1328+25	3C 287	CSS	-58	-245	1
1328+30	3C 286	CSS	-1	-3	2
1442+101	OQ 172	GPS	1091	22400	4, 8
1447+77	3C 305.1	CSS	-57	-259	1
1458+71	3C 309.1	CSS	63	228	1
1517+20	3C 318	CSS	456	1400	8
1641+17	3C 346	CSS	-32	-43	1
2223+21		GPS	-125	-1094	1
2134+004		GPS	349	3008	5
2247+14	4C 14.82	CSS	-3	-5	1
2248+71	3C 454.1	CSS	-49	-395	1
2249+18	3C 454	CSS	-87	-661	1
2252+12	3C 455	CSS	7	17	1

NOTES.—Compilation of Faraday rotation measures for GPS and CSS sources listed in Table 1. Col. (1), IAU name; col. (2), catalog name; col. (3), class (either CSS or GPS); col. (4), observed RM; col. (5), RM in the rest frame of the source; col. (6), a reference for the observed RM. Note that the high RM for 0201+113 in O'Dea et al. 1990 was not confirmed by Stanghellini et al. 1998b.

REFERENCES.—(1) Simard-Normandin et al. 1981; (2) Rudnick et al. 1983; (3) Rudnick & Jones 1983; (4) Aizu et al. 1990; Kato et al. 1987; (5) Stanghellini et al. 1998b; (6) O'Dea et al. 1990; (7) Mantovani et al. 1994; (8) Taylor et al. 1992.

of order 10^3 rad m⁻²? For a uniform medium

$$\text{RM} = 0.81n_e B_{\parallel} L \text{ rad m}^{-2}, \quad (5)$$

where RM is the intrinsic RM in rad m⁻², n_e is the electron density in cm⁻³, B_{\parallel} is the parallel component of the magnetic field in μG , and L is the path length in pc. For a path length of 100 pc, and a magnetic field of 10 μG in the ambient me-

dium, the electron density is of order unity:

$$n_e \approx 1.2 \left(\frac{\text{RM}}{10^3 \text{ rad m}^{-2}} \right) \left(\frac{B_{\parallel}}{10 \mu\text{G}} \right)^{-1} \left(\frac{L}{100 \text{ pc}} \right)^{-1} \text{ cm}^{-3}. \quad (6)$$

This calculation is meant to be merely illustrative; however, it does suggest that electron densities in the environment of GPS/CSS sources with large RMs could be very high. If the ambient

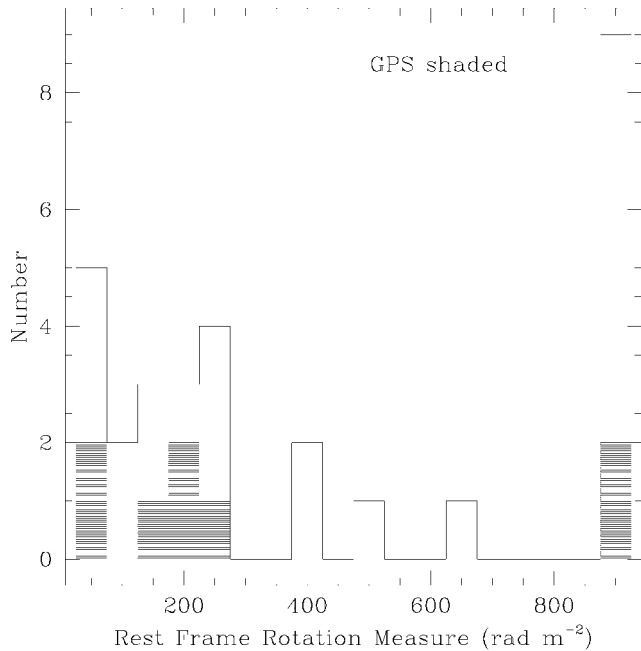


FIG. 7a

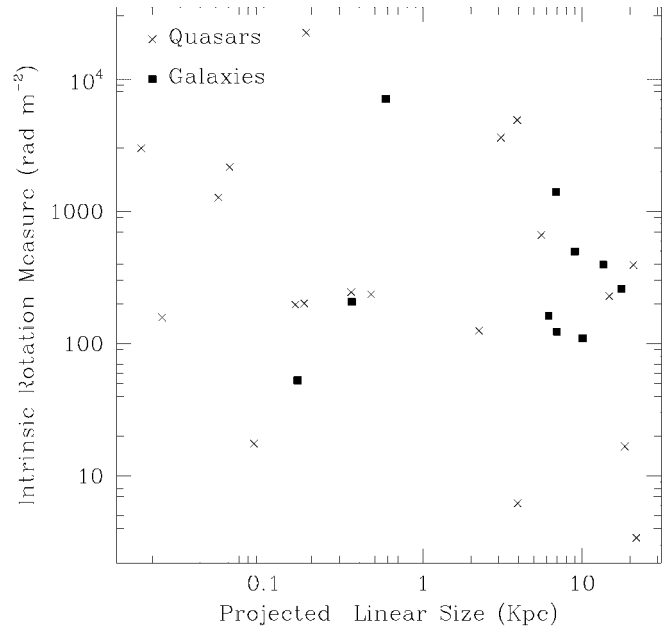


FIG. 7b

FIG. 7.—(a) Histogram of rest-frame Faraday rotation measure for the subset with measurements of the Fanti et al. CSS sample and the Stanghellini et al. GPS sample (*shaded*). Sources in the rightmost bin have values $\geq 10^3$ rad m^{-2} . (b) Rest-frame RM as a function of projected source size for the sources in (a). Galaxies are represented by solid squares, and quasars by crosses.

medium has a low ionization fraction (f), then the ambient density is proportionally larger ($n_H \approx n_e/f$). Thus, at this point the existence of large RMs in some CSS/GPS sources supports the hypothesis of a dense ambient medium surrounding the radio source. Note that if the high RMs turn out to be produced mainly in the nuclei, then this support will be diminished.

5. VARIABILITY, PROPER MOTIONS, BEAMING, AND UNIFIED SCHEMES

In general there is no strong evidence that the radio emission from GPS/CSS galaxies is significantly Doppler boosted. In fact, there is evidence to the contrary.

In the radio, GPS/CSS sources are the least variable class of compact extragalactic radio sources (see, e.g., Rudnick & Jones 1982; Seielstad, Pearson, & Readhead 1983; Waltman et al. 1991; Aller et al. 1992). Typically, only minor variations are seen, e.g., $\sim 10\%$ over a timescale of 1 yr. However, life is never this simple, and there are counterexamples of sources (all quasars) that are very variable, e.g., 0552+398, 1127-145, and 2134+004 (Wehrle et al. 1992). Some CSSs are observed to vary at low frequencies; however, these cases are thought to be due to extrinsic effects, e.g., refractive scintillation or ionospheric Faraday rotation (see, e.g., Mantovani et al. 1992). At this point not much is known about variability at other wave bands.

De Bruyn (1990) has used the limits on flux density variability in OQ 208 to place an interesting limit on the expansion

speed of the radio source. If the turnover in OQ 208 is due to synchrotron self-absorption, then below the turnover, where the source is optically thick, the flux density is proportional to the source solid angle. The observed limits on variability at 1.4 GHz imply an expansion speed of less than 10^3 km s^{-1} . This argument has been revisited by Stanghellini et al. (1997a) using improved knowledge of the milliarcsecond structure, deriving an upper limit to the expansion speed of 1.2×10^3 km s^{-1} .

Seven sources (0108+388, 0710+439, 0711+356, 1934-638, 2021+614, 2134+004, and 2352+495) now have upper limits to component proper motion that are subluminal, ranging from $0.05c$ to $0.5c$ (Pearson, Readhead, & Barthel 1987; Conway et al. 1992, 1994; Pauliny-Toth et al. 1984; Tzioumis et al. 1989; Taylor, Readhead, & Pearson 1996a; G. Taylor 1996, private communication). The observed upper limits are generally much larger than the “expected” hot spot advance speeds of $\sim 0.02c$ (see, e.g., Readhead et al. 1996b). Although 3C 216 has been shown to be superluminal (Barthel et al. 1988), it is now thought to be a large-scale double viewed close to the radio axis and not a true CSS (see, e.g., van Breugel et al. 1992; Taylor et al. 1995). There are a few sources that are apparently superluminal (e.g., CTA 102, Bååth 1987, Wehrle & Cohen 1989; 1946+708, Taylor & Vermeulen 1997; 3C 138, Cotton et al. 1997a; and possibly 0646+600, Akujor, Porcas, & Smoker 1996). The arm-length ratio and brightness ratios of the bidirectional jets in 1946+708 are consistent with Doppler effects. However, superluminal motion currently ap-

pears to be rare in GPS/CSS sources, unlike core-jet sources, which are very frequently found to be superluminal.

Wilkinson et al. (1994) have argued based on the similar number of CSOs (objects with radio cores) and compact doubles (i.e., CDs, objects without apparent cores) that the CSOs do not constitute a beamed subset of the CDs. Thus, all these arguments taken together are consistent with the hypothesis that the morphologies and luminosities of the GPS/CSS galaxies are not dominated by Doppler-boosted emission. This implies that these sources are *intrinsically* very powerful. On the other hand, there is evidence from variability that at least some of the GPS quasars are Doppler boosted.

The GPS/CSS quasars tend to be at higher redshift than the galaxies (§ 8.1) and tend to have higher radio powers by roughly an order of magnitude (§ 6). This is consistent with the quasar radio flux densities being moderately increased by Doppler boosting.

Fanti et al. (1990b), Saikia (1995), and Saikia et al. (1995) have considered the orientation-dependent properties of CSS sources in order to determine whether beaming is significant. Fanti et al. concluded that the radio luminosity of the CSS sources was not strongly affected by Doppler boosting and that the quasars seemed more asymmetric and distorted than expected purely on the basis of projection effects. Saikia has compared the fraction of total emission contributed by the core, projected linear size, misalignment angle, ratio of distances from the core to the lobes, and ratio of flux densities of the lobes for a sample of CSS sources and a sample of larger 3CR sources. He finds that the distributions of these orientation indicators are consistent with the differences in the CSS galaxies and quasars being due primarily to orientation, i.e., the quasars are closer to the line of sight than the galaxies. However, the CSS sources have more extreme values of these parameters than do the larger scale sources (i.e., the CSS sources are more asymmetric than the larger scale sources). Saikia suggests this is due to an additional effect—interactions with dense clouds in the environment.

6. GLOBAL RADIO PROPERTIES

The radio power and linear size are two fundamental observables of radio sources and are the parameters that are the subject of much theoretical work. In this section we present the results on the GPS and CSS sources, and in the next section we compare these properties with those of the large-scale 3CR sources.

6.1. Radio Power and Projected Linear Size

The distribution and trends in the physical properties of the CSS sources have been discussed in great detail by Fanti et al. (1990b). Additional results on CSS sources have been presented by Spencer et al. (1989) and Sanghera et al. (1995). O'Dea & Baum (1997) have presented an analysis of the radio power

and linear size of the Fanti et al. CSS sample and Stanghellini et al. GPS sample.

Histograms of the integrated radio power at 5 GHz in the rest frame (adapted from O'Dea & Baum 1997) are shown in Figure 8. It is clear that (1) the GPS and CSS sources have similar radio powers and (2) they are very luminous radio sources. Note that since the quasars tend to be at higher redshifts than the galaxies (§ 8), they have larger luminosities than the galaxies. All objects are above the FR 1/FR 2 break power of roughly 10^{25} W Hz⁻¹ at 5 GHz. Since Doppler boosting is not likely to affect the observed powers of at least the radio galaxies (§ 5), these large powers are intrinsic. Any model for these objects must be able to explain their enormous luminosities. In addition, it would be interesting to know how far down in power the GPS and CSS phenomena extends; thus, we eagerly await the results of studies of sources at fainter flux densities.

It is interesting to examine the relationship between radio power and total projected source size, since this is a constraint on evolutionary models. Figure 9 shows a scatter diagram, i.e., the radio power is basically independent of linear size.⁸ This is consistent with the result above that the GPS and CSS sources have similar ranges of radio power.

Histograms of the distribution of total projected linear sizes are shown in Figure 10. And the distribution of projected linear size with redshift is shown in Figure 11. The results are the following. (1) There is no trend for projected linear size to vary with redshift (except at high redshifts, where all the objects in these samples are GPS quasars). (2) Over the redshift range where the galaxies and quasars overlap, they have similar ranges of size. Thus, the quasars do not seem to be necessarily strongly foreshortened versions of the galaxies (cf. § 5).

6.2. Comparison between the GPS/CSS and the LRL 3CR

O'Dea & Baum (1997) have shown that at 5 GHz in the rest frame, the Stanghellini GPS and Fanti CSS sources are just as powerful as the 3CR in the Laing, Riley, & Longair (1983, hereafter LRL) revised sample. These GPS and CSS sources would apparently have been in the LRL 3CR if their spectra did not turn over. The power versus size plot was introduced by Baldwin (1982) as a tool with which to study radio source evolution. O'Dea & Baum plot power versus projected largest linear size (Fig. 12) for the complete GPS and CSS samples and the LRL 3CR for the redshift range $0.2 \lesssim z \lesssim 1.0$, where there is good overlap between the samples. At this range of redshifts, the LRL 3CR sources are almost exclusively classical doubles. Out to sizes of several kpc, the power is constant with size, and at larger sizes the power may decline slightly with increasing size (cf. Leahy & Williams 1984; Nilsson et al. 1993; Readhead et al. 1996a).

⁸ However, note the presence of a group of high-redshift, compact quasars with high radio powers in the upper left of the diagram.

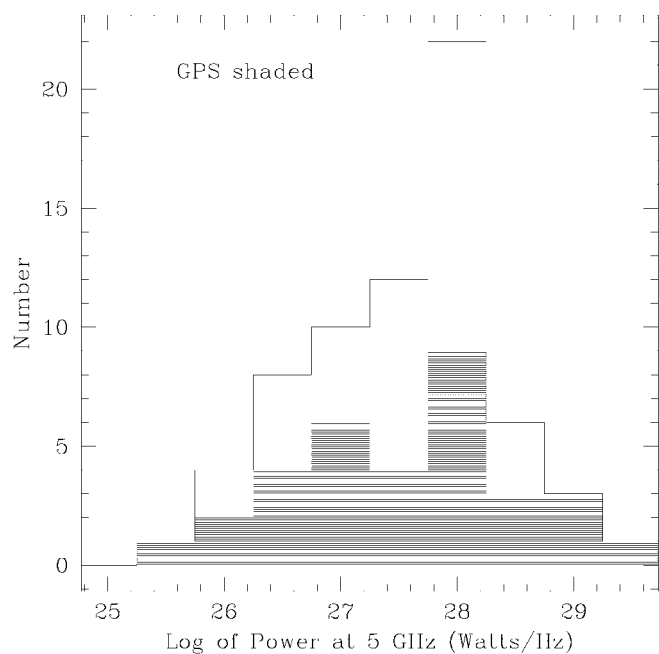


FIG. 8a

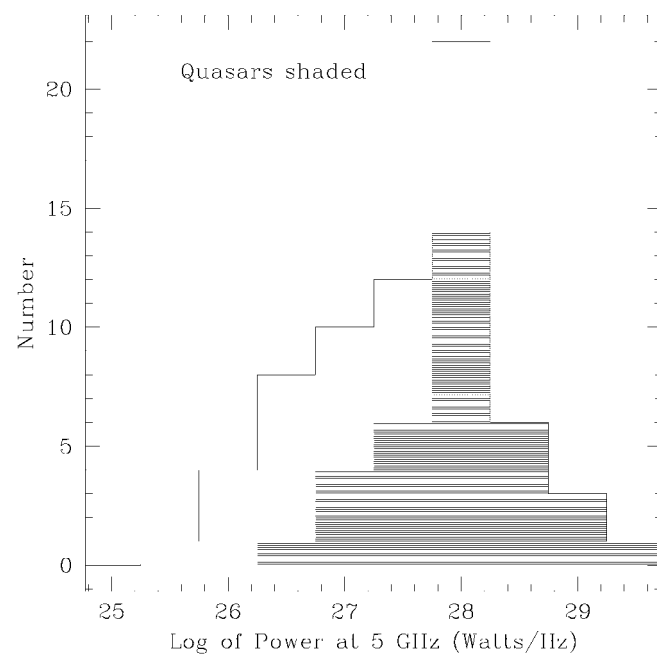


FIG. 8b

FIG. 8.—(a) Histogram of log of integrated radio power at 5 GHz in the rest frame for the Fanti et al. CSS sample and the Stanghellini et al. GPS sample (shaded). (b) Same as (a), but with the quasars shaded. Adapted from O’Dea & Baum (1997).

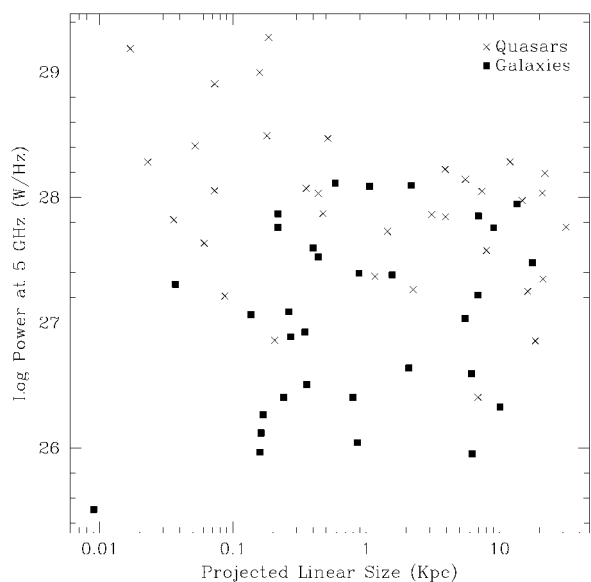


FIG. 9.—Log radio power at 5 GHz vs. the linear size for the Fanti et al. CSS sample and the Stanghellini et al. GPS sample. The quasars are represented by crosses, and the galaxies by solid squares. Adapted from O’Dea & Baum (1997).

The $P-l$ diagram is a “snapshot” of radio source evolution, and individual sources will trace out trajectories in the $P-l$ plane as they evolve. A constraint on radio source evolution comes from the number of sources as a function of size in the $P-l$ plane. O’Dea & Baum plot the number of sources in bins of $\Delta \log l = 0.5$ (see Fig. 13). The number is roughly constant with linear size ($N \propto l^0$) for the small sources (less than a few kpc), while for the larger sources the number increases with increasing size as $N \propto l^{0.4}$ approximately up to the penultimate bin.⁹ Note that other fits to the data are possible. The dotted line in Figure 13 shows a fit to all the data with slope 0.21, while the dashed line shows a fit to all the data except the last bin with slope 0.25. The increase of number with size has been seen previously in the large sources (see, e.g., Fanti et al. 1995; Readhead et al. 1996a; and references therein). However, the result that the number is approximately constant with size for the small sources is a new result made possible by the inclusion of the Stanghellini GPS and Fanti CSS sources. This result suggests that *the evolution of the small sources is qualitatively different from that of the larger sources*. This is perhaps not so surprising, since the small sources are still embedded in and are interacting with the ISM of the host galaxy. In § 12, I examine the implications of the difference in evolution for the small and large sources.

⁹ The last bin is probably affected by radio source lifetimes (i.e., sources at the largest observed sizes may have started to “turn off”).

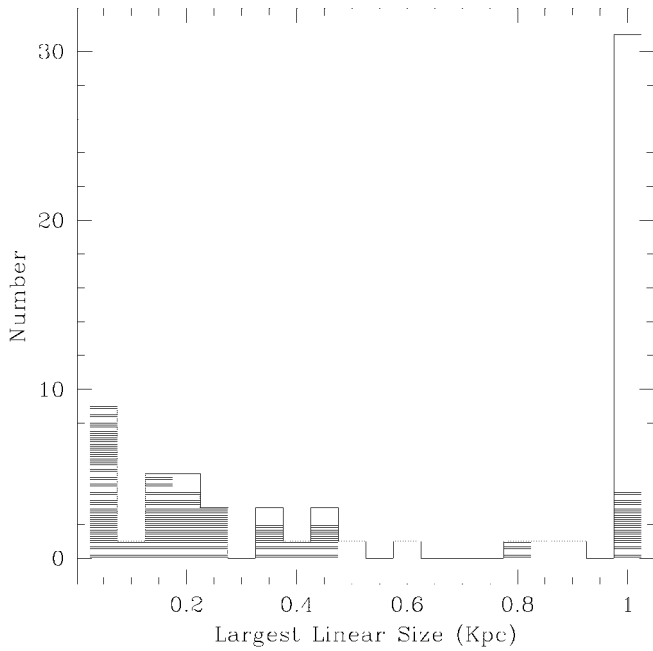


FIG. 10a

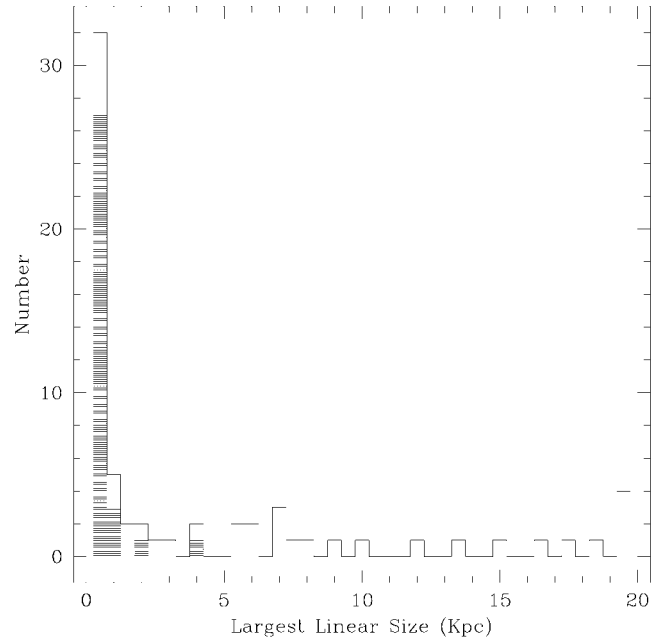


FIG. 10b

FIG. 10.—(a) Histogram of the total projected size for the Fanti et al. CSS sample and the Stanghellini et al. GPS sample (*shaded*). Sources in the rightmost bin have sizes ≥ 1 kpc. (b) Same as (a), but with scale adjusted to emphasize the CSS source distribution. Sources in the rightmost bin have sizes ≥ 20 kpc. Adapted from O’Dea & Baum (1997).

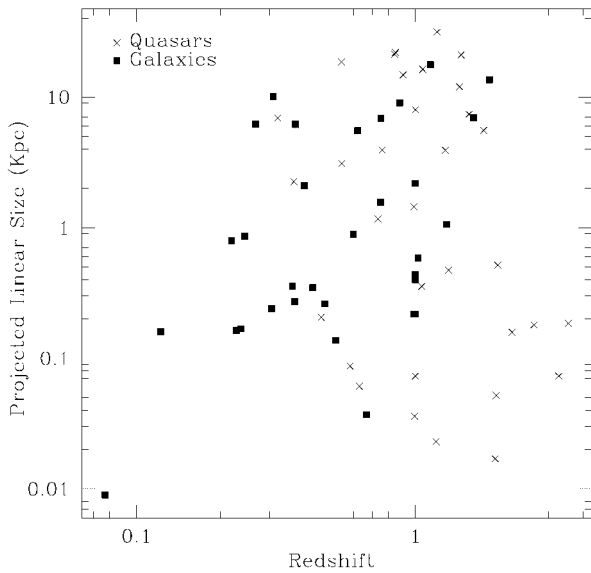


FIG. 11.—Projected linear size as a function of redshift for the combined sample of Fanti et al. CSS sources and Stanghellini et al. GPS sources. Adapted from O’Dea & Baum (1997).

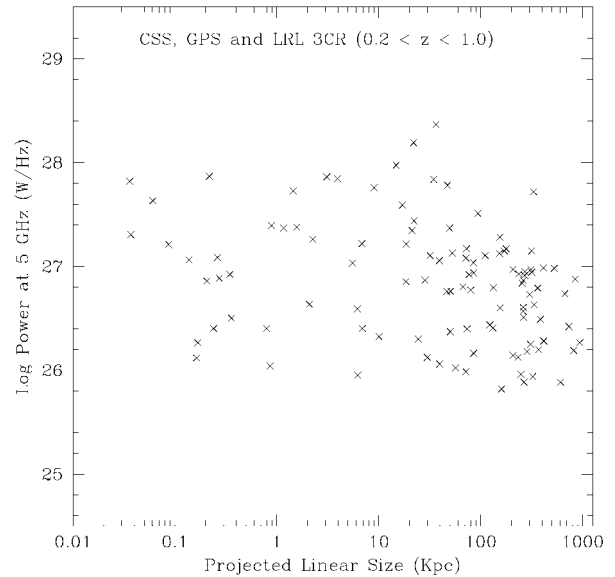


FIG. 12.—The log of power at 5 GHz vs. the projected linear size for sources in the redshift range $0.2 \leq z \leq 1.0$ from the LRL 3CR and the Fanti et al. CSS sample and the Stanghellini et al. GPS sample. Adapted from O’Dea & Baum (1997).

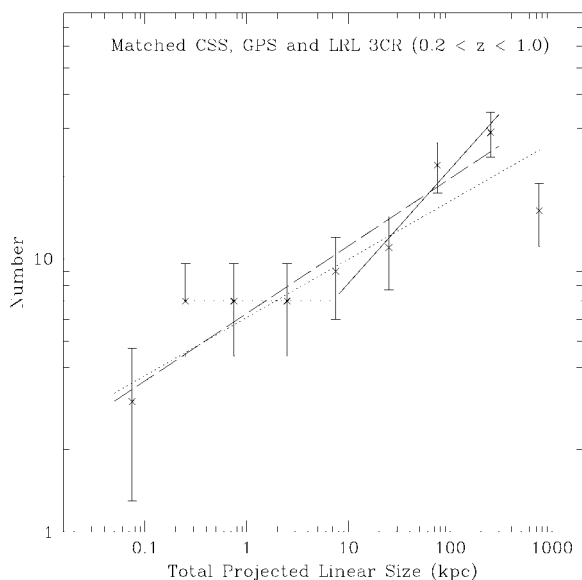


FIG. 13.—Distribution of sources in bins of 0.5 log (size) for the Fanti et al. CSS sample, the Stanghellini et al. GPS sample, and the LRL 3CR sample in the redshift range $0.2 \leq z \leq 1.0$. The GPS and CSS sources are matched in sky coverage to that of the LRL sample. The error bars are $N^{1/2}$. The solid lines are a constant value for the GPS and CSS sources and a slope of 0.4 for the LRL 3CR. The dashed line with slope 0.25 is a least-squares fit to all the data except the last point, which may be missing sources that have turned off. The dotted line with slope 0.21 is a fit to all the points.

7. FAR-INFRARED PROPERTIES

The infrared properties of the GPS and CSS sources can in principle shed light on the properties of the central engine and its immediate environment. Consider the expected mid–far-infrared (MFIR) properties of GPS/CSS sources compared to those of a sample of classical double radio sources with the same extended radio power and redshift. If the nucleus in GPS sources is surrounded by gas and dust with a higher covering factor than in “normal” extended radio galaxies, then we might expect a higher fraction of the optical–UV continuum light to be reprocessed and to emerge as MFIR radiation. Thus, in this

scenario, we might expect the GPS sources to be brighter in the MFIR than “normal” radio sources. On the other hand, it is possible that the jets in the GPS sources convert a higher fraction of their energy into radio luminosity because of the interaction with the dense and clumpy environment (see, e.g., Eilek & Shore 1989; Gopal-Krishna & Wiita 1991; De Young 1993). This enhanced efficiency means that the GPS sources will be intrinsically weaker than a sample matched in radio power. In this case we might expect the GPS sources to be weaker in the MFIR than the comparison sample.

Heckman et al. (1994) constructed samples of GPS and CSS galaxies and quasars and matched them in radio power at 5 GHz and in redshift with comparison samples of classical double 3CR radio galaxies and quasars. They have determined the *IRAS* flux densities for the ensembles of objects using the SUPERSCANPI algorithm at IPAC. Note that most GPS and CSS sources are not detected by *IRAS*. Thus, these results only apply to the ensemble.

A summary of the Heckman et al. (1994) results is given in Table 6. Heckman et al. find that the 3CR galaxy comparison sample is detected at wavelengths $\geq 25 \mu\text{m}$, while the GPS galaxies are detected at only $60 \mu\text{m}$ in the mean value, but not in the median, consistent with the mean value being dominated by a few larger values. However, the limits on the GPS galaxies are similar to the detections of the comparison sample, so no strong statements can currently be made. The data are consistent with the GPS galaxies and the comparison sample having similar MFIR infrared properties and rest-frame $50 \mu\text{m}$ luminosities $\leq 10^{12} L_{\odot}$. On the other hand, the quasars, although at higher mean redshift, are detected at higher flux density levels and at more wavelengths than the galaxies. The GPS/CSS quasars are detected at wavelengths $\geq 25 \mu\text{m}$, while the 3CR comparison sample is detected at $\geq 12 \mu\text{m}$. The two samples have similar MFIR flux densities to within a factor of about 2. The $50 \mu\text{m}$ luminosities of the GPS/CSS quasars are roughly $3 \times 10^{12} L_{\odot}$. Note that the MFIR luminosity of the GPS/CSS sources is comparable to that of the ultraluminous *IRAS* galaxies (see, e.g., Sanders et al. 1988). The plot of the spectral energy dis-

TABLE 6
SUMMARY OF MEAN INFRARED PROPERTIES

Sample (1)	N (2)	z (3)	$\log P_{5 \text{ GHz}}$ (W Hz^{-1}) (4)	$S_{12 \mu\text{m}}$ (mJy) (5)	$S_{25 \mu\text{m}}$ (mJy) (6)	$S_{60 \mu\text{m}}$ (mJy) (7)	$S_{100 \mu\text{m}}$ (mJy) (8)	$L_{50 \mu\text{m}}$ (ergs s^{-1}) (9)
RG (z, P)	51	0.753	27.0	< 9	16 ± 4	25 ± 5	51 ± 10	2.3×10^{45}
GPSCSSG (z, P)	33	0.766	27.1	< 12	< 15	< 27	< 102	3.3×10^{45}
Q (z, P)	28	0.945	27.3	18 ± 4	29 ± 4	51 ± 5	114 ± 29	2.1×10^{46}
GPSCSSQ (z)	22	0.934	27.6	< 12	21 ± 7	39 ± 8	92 ± 24	1.0×10^{46}
GPSCSSQ (P)	11	0.766	27.2	< 24	< 21	51 ± 11	227 ± 34	...

NOTES.—Col. (1): RG and Q are the 3CR comparison samples of radio galaxies and quasars, respectively. The letters in parentheses designate the criteria for matching the sample, e.g., z means that the sample was matched on redshift. Col. (2): Number of objects in the sample. Col. (3): Mean redshift of the sample. Col. (4): Mean log power at 5 GHz. Cols. (5)–(8): Median flux density of the sample at 12, 25, 60, and $100 \mu\text{m}$, respectively, from SUPERSCANPI. Col. (9): Characteristic luminosity νP_{ν} in the rest frame at approximately $50 \mu\text{m}$.

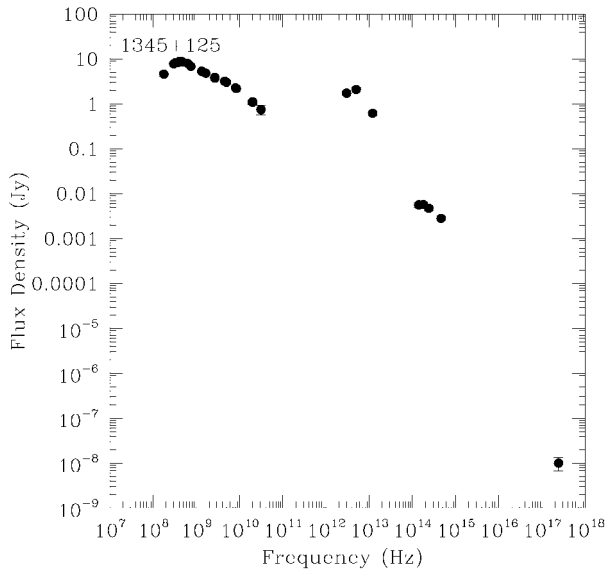


FIG. 14a

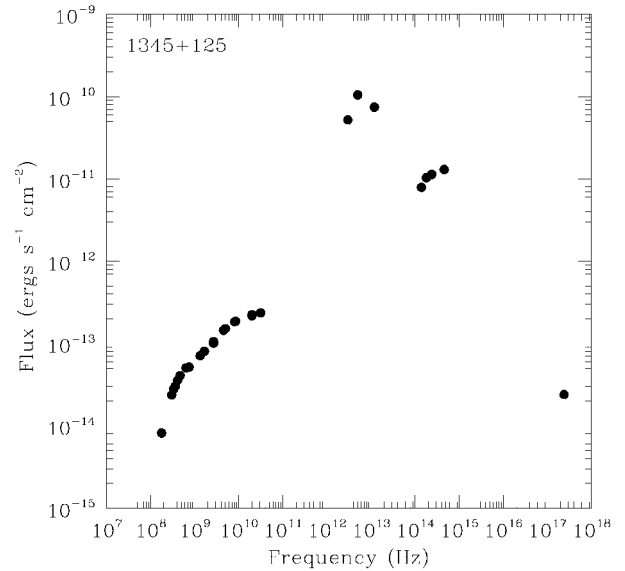


FIG. 14b

FIG. 14.—(a) Broadband spectrum F_ν (Jy) vs. ν (Hz) of the GPS galaxy 1345+125, including radio, *IRAS*, near-IR to optical, and X-ray measurements. (b) Same data as (a), but showing νF_ν (ergs s⁻¹ cm⁻²) vs. ν (Hz). Note that the energy output peaks in the mid-IR.

tribution for the GPS radio galaxy 1345+125 (Fig. 14) shows that the energy output peaks in the mid-IR around $60 \mu\text{m}$ similar to the sources studied by Vader et al. (1993).

Hes, Barthel, & Hoekstra (1995) performed a study of the *IRAS*-detected 3CR quasars and radio galaxies. They also did not find strong evidence for a difference in properties of CSS sources with non-CSS sources. Thus, the similarity of the GPS/CSS samples with their comparison samples is consistent with neither the covering factor of the circumnuclear dust nor the jet efficiency being extremely different (i.e., to within a factor of a few) in the GPS/CSS sources and the classical doubles. Preliminary results from *ISO* are also consistent with this conclusion (Fanti et al. 1998, in preparation).

8. OPTICAL PROPERTIES

In contrast to the wealth of information on the radio properties of the GPS/CSS sources, until recently we have known very little about their optical properties. Recent work is beginning to give us some clues, but our picture is far from complete and much additional work remains to be done. Here I review our current understanding of the redshift distribution, host galaxy magnitudes, morphology, colors, polarization, and emission-line properties where known.

8.1. Redshift Distribution

Fanti et al. (1990b) and O’Dea et al. (1991) presented the redshift distribution of the CSS and GPS sources, respectively. Note that there are still six sources with unknown redshifts in the complete sample. Figure 15 shows the distribution of redshift for the combined sample, with GPS/CSS and galaxies/

quasars distinguished in the two plots. The main results are these: (1) the GPS and CSS sources have similar redshift distributions; (2) there are similar numbers of quasars and galaxies in the GPS/CSS sources; (3) the quasars tend to be at higher redshifts than the galaxies (i.e., all objects at $z \geq 2$ are quasars); and (4) the $z \geq 2$ quasars are preferentially GPS rather than CSS. Recall that the GPS sources and the PW subset of the CSS sources are selected at centimeter wavelengths, where the contributions from Doppler-boosted jets are most visible. Thus, the results that there are similar numbers of quasars and galaxies and that the quasars predominate at the higher redshifts are both consistent with some Doppler boosting of the centimeter-wavelength radio emission in the quasars.

The tendency for quasars at high redshifts to be GPS sources was noted by Peterson et al. (1982), Menon (1983, 1984), Savage & Peterson (1983), and Savage et al. (1990) and was explored in more detail by O’Dea (1990). This tendency seems to be real. The exact fractional contribution of GPS quasars to the radio-loud quasar population at high redshifts is uncertain but currently appears to be around $\sim 30\%$. Thus, red, stellar GPS sources are strong candidates for high-redshift quasars and should be exploited as such.

The result that the GPS and CSS galaxies are found primarily at low to intermediate redshifts $0.1 \lesssim z \lesssim 1$ has interesting implications for source evolution. It is in this redshift range that the powerful radio sources begin to be found at the centers of clusters, rather than in the sparser environments they frequent at low redshift (see, e.g., Hill & Lilly 1991), and it is here that the peculiar “alignment” effect between the optical continuum light, the optical line-emitting gas, and the extended radio

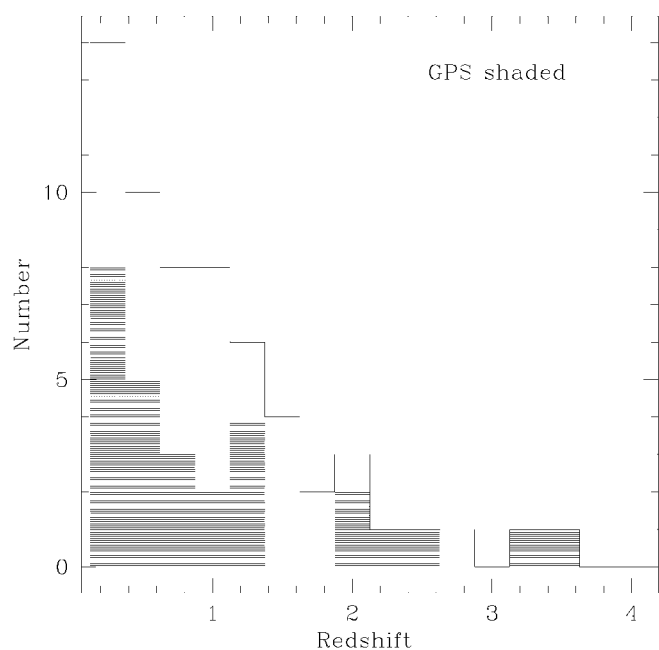


FIG. 15a

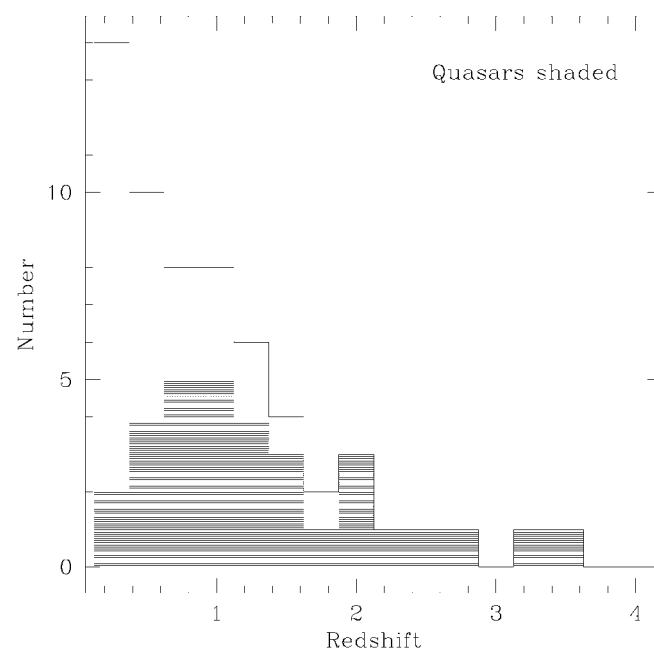


FIG. 15b

FIG. 15.—(a) Histogram of redshifts for the Fanti et al. CSS sample and the Stanghellini et al. GPS sample (*shaded*). (b) Same as (a), but with the quasars shaded.

source begins to emerge (see, e.g., McCarthy et al. 1987; Chambers et al. 1987; Miley & Chambers 1989). Thus, the appearance of GPS/CSS sources at these redshifts, and their apparent absence at lower redshifts, may indicate that these are indeed young or frustrated sources whose birth is tied to the dynamical processes of evolution occurring in clusters and groups of galaxies (e.g., collapse of compact groups—see, e.g., Mamon 1987). In particular, the higher frequency of mergers at these redshifts (see, e.g., Roos 1985; Zepf & Koo 1989; Carlberg 1990) may play an important role in their formation.

One remaining question is, where are the low-redshift ($z < 0.1$) counterparts of the GPS and CSS sources? Are they hiding as LINERs (e.g., 1718–649; Tingay et al. 1997) or Seyferts (e.g., OQ 208; Stanghellini et al. 1997a)?

8.2. Host Galaxy Morphologies

Gelderman (1994, 1996) obtained images through broadband B , V , R filters of a sample of 20 CSS sources.¹⁰ He classified amounts of disturbance and interaction using the parameters DC, IC, Q defined by Dahari (1994, 1985a, 1985b). He finds that there is evidence that *every* CSS source in his sample is either disturbed or interacting according to Dahari's criteria. Gelderman also notes the trend for the CSS sources to show evidence for diffuse linear features, such as tidal tails, bridges, and shells. Since these features are produced in simulations of

interactions involving disk systems, Gelderman suggests that the CSS interactions involve at least one gas-rich object.

The morphologies of the GPS host galaxies have been studied by Biretta, Schneider, & Gunn (1985), O'Dea, Baum, & Morris (1990a), Stanghellini et al. (1993), de Vries, Barthel, & Hes (1995), and these results have been summarized and analyzed by O'Dea et al. (1996a). In the sample considered by O'Dea et al. (1996a), there are 30 objects for which there is sufficient signal-to-noise to permit a determination of the basic morphology. The observations used generally reach a sensitivity (i.e., lowest, 3σ contour level) of about $24.5 \text{ mag arcsec}^{-2}$ (observed) in the r band. O'Dea et al. (1996a) find that 17 of these objects (57%) have distorted isophotes and that four galaxies (13%) have a second nucleus in projection (within a few arcsec or within 10 kpc).

O'Dea et al. (1996a) also determined the projected distance to the closest *apparent* companion or second nucleus of the GPS galaxies. The redshifts of the possible companions are unknown, so their relationship to the GPS source is currently unknown. The median angular separation is $\sim 5''$, and the median projected linear separation is ~ 20 kpc. If these possible companions are confirmed, then their relative closeness to the GPS galaxy is consistent with the other evidence that these sources are interacting and/or merging. Thus, a large fraction of the CSS/GPS radio galaxies show evidence for interaction and/or mergers, suggesting that these processes must be relevant to or at least associated with the formation of CSS/GPS radio sources.

¹⁰ The three additional objects in the sample are now reclassified as large-scale doubles seen close to the radio axis. See § 3.

Other studies of powerful radio galaxies have found similar fractions of distorted objects (see, e.g., Heckman et al. 1986; Smith & Heckman 1989a, 1989b). Smith & Heckman (1989b) found similarly high fractions (54%) with distorted isophotes and (20%) with double nuclei in their sample of powerful radio galaxies at surface brightness levels (in the rest frame) brighter than 25 mag arcsec⁻². Thus, the results for the morphologies of CSS/GPS radio galaxies are consistent with those found for the powerful radio galaxies with extended radio structure. We note that at low redshift, FR 2 galaxies tend to exhibit signs of interaction much more often than FR 1 galaxies (Heckman et al. 1986; Smith & Heckman 1989b; Baum & Heckman 1989; Ledlow & Owen 1995). Thus, the CSS/GPS hosts are more like FR 2 hosts than FR 1 hosts in this respect.

8.3. The Alignment Effect

At high redshifts ($z \geq 0.6$) in the large-scale radio sources there is a component of blue light that is aligned with the radio source axis (see, e.g., McCarthy et al. 1987; Chambers et al. 1987; McCarthy 1993 and references therein). The currently most likely explanations for the aligned component include (1) young stars from a “jet-induced starburst” (see, e.g., De Young 1989; Rees 1989; Daly 1990; Begelman & Cioffi 1989), (2) scattered nuclear continuum (Tadhunter, Fosbury, & di Serego Alighieri 1988; Fabian 1989), (3) inverse Compton scattering from the radio-emitting electrons (Daly 1992), and (4) nebular continuum (Dickson et al. 1995), or some combination of these.

Using ground-based imaging, Gelderman (1994) found a general alignment between the optical and radio position angles in 13 CSS sources. Röttgering et al. (1996) have presented *Hubble Space Telescope* (*HST*) observations of the alignment effect in two CSS sources. de Vries et al. (1997b) using *HST*'s second Wide Field Planetary Camera (WFPC2) images in a broad red filter also find a strong alignment effect in 12 CSS sources (see Fig. 16 for a couple of examples), one of which is in common with Röttgering et al. (1996). Lehnert (1996) has presented an independent analysis of the quasars in the de Vries et al. sample and reached the same conclusions. There is good agreement between the alignments seen by Gelderman and de Vries et al. for the few sources in common. The alignment angles (optical-radio position angle) are shown in Figure 17 for the Gelderman and de Vries et al. CSS sources and the O'Dea et al. (1996a) GPS galaxies. The GPS galaxies tend not to show the alignment effect; however, this may be due to the lack of observations with sufficient resolution. As noted by de Vries et al., the CSS sources show the alignment effect at all redshifts, in contrast to the large-scale sources, which only show it at high redshift (Fig. 17b).

Analysis of *HST* WFPC2 linear ramp filter observations centered on rest-frame [O II] $\lambda 3727$ or [O III] $\lambda 5007$ suggests that the dominant contribution to the alignment effect seen in the *R* band is emission-line gas (de Vries et al. 1998a). This is consistent with Gelderman & Whittle's (1994) result that the

CSS sources are very luminous in optical emission lines. In addition, Bicknell et al. (1997) expect emission-line gas (shocked by the radio source) to be aligned with the CSS radio sources. Thus, the emission-line nature of the aligned component supports the hypothesis that the CSS sources interact strongly with their gaseous environment.

8.4. Absolute Magnitudes and the Hubble Diagram

Work in progress by Gelderman and collaborators will eventually allow accurate magnitudes to be obtained for CSS sources. This section concentrates on recent work on the GPS host galaxies by O'Dea et al. (1996a).

The absolute magnitudes in the Cousins R_c band are between -22 and -24.0 (which corresponds to the range from M_* to 2 mag brighter). This range of absolute magnitudes is consistent with the host galaxies of other powerful radio galaxies (see, e.g., Owen & Laing 1989; Owen & White 1991; Smith & Heckman 1989b) and first-ranked cluster galaxies (Postman & Lauer 1995). Thus, the distribution of optical absolute magnitudes is at least consistent with these sources being the progenitors of the large-scale radio sources. Note, however, that examination of the R_c Hubble diagram below does reveal differences between the GPS and 3CR host galaxies.

Figure 18 shows the R_c band Hubble diagram for both the GPS sources and powerful *extended* radio galaxies (mostly from 3CR). The GPS Hubble diagram has been discussed by Stanghellini (1992), de Vries (1995), Snellen et al. (1996b), and O'Dea et al. (1996a). The good agreement between the GPS and extended radio galaxies (especially at $z \lesssim 0.5$) suggests that to first order the host galaxies of the GPS sources and extended sources are essentially the same. However, there is a suggestion that at redshifts of order unity the 3CR galaxies are brighter by about 1 mag than the GPS galaxies. In addition, O'Dea et al. (1996a) show that the GPS galaxies have a steeper slope than the sample as a whole. Since the 3CR galaxies are now completely identified, the offset in magnitude is due not to incompleteness in the 3CR.

One possibility is that the extra light in the 3CR galaxies could be related to radio power—i.e., if the 3CR galaxies are stronger radio sources, then they may have more of the extra component. O'Dea et al. (1996a) showed that there are no systematic differences between the GPS and 3CR galaxies regarding the relationship between optical magnitude and radio power. Thus, the result that, at high redshift, the 3CR galaxies are brighter than the GPS galaxies is not due to the 3CR galaxies having more powerful radio sources.

O'Dea et al. compared the data with models computed with the latest version of the Bruzual-Charlot population synthesis code (described by Charlot, Worthey, & Bressan 1996) assuming a single 0.5 Gyr duration burst of star formation at some formation redshift z_* , followed by “passive” evolution. The models are normalized in magnitude to the data at low redshift. The “no evolution” model is that for an average elliptical at

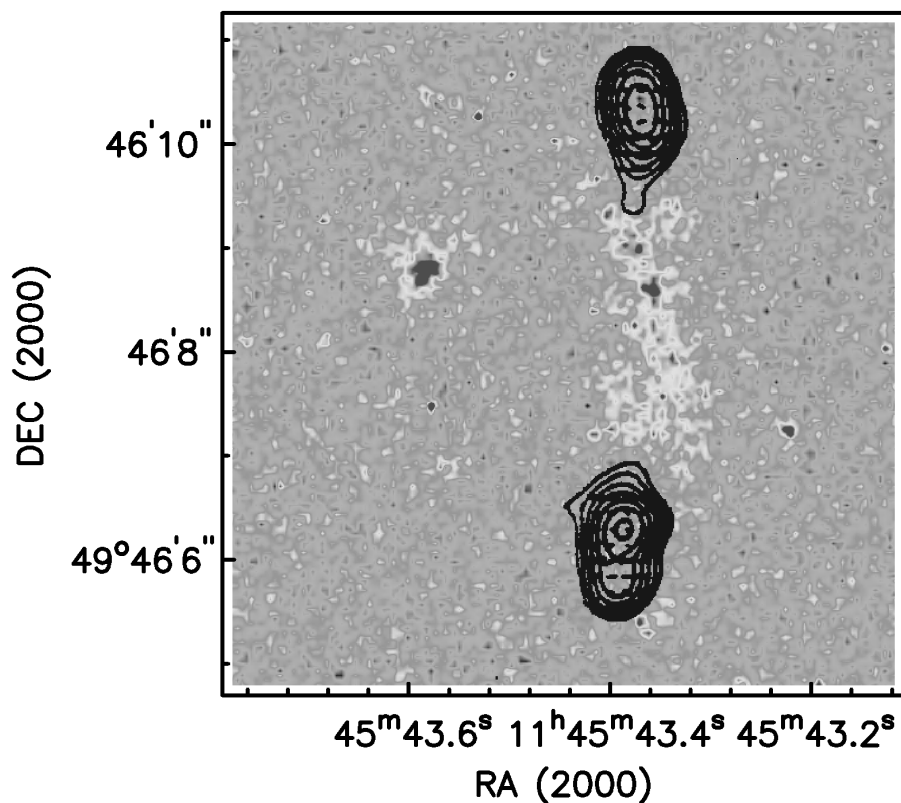


FIG. 16a

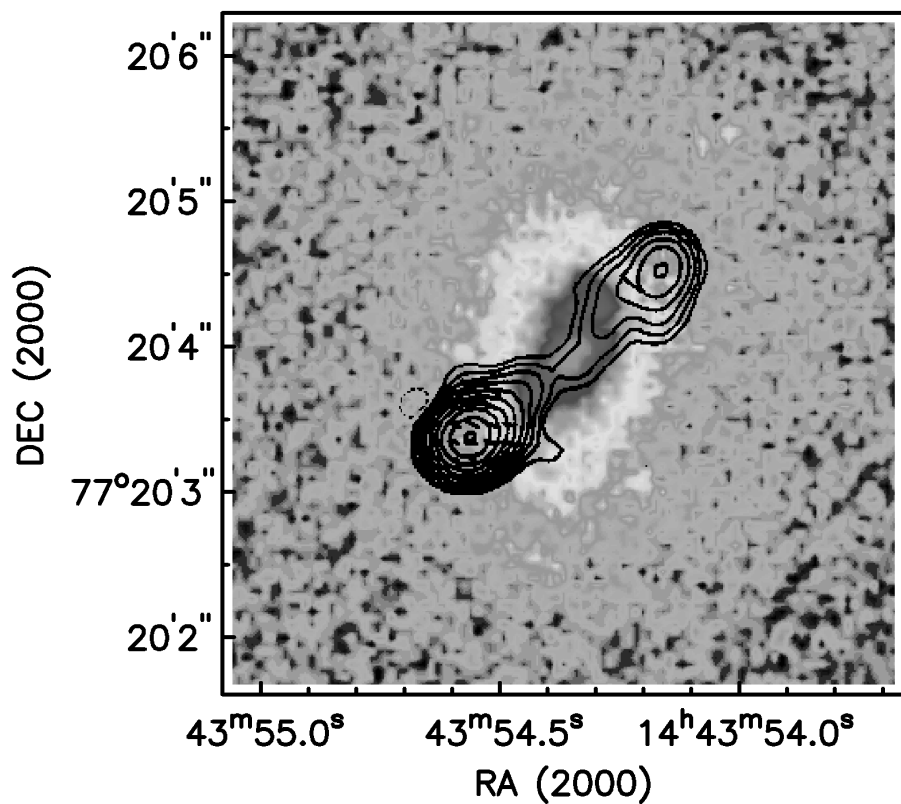


FIG. 16b

FIG. 16.—Radio contours overlaid on gray scale of *HST* WFPC2 F702W image from W. H. de Vries (1997, private communication; see also de Vries et al. 1997b). Note the strong alignment between the radio and optical. (a) 3C 266; (b) 3C 303.1.

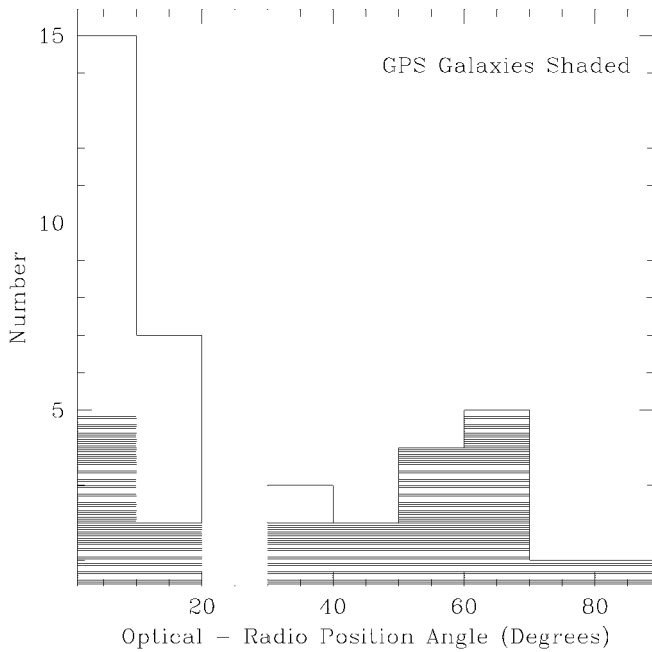


FIG. 17a

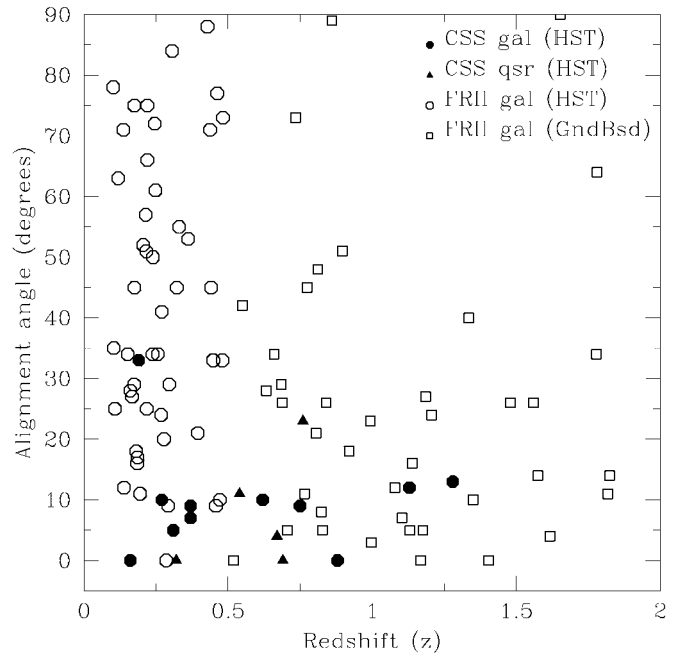


FIG. 17b

FIG. 17.—(a) Histogram of alignment angle (optical-radio position angle) for CSS sources from Gelderman (1994) and de Vries et al. (1997b) and GPS sources from O’Dea et al. (1996a). GPS sources are shaded. (b) Plot of alignment angle vs. redshift for CSS and large-scale 3CR sources (de Vries et al. 1997b). Note that the CSS sources have a strong alignment at all redshifts, while the large-scale 3CR sources are aligned at high redshift ($z \gtrsim 0.6$).

age 13.5 Gyr (see Fig. 5 of Bruzual & Charlot 1993). Figure 18 shows that the GPS galaxies are consistent with both the nonevolving elliptical model and passive evolution of an old stellar population ($z_f \gtrsim 5$). Models in which the stellar populations are younger (the elliptical model with $z_f = 2$ and the Sa model with $z_f = 5$) tend to be brighter than the GPS sources at redshifts $z \approx 1$. The 3CR galaxies at $z \gtrsim 1$ are brighter than predicted by these passive evolution models with an old stellar population (cf. Spinrad 1986; Spinrad & Djorgovski 1987; Djorgovski 1987). The fact that the GPS galaxies agree with the models for passive evolution of old stellar populations suggests that difference between the GPS and 3CR galaxies is not due to the GPS galaxies being redder than normal elliptical galaxies, but to the 3CR galaxies being bluer than normal elliptical galaxies. This is also consistent with the observed agreement of the GPS sources with the 3CR on the K -band Hubble diagram (de Vries et al. 1998b).

As discussed above, the GPS sources are missing the blue aligned component that is seen in larger scale radio galaxies. This lack of a blue component may be responsible for their different behavior on the Hubble diagram (see also Snellen et al. 1996b). One consequence of this is that the stellar evolution of GPS galaxies may be simpler than the 3CR galaxies with large-scale radio sources. Thus, the “optically boring” GPS galaxies may provide examples of “normal” giant elliptical galaxies at high redshift (Snellen et al. 1996b; O’Dea et al. 1996a; Bremer & Snellen 1996).

8.5. Optical Colors

There are not sufficient uniform data on the CSS sources to warrant a discussion of their colors. However, work in progress by Gelderman et al. and de Vries et al. should provide the necessary information. The $r - i$ colors of a subset of GPS galaxies (from Stanghellini et al. 1993) have been compared with the Bruzual-Charlot stellar evolution models by O’Dea et al. (1996a). Figure 18 shows that the colors are in good agreement with those of passively evolving ellipticals with an old stellar population. Even the colors of a Sa galaxy are too blue to be consistent with the GPS colors.

The lack of evidence for substantial amounts of young stars in the $r - i$ colors of the GPS host galaxies is consistent with the result that the GPS sources tend not to show an alignment effect. However, it is somewhat surprising given the fact that the GPS galaxies appear to be merging/interacting with companions and may have recently acquired large amounts of gas. This implies that a starburst triggered either by the merger or by the radio source should be visible. The lack of evidence for a circumnuclear starburst in the GPS galaxies may be due to the inner regions of the galaxies being very “dust enshrouded.”

8.6. Near-IR Colors

Anecdotal evidence suggests that at least some GPS sources have reddened nuclei that become bright in the near-IR (O’Dea et al. 1992; Stickel et al. 1996a, 1996b; Akujor et al. 1996;

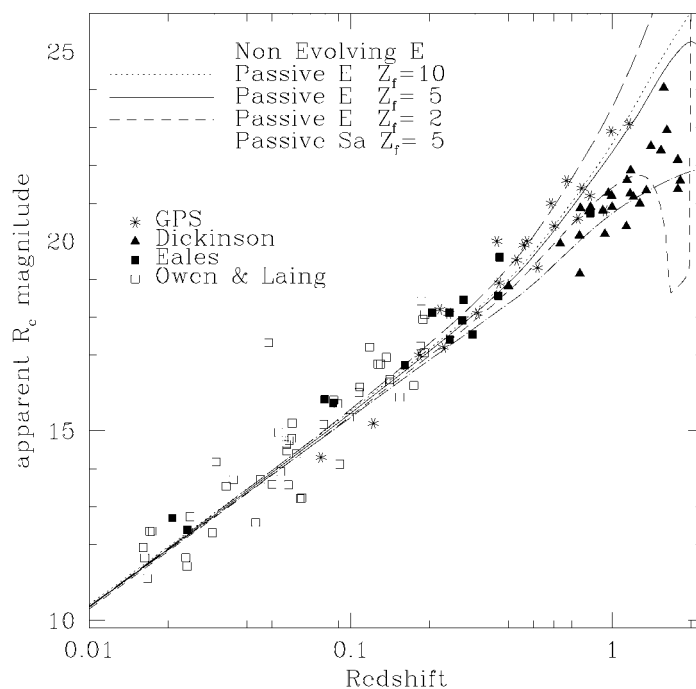


FIG. 18a

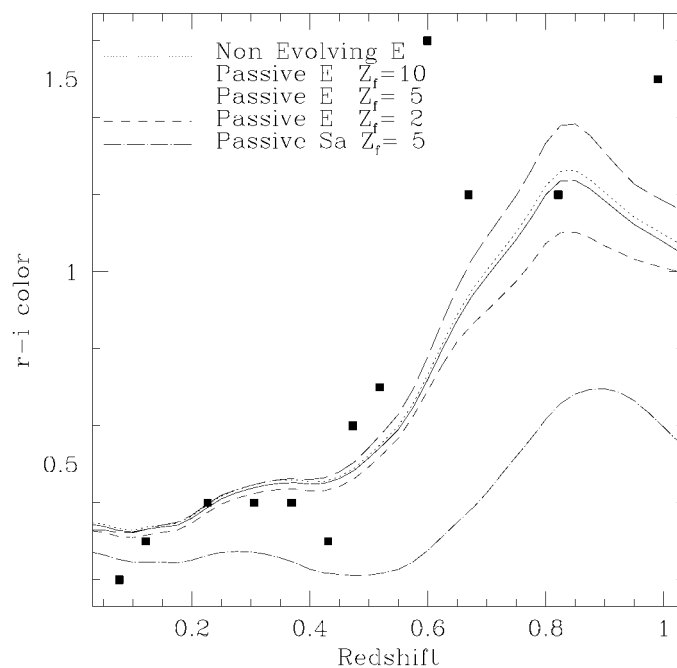


FIG. 18b

FIG. 18.—(a) The Cousins R_c band Hubble diagram for powerful radio galaxies. Magnitudes are not K -corrected. GPS galaxies are represented by asterisks, extended radio galaxies from Owen & Laing (1989) by open squares, 3CR galaxies from Eales (1985) by solid squares, and 3CR galaxies from Dickinson (1995, private communication) by solid triangles. Includes models from Bruzual & Charlot (1993). The key for the models is as follows: *Long-dashed curve*, nonevolving E galaxy; *dotted curve*, E galaxy with $z_f = 10$; *solid curve*, E galaxy with $z_f = 5$; *short-dashed curve*, E galaxy with $z_f = 2$; *dotted-long-dashed line*, Sa galaxy with $z_f = 5$. All models assume $H_0 = 75$ and $q_0 = 0.1$. (b) $r-i$ color vs. redshift for GPS host galaxies. The key to the plotted models is as follows: *Long-dashed curve*, nonevolving E galaxy; *dotted curve*, E galaxy with $z_f = 10$; *solid curve*, E galaxy with $z_f = 5$; *short-dashed curve*, E galaxy with $z_f = 2$; *dotted-long-dashed line*, Sa galaxy with $z_f = 5$. All models assume $H_0 = 75$ and $q_0 = 0.1$. Adapted from O'Dea et al. (1996a).

Bremer & Snellen 1996; Snellen et al. 1996c). Stickel et al. (1996a) report that some GPS “galaxies” are variable in the near-IR, suggesting that these are in fact members of the class of extremely red objects known as “red quasars” (Rieke, Lebofsky, & Kinman 1979; Rieke, Wisniewski, & Lebofsky 1982) or perhaps “optically quiet quasars” (Cotton, Owen, & Mahoney 1989; Kollgaard et al. 1995).

de Vries et al. (1998b, 1998c) present the results of a study of the spectral energy distribution across the R , J , H , and K bands of samples of GPS, CSS, and extended 3CR radio galaxies. They find that GPS, CSS, and 3CR sources have similar broadband spectra in the near-IR, consistent with them having similar stellar populations and AGNs ($r - K$ colors presented by Snellen et al. 1996a are also consistent with this). The distribution of the ratio of nuclear to extended light at K band in all three samples is comparable—consistent with only a few GPS or CSS or 3CR galaxies being “red quasars.” The sources that are red quasars are likely to be obscured by material in the host galaxy rather than an intervening galaxy.

de Vries et al. find the $R - K$ spectral energy distribution (SED) is best-fitted with a metallicity that is consistent with solar and fairly old stellar populations (older than 5 Gyr) implying redshift of formation in the range 5–10 depending on the cosmology. de Vries et al. also find an extra near-IR component is needed that can be modeled by emission from dust at a temperature of ~ 1000 K. If this is the correct interpretation, this may be produced by circumnuclear material heated by the AGN, perhaps in the putative obscuring torus.

8.7. Optical Polarization

Polarization measurements for GPS and CSS sources (mostly quasars) compiled from the literature are shown in Table 7. In general the polarizations are low ($\leq 1\%$). The fact that the GPS/CSS polarizations are so low compared to the polarizations of core-dominated quasars led Wills et al. (1992) to suggest that the GPS and CSS quasars are not as strongly beamed as the core-dominated quasars. These low polarizations are comparable to those found in rest-frame optical observations of extended lobe-dominated radio galaxies (see, e.g., Antonucci 1984; Tadhunter et al. 1992). These observations are consistent with a scattered (in galaxies) or beamed (in quasars) optical component generally being weak or diluted in GPS and CSS sources. However, in marked contrast to this trend is PKS 0116+082, which is a variable and strongly polarized CSS NLR galaxies (Cohen et al. 1997).

Another interesting counterexample is the archetypal compact double source 1934–638. Tadhunter, Shaw, & Morganti (1994) detected optical polarization of $\sim 3.5\%$ in 1934–638. The polarization E -vector is oriented within 10° of perpendicular to the axis of the compact double radio source. Tadhunter et al. suggest that the observed polarization is probably scattered nuclear light, though dichroic absorption in a dust band perpendicular to the radio axis and synchrotron emission as-

TABLE 7
OPTICAL POLARIZATION

Object	Type	ID	% P	θ	Reference	
0023–26	CSS	G	< 2.0	...	1
0116+319	CSS	G	< 1.15	...	2
0116+082	CSS	G	5–15 (var)	30–100	3
0134+329	CSS	Q	1.4 ± 0.2	148 ± 5	4
0153+744	GPS	Q	1.1 ± 0.3	106 ± 7	5
0237–233	GPS	Q	0.3 ± 0.3	...	4
0248+430	GPS	Q	1.01	...	6
0407–658	GPS	Q	0.7 ± 0.4	136 ± 15	4
0500+019	GPS	G	2.9 ± 2.9	...	7
0518+165	CSS	Q	2.2 ± 2.2	...	4
0528–250	GPS	Q	1.16	...	6
0538+498	CSS	Q	2.3 ± 0.9	169 ± 11	5
0552+398	GPS	Q	2.34	...	6
0646+600	GPS	Q	8.6 ± 1.2	118 ± 5	7
0711+356	GPS	Q	1.0 ± 1.0	29 ± 24	5
0738+313	GPS	Q	0.32	...	6
0740+380	CSS	Q	1.18	...	6
0743–006	GPS	Q	0.43	...	6
1143–245	GPS	Q	1.61	...	6
1151–34	CSS	Q	< 0.9	...	1
1250+568	CSS	Q	1.30	...	6
1306–09	CSS	G	6.3 ± 1.3	...	1
1328+254	CSS	Q	0.6 ± 0.7	...	4
1328+307	CSS	Q	1.3 ± 0.5	47 ± 11	4
1345+125	GPS	G	1.44 ± 0.44	66 ± 13	8
1404+286	GPS	Q	0.61	...	2, 6
1416+067	CSS	Q	0.77	...	6
1458+718	CSS	Q	0.93	...	6
1637+626	CSS	G	< 10.4	...	9
1934–638	GPS	G	3.5 ± 0.5	8 ± 3	10
2021+614	GPS	G	0.3 ± 0.3	...	5
2126–158	GPS	Q	0.87	...	6
2149+056	GPS	G	7.8 ± 3.0	30 ± 13	7
2135–20	CSS	Q	< 2.7	...	11
2223+210	GPS	Q	0.44	...	6
2352+495	GPS	G	1.2 ± 2.0	...	5

NOTES.—Optical polarization measurements (primarily V band) from the literature. Includes sources not in the complete samples. In 1345+125 the polarization may be dominated by the Seyfert galaxy, which is merging with the radio galaxy; see Gilmore & Shaw 1986.

REFERENCES.—(1) Morganti et al. 1997; (2) Marchã et al. 1996; (3) Cohen et al. 1997; (4) Impey & Tapia 1990; (5) Impey et al. 1991; (6) Wills et al. 1992, median values of fractional polarization only; (7) Fugmann & Meisenheimer 1988; (8) Young et al. 1996; (9) Tadhunter et al. 1992; (10) Tadhunter et al. 1994; (11) Shaw et al. 1995.

sociated with the radio source are also possible. Polarization observations are needed of other GPS and CSS galaxies, especially those exhibiting the alignment effect (§ 8.3).

8.8. Emission-Line Luminosities

Gelderman & Whittle (1994) present low-dispersion spectra (and high-dispersion spectra of the region around $[\text{O III}] \lambda 5007$) of a sample of 20 CSS sources (both galaxies and quasars). Gelderman & Whittle found that the CSS sources have relatively strong, high equivalent width, high-excitation line emission, with broad, structured $[\text{O III}]$ profiles. They suggest that

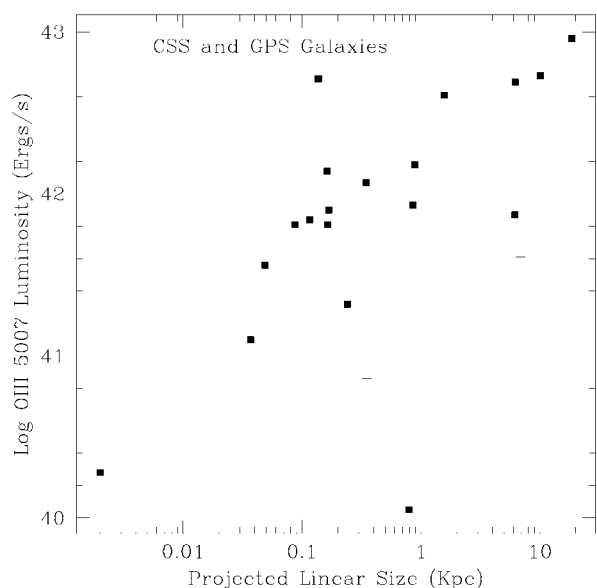


Fig. 19.—[O III] $\lambda 5007$ luminosity vs. projected linear size for a sample of assorted CSS and GPS galaxies (not necessarily from the complete samples). Adapted from Baum et al. (1998). Horizontal lines are upper limits on emission-line luminosity. For these sources without detected emission lines, the redshift is estimated using the R -band Hubble diagram.

these properties are consistent with strong interactions between the radio source and the ambient line-emitting gas.

At this point, there are only a few GPS galaxies with high quality optical spectra (Lawrence et al. 1996), though work in progress should remedy this. Baum et al. (1998) have compiled emission-line data from the literature and work in preparation. The numbers of objects are small, and some sources are included that are not in the complete samples. Given the redshift distribution of the sources, it is not surprising that [O III] $\lambda 5007$ is the most common bright emission line visible in the spectra. Figure 19 shows the [O III] $\lambda 5007$ luminosity plotted against the projected linear size for the Gelderman & Whittle CSS galaxies and assorted GPS galaxies from the literature. Baum et al. (1998) find that the GPS sources tend to have lower line luminosities than the CSS sources.

Readhead et al. (1996b) noted that four CSOs (also included here) were consistent with the relationship between jet power and emission-line luminosity found for large-scale sources by Rawlings & Saunders (1991; see also Baum & Heckman 1989). Baum et al. have compared the CSS and GPS sources with the large-scale sources studied by Zirbel & Baum (1995). In order to do this, Baum et al. have (1) (in cases where $H\alpha + [N II]$ is not available) converted the [O III] fluxes to $H\alpha + [N II]$ using the prescription given by Zirbel & Baum, (2) extrapolated the flux densities to 408 MHz, and (3) scaled the results to their values of H_0 and q_0 . The resulting plot of $H\alpha + [N II]$ luminosity versus total radio power at 408 MHz is shown in Figure 20. Also shown are the Zirbel & Baum fits to the re-

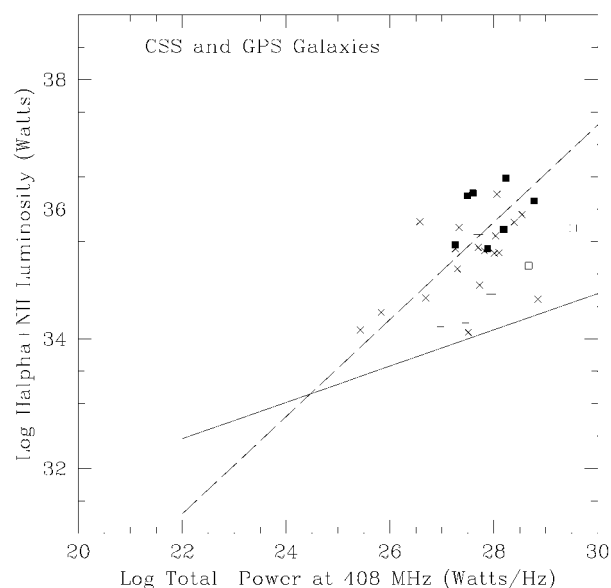


Fig. 20.— $H\alpha + N II$ luminosity vs. total power at 408 MHz (scaled to $H_0 = 50 \text{ km s}^{-1} \text{ Mpc}^{-1}$ for comparison with the results of Zirbel & Baum 1995). Adapted from Baum et al. (1998). The GPS and CSS galaxies detections are represented by crosses and solid squares, respectively. Upper limits to the emission-line luminosity are the horizontal lines and open squares for the GPS and CSS sources, respectively. The dashed and solid lines are the Zirbel & Baum fits to the FR 2 and FR 1 radio galaxies, respectively. Compare with Fig. 9 of Zirbel & Baum.

lationships for FR 2 and FR 1 galaxies. Figure 20 can be compared to Figure 9 of Zirbel & Baum. Baum et al. find that (1) the CSS sources fall on (or even a bit above) the relationship defined by the FR 2 galaxies (cf. Hirst, Jackson, & Rawlings 1996); and (2) the GPS sources have a larger scatter on the emission-line–radio plane than the CSS galaxies or FR 2 sources and extend down to lower emission-line luminosities for a given radio luminosity. These results could be consistent with a model in which at least some of the GPS nuclei are more dust enshrouded than the CSS sources or are intrinsically fainter in ionizing photons for a given radio luminosity. Constraints on radio source evolution (§ 12 and Fanti et al. 1995; Readhead et al. 1996a; O’Dea & Baum 1997) suggest that the GPS sources drop strongly in radio luminosity as they grow. O’Dea & Baum have suggested that some of the GPS sources may evolve into FR 1 sources. If this is the case, then the pre-FR 1 GPS sources may have lower ionizing photon luminosities and emission-line luminosities than the pre-FR 2 GPS sources as the large sources do (see, e.g., Baum, Zirbel, & O’Dea 1995).

There are effects that could in principle influence the relationship between radio and emission-line luminosity. Consider the case where the emission lines are primarily energized by the ionizing nuclear continuum. If the jet thrust and ionizing continuum are constant over the lifetime of the radio sources and the radio luminosity declines by 1–2 orders of magnitude as required in the current evolutionary schemes (Fanti et al.

1995; Readhead 1995; Readhead et al. 1996a; Begelman 1996; O'Dea & Baum 1997), then the ratio of optical line to radio luminosity should increase over the lifetime of the radio source. This would imply that the GPS and CSS sources should have lower optical line luminosities for a given radio luminosity than the large-scale doubles. This is not seen—the CSS sources are at least as bright in emission lines as the extended sources for a given radio luminosity (see also Gelderman 1994). There are several possible implications. (1) Perhaps the simple picture of strong luminosity evolution is not correct. (2) There may be an additional source of ionization in the CSS sources, e.g., shocks generated by the radio source (Bicknell et al. 1997). The broad and structured [O III] profiles seen by Gelderman & Whittle (1994) support such an interaction of the radio source with emission-line gas. (3) The cold gas presumably acquired at the onset of nuclear activity may not yet have settled into a disk perpendicular to the radio source, resulting in a much larger fraction of the gas ionized by either the nuclear continuum or interaction with the radio source. Note that this is also consistent with the alignment effect observed in CSS sources.

In summary, the high emission-line luminosities in CSS and some GPS sources are consistent with an additional source of ionization (interaction with the radio sources) and/or a larger mass for the ionized nebula. The dispersion of emission-line luminosities in GPS sources suggests that at least some sources (1) are very dust enshrouded, (2) are weak sources of ionizing photons, or (3) will evolve into FR 1 sources.

8.9. Emission-Line Diagnostics of Reddening and Density

Very little is currently known about the emission-line properties of the GPS and CSS galaxies. The existing anecdotal evidence is that there is evidence for large reddening and high densities in the NLR of at least some objects (e.g., 2021+614, Bartel et al. 1984a; 1934–638, Fosbury et al. 1987 and Fosbury 1990).

Baker & Hunstead (1995, 1996) have compared composite spectra of different subclasses of quasars from the Molonglo quasar sample. The CSS quasar's steep power-law continuum, the high Balmer decrement, low ratio of Ly α /C IV, and weak 3000 Å bump are all consistent with dust absorption being stronger in the CSS quasars than in the other types. Baker & Hunstead also find that absorption-line systems associated with the quasar are common in CSS sources. In addition, the low ionization narrow lines have large equivalent widths consistent with an additional source of ionization for the gas, e.g., shocks (cf. Bicknell et al. 1997).

On the other hand, Morganti et al. (1997) present optical spectra of seven CSS sources (five with only NLRs and two with broad-line regions, or BLRs) from a southern subset of the Wall & Peacock (1985) sample. Morganti et al. note that two of the objects have large Balmer decrements, but in general they find that the emission-line properties are generally not distinguishable from those of large-scale radio sources in terms

of their [O III] λ 3727 luminosity or their location on diagnostic line-ratio diagrams. They suggest that the emission-line properties do not show any evidence that these are “frustrated” sources.

9. X-RAY PROPERTIES

At this point there are no systematic studies of the X-ray properties of large samples of GPS and CSS sources. The few observations that have been done are nevertheless very interesting and are reviewed below. Observations of a much larger sample with *AXAF* will be necessary before we understand the X-ray properties of CSS and GPS sources. X-ray observations from the literature are summarized in Table 8. Generalizing from the limited data, it appears that the GPS and CSS *quasars* can be very luminous in the X-rays ($L_x \sim 10^{45}$ – 10^{46} ergs s $^{-1}$), consistent with them containing a very powerful central engine. On the other hand, the GPS and CSS *galaxies* tend to be much less luminous than the quasars with luminosities below $L_x \sim 10^{44}$ ergs s $^{-1}$ and in some cases of order $L_x \sim 10^{42}$ ergs s $^{-1}$. The large difference between quasar and galaxy X-ray luminosities is consistent with that seen in the large-scale radio sources (see, e.g., Siebert et al. 1996).

There is evidence for an additional column of X-ray absorbing material (in excess of the Galactic value) in some GPS quasars (Elvis et al. 1994) and the GPS broad-line radio galaxy OQ 208 (Zhang & Marscher 1994). This extra absorption may be associated with high-redshift quasars in general and not just with GPS sources. Elvis et al. estimate the extra column density to be of order 10^{22} cm $^{-2}$. Possible locations for the material include (1) intervening Ly α systems, (2) cluster cooling flows, and (3) material associated with the quasar. Elvis et al. (1994) examine the radio and optical properties of the quasars with extra absorption and suggest that the absorbing material is associated with the quasar. If this is the case, then the absorption may take place in circumnuclear gas on the subkiloparsec scale. Baker, Hunstead, & Brinkmann (1995) detect X-rays from CSS quasars only one-third as often as non-CSS quasars in the Molonglo quasar sample. This could be due to larger absorbing columns in the CSS quasars or to a difference in the quasar spectra. Baker & Hunstead (1996) find associated absorption-line systems to be extremely common in their CSS quasars, suggesting the presence of large columns associated with the quasar.

O'Dea et al. (1996b) obtained sensitive *ROSAT* observations of two GPS galaxies, 1345+125 and 2352+495. The 3σ upper limits to the X-ray luminosity are about $L_x < 3 \times 10^{42}$ ergs s $^{-1}$. The X-ray luminosities are too low to be consistent with emission from a typical Abell cluster but are consistent with the X-ray luminosity of early-type galaxies ($L_x \sim 10^{39}$ – 10^{41} ergs s $^{-1}$, Forman, Jones, & Tucker 1985) and of groups or poor clusters of galaxies with central dominant galaxies ($L_x \sim 10^{41}$ – 10^{43} ergs s $^{-1}$; see, e.g., Kriss, Cioffi, & Canizares 1983). The optical fields around 1345+125 (Hutchings, Johnson, &

TABLE 8
 X-RAY OBSERVATIONS OF CSS AND GPS SOURCES

Object	Type	ID	X-Ray Luminosity (ergs s ⁻¹)	Band (keV)	Reference	Comment
0026+346	GPS	G	7.9 × 10 ⁴³	0.2–2.0	1	OQQ?
0108+388	GPS	G	< 1.0 × 10 ⁴⁴	0.5–4.5	2	
0134+329	CSS	Q	1.0 × 10 ⁴⁵	0.2–2.4	3	
0237–233	GPS	Q	6.6 × 10 ⁴⁶	0.2–4.5	4	
0420–388	GPS	Q	3.4 × 10 ⁴⁶	2–10	5	
0500+019	GPS	G	4.4 × 10 ⁴⁴	0.2–2	1	OQQ
0518+165	CSS	Q	1.5 × 10 ⁴⁵	0.2–2.4	3	
0528–250	GPS	Q	< 3.8 × 10 ⁴⁶	0.2–4.5	4	
0538+498	CSS	Q	4.9 × 10 ⁴⁴	0.5–4.5	2	
0636+680	GPS	Q	4.1 × 10 ⁴⁶	2–10	5	
0738+313	GPS	Q	1.4 × 10 ⁴⁵	0.2–4.5	4	
0740+380	CSS	Q	4.4 × 10 ⁴⁵	0.2–4.5	4	
0758+143	CSS	Q	2.0 × 10 ⁴⁵	0.2–4.5	4	
1127–145	GPS	Q	1.1 × 10 ⁴⁶	0.2–4.5	4	
1250+568	CSS	Q	2.2 × 10 ⁴⁴	0.2–4.5	4	
1416+067	CSS	Q	9.7 × 10 ⁴⁵	0.2–4.5	4	
1442+101	GPS	Q	8.8 × 10 ⁴⁶	0.2–4.5	4	
1328+254	CSS	Q	2.8 × 10 ⁴⁵	0.2–2.4	3	
1328+307	CSS	Q	4.7 × 10 ⁴⁴	0.2–2.4	3	
1345+125	GPS	G	≤ 1.7 × 10 ⁴²	0.2–2	6	Marginal detection ?
1358+624	GPS	G	< 1.8 × 10 ⁴⁴	0.5–4.5	2	
1404+286	GPS	Q	1.0 × 10 ⁴²	0.3–2.5	7	
1458+718	CSS	Q	3.0 × 10 ⁴⁵	0.2–2.4	3	
1517+204	CSS	G	< 4.3 × 10 ⁴⁴	0.7–2.0	8	
1614+051	GPS	Q	2.7 × 10 ⁴⁶	0.2–4.5	4	
1637+626	CSS	G	< 6.5 × 10 ⁴³	0.7–2.0	8	
2000–330	GPS	Q	5.2 × 10 ⁴⁶	2–10	5	
2106–409	GPS	G	2.9 × 10 ⁴⁵	0.2–2	1	OQQ
2126–158	GPS	Q	3.9 × 10 ⁴⁷	2–10	5	X-ray absorption
2223+210	GPS	Q	1.0 × 10 ⁴⁷	0.2–4.5	4	
2352+495	GPS	G	< 1.4 × 10 ⁴²	0.2–2	6	

NOTES.—X-ray observations from the literature. Luminosities are converted to the distance scale used in this review.

REFERENCES.—(1) Kollgaard et al. 1995; (2) Bloom & Marscher 1991; (3) Prieto 1996; (4) Wilkes et al. 1994; (5) Elvis et al. 1994; (6) O’Dea et al. 1996b; (7) Zhang & Marscher 1994; (8) Crawford & Fabian 1996.

Pyke 1988; Baum et al. 1988; Stanghellini et al. 1993) and 2352+495 (O’Dea et al. 1990a) are consistent with such a sparse environment.

O’Dea et al. use the X-ray constraints to show that the pressure from a hot ISM in the host galaxies is orders of magnitude too low to confine the radio sources. If the source advance is not slowed by collisions with clouds (O’Dea et al. 1991; Carvalho 1994, 1998; De Young 1991; Balsara 1991) and the lobes are in ram pressure balance with the hot ISM, then the advance speed (v_a) is given by

$$v_a \geq 0.026c \left(\frac{P_l}{10^{-6} \text{ dyn cm}^{-2}} \right)^{1/2} \left(\frac{n}{1 \text{ cm}^{-3}} \right)^{-1/2}, \quad (7)$$

where P_l is the lobe pressure in dyn cm⁻² and n is the ambient density in cm⁻³ (cf. Readhead et al. 1996b). This suggests that the radio sources are not confined and might expand to become large-scale radio sources (see, e.g., Phillips & Mutel 1982;

Carvalho 1985; Hodges & Mutel 1987; De Young 1993; Fanti et al. 1995; Begelman 1996; Readhead et al. 1996a, 1996b; O’Dea & Baum 1997). Alternatively, the radio sources could be confined by another component of the ISM, e.g., dense, *cold* gas. O’Dea et al. also show that the X-ray luminosity in 1345+125 and 2352+495 is too low to be consistent with large cooling flows in the host galaxies and/or surrounding ICM. A conservative upper limit to the mass accretion rate is a few $M_\odot \text{ yr}^{-1}$.

9.1. Are the AGNs in GPS Radio Galaxies Obscured?

The lack of a detection of the central engine in X-rays in the GPS sources could be because either (1) the AGNs are intrinsically weak in X-rays or (2) the soft X-rays to which these *ROSAT* observations are sensitive are obscured by large columns of cool gas surrounding the nuclei. O’Dea et al. (1996b) estimate that intrinsic absorbing columns of a few

TABLE 9
COLD GAS CONTENT OF THE HOST GALAXIES

Object	Type	ID	Gas Mass (M_{\odot})	Method	References	Comment
0116+319	CSS	G	2×10^{10}	Dust at 1 mm	1	1
0116+319	CSS	G	2×10^8	H I absorption	2, 3	2, 3
0134+329	CSS	Q	3×10^{10}	CO (1 \rightarrow 0)	4	
1345+125	GPS	G	7×10^{10}	CO (1 \rightarrow 0)	5	4
1345+125	GPS	G	1×10^8	H I absorption	6	2, 3
1404+286	GPS	Q	1×10^{11}	Dust at IR	7	1
1404+286	GPS	Q	$< 2 \times 10^7$	H I absorption	2	2, 3
1718-649	GPS	G	3×10^{10}	H I emission	8	
1934-638	GPS	G	$< 5 \times 10^{10}$	CO (1 \rightarrow 0)	9	
2352+495	GPS	G	$< 3 \times 10^8$	CO (1 \rightarrow 0) absorption	10	2, 5
2352+495	GPS	G	$< 4 \times 10^9$	H I absorption	10	2

NOTES.—Estimates of the mass of cold gas in the host galaxies, taken from the literature and scaled to our distance scale. Comments are as follows: (1) Assumes a gas-to-dust ratio of 100. (2) Assumes that the gas with the estimated column density is within 1 kpc of the nucleus, similar to ULIRGs. (3) Assumes a spin temperature of 100. (4) In 1345+125 the CO may be associated with the Seyfert nucleus instead of the radio nucleus (see, e.g., Dickey et al. 1990). (5) The nondetection of CO absorption may be affected by radiative excitation (Maloney et al. 1994).

REFERENCES.—(1) Knapp & Patten 1991; (2) van Gorkom et al. 1989; (3) Mirabel 1990, Conway 1996; (4) Scoville et al. 1993, Wink et al. 1997; (5) Mirabel et al. 1989; (6) Mirabel 1989; (7) Knapp et al. 1990; (8) Véron-Cetty et al. 1995, Fosbury et al. 1977; (9) O’Dea et al. 1994b; (10) Readhead et al. 1996b.

times 10^{22} cm^{-2} are sufficient to hide X-ray luminosities of between 10^{43} and 10^{44} ergs s^{-1} . The existence of a powerful AGN that emits most of its energy in the IR is consistent with the amount of reprocessed luminosity observed in the mid-IR (Heckman et al. 1994) and the evidence for hot dust in the near-IR (de Vries et al. 1998c). *ASCA* observations are in progress to determine whether there is indeed a luminous hidden nucleus.

10. THE GAS CONTENT OF THE HOST GALAXIES

There are several pieces of evidence that suggest that the host galaxies of the GPS and CSS galaxies may contain significant amounts of dense gas. (1) The radio sources are strongly depolarized and some sources show very large Faraday rotation measures (§ 4). (2) The emission-line nebula in some sources show evidence for strong reddening and high densities (§ 8.9). And some GPS galaxies seem underluminous in emission lines (§ 8.8). (3) The CSS sources show the alignment effect (§ 8.3). (4) Some GPS quasars show evidence for large columns of X-ray absorbing gas and some GPS galaxies may have large columns that obscure the soft X-rays (§ 9). (5) The radio morphologies are often distorted, suggesting interaction with dense clouds (§ 3).

The presence of dense gas in the host galaxies has implications for how the radio sources will evolve (see, e.g., Bicknell et al. 1997). Interaction of the radio source with dense gas can slow the propagation of the jets (see, e.g., Balsara 1991; O’Dea et al. 1991; De Young 1993; Carvalho 1994, 1998) or possibly even “frustrate” them so they are unable to escape the subkiloparsec scales (see, e.g., Wilkinson et al. 1984a; van Breugel

et al. 1984b; O’Dea et al. 1991). Thus, I review here the evidence for direct detection of dense gas in the host galaxies of GPS and CSS sources.

For comparison, “normal” elliptical galaxies tend to have masses of cold gas in the range 10^7 – $10^8 M_{\odot}$ (see, e.g., Lees et al. 1991), while the very gas-rich ultraluminous *IRAS* galaxies (ULIRGs) have gas masses in the range 10^9 – $5 \times 10^{10} M_{\odot}$ (see, e.g., Sanders, Scoville, & Soifer 1991). Powerful radio galaxies tend to have cold gas masses that overlap both those ranges at about 10^8 – $10^{10} M_{\odot}$ (see, e.g., Knapp, Bies, & van Gorkom 1990; Mazzarella et al. 1993; O’Dea et al. 1994b; Evans et al. 1996).

Estimates (or limits) on the mass of cold atomic or molecular gas in GPS and CSS sources are given in Table 9. Estimates of molecular gas mass from either CO or thermal IR are very high for the few sources that have been detected and are in the range 10^{10} – $10^{11} M_{\odot}$. These are close to the upper end of the distribution of gas masses. Given the small numbers and the likelihood of strong selection effects, this result should be viewed with caution. However, it does indicate that at least some GPS and CSS sources are in very gas-rich host galaxies. As a counterexample, the CSO 2352+495 seems relatively gas poor, though this could be due to radiative excitation of the gas as discussed by Readhead et al. (1996b).

Conway (1996) notes that four out of 28 large-scale radio galaxies observed by van Gorkom et al. (1989), and three out of five CSOs show H I absorption. The much higher detection fraction in the CSOs could be due to them having much more gas in their nuclei than the large-scale sources. An alternate explanation favored by Conway is that the CSOs are better

suitable to probe H I disks in the nuclei because of their symmetric and high surface brightness.

Curiously, the estimates/limits of atomic hydrogen are significantly less than those for molecular hydrogen. This suggests that (1) the gas is predominantly molecular, (2) most of the atomic gas avoids the line of sight to the radio source, or (3) the mass of molecular gas is overestimated.

11. WHAT ARE THE CSS/GPS SOURCES?

The GPS and CSS sources have remained outside the mainstream paradigm for powerful radio sources since their discovery. Below I review the three main hypotheses for their nature. These ideas were all suggested to explain the facts that these sources are (1) compact, (2) very radio luminous (as powerful as the large 3CR classical doubles), and (3) a significant fraction of the radio source population. The simplest hypothesis, that the compact sources evolve with constant radio luminosity and constant advance speed into the large ones, fails because of their large relative numbers, i.e., if the GPS sources have lifetimes that are 10^{-3} of the large classical doubles, then they should also be 10^{-3} less numerous, yet they are at least 10% of the bright radio source population.

11.1. Transient Sources

Readhead et al. (1994) suggested that the CSOs might be transient events with relatively short lifetimes of $\lesssim 10^4$ yr (see also Readhead et al. 1996b). Given the short lifetimes of the implied CSO phase, most elliptical galaxies with luminosities of at least $0.3L_*$ or more would pass through a CSO phase at least once. Since we now know that the host galaxies of the CSO (and in general GPS) galaxies are L_* or brighter, this decreases the possible parent population of CSOs and increases the number of times each galaxy must go through a CSO phase. In its current simple form, this hypothesis lacks predictive power. At this point there are no strong arguments either for or against it, other than Occam's razor.

11.2. Old, Confined (Frustrated) Sources

One explanation for the large relative numbers of GPS and CSS sources compared with the large classical doubles is that they have similar ages. This requires that the GPS and CSS sources are kept compact for a significant fraction of their lifetimes. Partly because of radio morphologies, which suggested that the sources were undergoing strong interaction, it was suggested that the CSS sources were confined by interaction with dense gas in their environment (see, e.g., Wilkinson et al. 1984a; van Breugel et al. 1984b). O'Dea et al. (1991) suggested that the GPS sources could be confined by interaction with dense clouds in their environment. Gopal-Krishna (1995) suggested that distortions of the central gaseous torus during a merger could cause the jet to collide with dense gas. As discussed in § 10, there are now multiple pieces of evidence for dense gas in the environments of GPS and CSS sources.

Gopal-Krishna & Wiita (1991) suggested that CSS sources are members of an intrinsically less radio-luminous source population, and that their radio luminosity is enhanced to its observed values because of its dense environment. They note that work by Eilek & Shore (1989) shows that the efficiency of conversion of jet kinetic energy into radio luminosity can vary depending on age and environment of the source. Gopal-Krishna & Wiita suggest that the efficiency is a factor of about 6 higher in the CSS sources and that since they are intrinsically weaker by this factor, their environments are sufficient to confine them.

There is evidence that the jet kinetic energy and the flux of ionizing photons from the nucleus are proportional (see, e.g., Baum & Heckman 1989; Rawlings & Saunders 1991; Baum, Zirbel, & O'Dea 1995). This would suggest that the CSS sources should have a ratio of optical line to radio luminosity, which is low compared to the large-scale classical doubles. However, this is not seen (§ 8.8). In addition, the ratio of MFIR to radio luminosity should also be low compared to the large-scale classical doubles, and again this is not seen (§ 7). Thus, the hypothesis that they are intrinsically fainter but more efficient (by factors of more than a few) is not supported by the current data. However, if the optical line emission and MFIR emission can also be enhanced in the CSS sources (e.g., through interaction with the radio source or the presence of additional gas and dust in the host galaxy), such an increase in efficiency would be permitted.

De Young (1993) carried out simple numerical hydrodynamical simulations of a jet propagating in a smooth medium and in a medium with a fine "mist" of dense clouds (cloud radius of 1 pc). Both cases gave similar results, and De Young found that most CSS sources could be confined if the average density in the ISM were $\sim 1-10 \text{ cm}^{-3}$. The most powerful sources would require even higher densities for confinement. For the case of a smooth medium with constant density, the total gas mass required is

$$M = 1 \times 10^9 M_{\odot} \left(\frac{n_0}{10 \text{ cm}^{-3}} \right) \left(\frac{R}{1 \text{ kpc}} \right)^3, \quad (8)$$

where R is the radius, and n_0 is the density. And for the case of a density varying with radius as R^{-2} , which describes steady infall, the enclosed mass is

$$M = 3 \times 10^9 M_{\odot} \left(\frac{n_1}{10 \text{ cm}^{-3}} \right) \left(\frac{R}{1 \text{ kpc}} \right), \quad (9)$$

where n_1 is the density at 1 kpc. It seems unlikely that a uniform dense medium of mass $10^{12} M_{\odot}$ extends out to the 10 kpc required to confine CSS sources, though the CSS sources may well interact with clouds of gas that are infalling into the center of the galaxy.

Carvalho (1994, 1998) has presented a simple analytic model of jet interactions with dense clouds and concludes that inter-

action with dense clouds would slow down the jet more than propagation through a smooth medium with the same average density. He finds that interaction with clouds could result in GPS sources having lifetimes as old as that of the large-scale doubles. Carvalho suggests that the GPS sources could be confined by a clumpy medium with a mass of $\sim 10^9\text{--}10^{10} M_{\odot}$ on the scale of hundreds of pc. Such masses are in general consistent with the small number of observations in Table 9 and are similar to those observed in the ULIRGs. Thus, it appears that interactions with dense gas could confine the radio sources. However, it is not yet clear whether sufficient gas generally exists in these sources to achieve confinement.

If the presence of large amounts of dense gas in the host galaxies is confirmed via sensitive observations of a large number of objects, this would support the “frustrated” source hypothesis. A scenario would be that an encounter with a gas-rich companion has resulted in large amounts of gas being accreted by the host galaxy. As shown in numerical simulations (Hernquist 1989; Barnes & Hernquist 1991; Bekki & Noguchi 1994; Hernquist & Mihos 1995) and observed in the ULIRGs (see, e.g., Scoville et al. 1994), the gas sinks to the center of the galaxy (to subkiloparsec scales). The gas can then trigger/feed the nuclear activity and confine the resulting radio source. The accumulation of dense gas in the nucleus should also trigger a large starburst (see, e.g., Sanders et al. 1988; Norman & Scoville 1988; Mihos & Hernquist 1994). The clouds will confine the radio source for the shorter of the following times: (1) the time for the jet to push aside or drill through the clouds (see, e.g., De Young 1991; Carvalho 1994, 1998) or (2) the time it takes for a starburst-driven superwind to disperse the clouds (see, e.g., Heckman, Armus, & Miley 1990). These timescales can both be of order $\gtrsim 10^7$ yr and will result in confinement of GPS sources to the subkiloparsec scale for most if not all of their lifetime. One prediction of this scenario is that there should be a large starburst in GPS and CSS sources. GPS galaxies have $r - i$ colors consistent with passively evolving ellipticals and do not show significant amounts of blue light from young stars. High-resolution near-IR imaging is needed to detect dust-obscured starbursts.

11.3. Young, Evolving Sources

The idea that GPS sources are young was suggested by Shklovsky (1965) for the case of 1934–638 and by Blake (1970) for an early sample of GPS sources based on their peaked spectra and compact size. Readhead & Hewish (1976) suggested that if Scheuer’s (1974) beam model is correct, the small 3CR sources should evolve into the larger ones. Phillips & Mutel (1982) pointed out the simple symmetric radio structure in four GPS radio galaxies (then called compact doubles) and suggested that they were young versions of the large classical doubles. Carvalho (1985) presented a simple analytic model (based on Scheuer 1974) for the evolution of GPS sources that guided much of the later discussion. Mutel and

collaborators (Hodges & Mutel 1987; Mutel & Phillips 1988; Mutel, Su, & Song 1990) applied Carvalho’s model to small samples of GPS, CSS, and large-scale doubles and suggested that these sources represented an evolutionary sequence. Begelman (1996) presented an analytic self-similar evolution model for CSOs that was adapted by Bicknell et al. (1997) to explain the relationship between the radio source and the emission-line nebula. Saikia et al. (1996) presented simulations of self-similar radio source models, while De Young (1996) has presented simulations of non-self-similar jet evolution, both of which seem to produce consistent evolution. Snellen et al. (1998) have presented a relativistic plasmon model for GPS sources.

The hypothesis that the GPS sources evolve through a CSS stage on their way to become large sources is in general consistent with observations of CSS sources (Fanti et al. 1990b, 1995), CSOs (Readhead 1995; Readhead et al. 1996a, 1996b), and combined samples of GPS and CSS sources (O’Dea & Baum 1997) and comparisons of these samples with large-scale powerful sources. Bremer, Fabian, & Crawford (1997) have suggested that radio sources in central cluster galaxies with cooling flows are GPS sources when young. However, the converse is not necessarily true, i.e., it is clear that not all GPS sources are in cooling flows (§ 9).

The main arguments in favor of evolution are the following. (1) The GPS and CSS sources have morphologies similar to those of the large-scale sources (§ 3). (2) Although there is gas in their environments, there is currently no compelling evidence that there is *enough* dense gas to confine the majority of the GPS and CSS sources (§§ 10 and 11.2). (3) In the absence of confinement by cold gas, the internal pressure in GPS and CSS radio sources is sufficient to allow expansion in ram pressure balance with expected ISM densities at velocities of a few to 10% of the speed of light (Phillips & Mutel 1982; Mutel, Hodges, & Phillips 1985; Fanti et al. 1990b; Readhead 1995; Readhead et al. 1996b). (4) The GPS and CSS sources do not show evidence for a large halo of diffuse emission (i.e., a “wastebasket”), which is expected if they are confined for their lifetimes (Readhead et al. 1996b).

At the present time, the weight of the evidence seems to favor the young and evolving source model for GPS and CSS sources. However, the answer is not definitive, and in fact more than one explanation may apply to this population of sources.

12. CONSTRAINTS ON EVOLUTION

If the GPS and CSS sources do indeed evolve into larger sources, then their global properties as well as those of the large-scale sources (§ 6) must constrain their evolution (Carvalho 1985; Fanti et al. 1995; Begelman 1996; Readhead et al. 1996a; O’Dea & Baum 1997). Fanti et al. (1995) have given the relationship between the observed variation of number with linear size, and that along evolutionary tracks assuming power-law dependencies of the parameters. Fanti et al. assume that

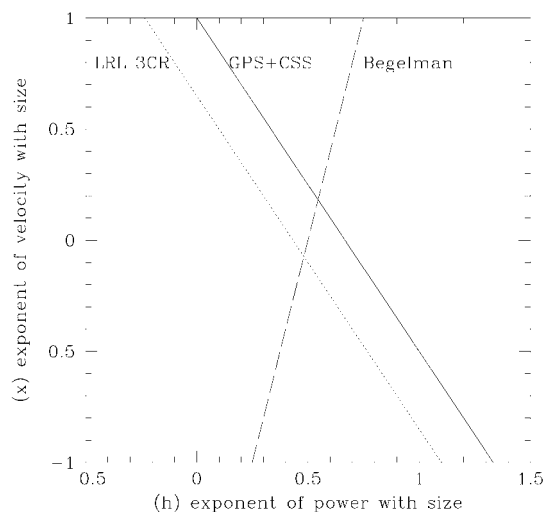


FIG. 21.—Constraints on evolution models from $N(l)$ vs. l . The GPS and CSS sources are shown by the solid line, and the LRL 3CR sources by the dotted line. The dashed line is the prediction from the Begelman model. Adapted from O’Dea & Baum (1997).

velocity depends on linear size l as $v \propto l^x$, and power on linear size as $P \propto l^{-h}$ and the luminosity function is $\rho(P) \propto P^{-b}$. Then the relationship between the exponents is given by

$$x = m - hb, \quad (10)$$

where m is the exponent on the observed relation $dN/dl \propto l^{-m}$, $m = 1 - \delta$, and δ is the slope measured on Figure 13 (see also O’Dea & Baum 1997).

The constraints from the data (Fig. 13) are shown in Figure 21 assuming slopes of 0 and 0.4 for the GPS/CSS and large-scale sources, respectively. As discussed in § 6, depending on which points are chosen, a range of slopes can fit the data. Fits to all the data with a single line result in a slope near 0.2, which is bracketed by the values of 0 and 0.4 shown in Figure 21. As an illustration of the constraints that can be placed on evolution, I also show the prediction of the Begelman (1996) self-similar source model. The location of the intersection between the constraints and the model are where Begelman’s model is consistent with the data.

The observations are consistent with a picture in which the sources expand with constant velocity, and the radio power drops as roughly $P \propto l^{-0.5}$. A possible evolutionary track is illustrated in Figure 22. The implied drop of radio power over the lifetime of the sources is at least an order of magnitude and suggests that at least some of the GPS and CSS sources will evolve into lower luminosity FR 1 radio sources.

Note that if the suggested flatter slope of N versus l (Fig. 13) for the GPS and CSS is correct, this has implications for the evolution of the sources. Reynolds & Begelman (1997) have suggested that the radio sources are intermittent on time-

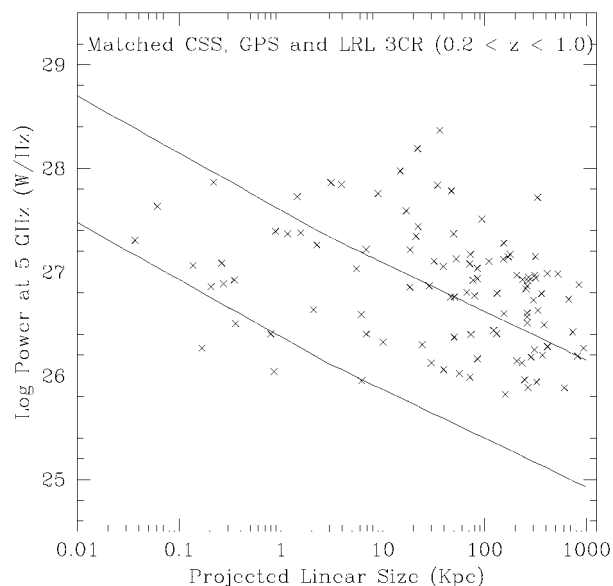


FIG. 22.—Illustrative plot of possible evolutionary tracks on the P vs. l plot. Adapted from O’Dea & Baum (1997).

scales of $\sim 10^4$ – 10^5 yr.¹¹ Alternatively, the flatter slope could mean that for a given variation of velocity with linear size, the GPS and CSS sources decline in radio power somewhat more rapidly than the large-scale sources. O’Dea & Baum (1997) have suggested that this is due to a drop in the efficiency of conversion of jet kinetic energy into radio luminosity as the source expands and ages (cf. Eilek & Shore 1989; Gopal-Krishna & Wiita 1991). As discussed in § 11.2, a modest increase in efficiency for the smaller sources is not ruled out by the current data.

13. CONCLUDING REMARKS

After almost two decades of work on the GPS and CSS sources we have obtained a much clearer picture of what their essential properties are. However, there is still controversy about their origin and relationship to the large-scale powerful sources. In this section I give my own perspective on these enigmatic sources.

The idea that they are some kind of *exotic* class of radio source unrelated to the large sources (i.e., transient sources) is probably not completely ruled out. But in my opinion, the similarities of many of their global properties, including optical host galaxies, emission-line properties, and near-IR properties, to those of the large sources suggest that they are similar types of AGNs in similar types of galaxies and are indeed related to the large sources. This is not to say that the GPS/CSS sources do not hold a few surprises for us.

It seems clear that the GPS/CSS radio sources do interact

¹¹ Intermittence was previously suggested by Baum et al. (1990) to explain the GPS sources with extended radio structure.

with their ambient medium, and much more strongly than do large sources at low and intermediate redshifts. However, at this point, the “smoking gun” of large gas masses ($\geq 10^{10} M_{\odot}$) in the host that would imply confinement/frustration has not been found. However, only a handful of objects have been searched carefully (§ 10). As we all know, absence of evidence does not mean evidence of absence. So it is important to conduct deep searches for gas in a significant number of GPS and CSS sources. Work in progress with the new low-frequency receivers at WSRT should help answer this question.

At the present time, the hypothesis that is not ruled out by any data is that the GPS and CSS sources are young versions of the large radio sources. The fact that many of the global properties of GPS/CSS sources are similar to those of the large sources supports this. In addition, the striking resemblance of the radio morphologies, especially those of the CSOs, also argues for an evolutionary relationship.

If true, this is very exciting, since we will finally be able to use samples of GPS/CSS in combination with samples of large sources to place constraints on the evolution of radio sources. The current analysis suggests a significant decline in radio luminosity as the sources evolve. Thus, the GPS and CSS in the bright samples studied so far will evolve into intermediate luminosity radio sources. If this is the case, the progenitors of the LRL classical doubles have not been found. This may be because they are so rare, i.e., we expect 0.1% of the population to be visible in the GPS state at any time, and/or because the very powerful sources have radio spectra that peak above 5 GHz when they are young.

14. FUTURE WORK

There are many pieces of the puzzle still needed to clarify the properties of the GPS and CSS sources and their place in the powerful radio source paradigm.

1. Fainter samples of sources should be studied to fill in the P - l plane.
2. The polarization properties and Faraday RMs of the sources need to be determined with high spatial resolution.
3. High dynamic range radio images of GPS sources (especially quasars) need to be obtained to determine the true range of morphology and to locate the cores.
4. Deep multicolor optical imaging of the hosts and envi-

ronments of GPS and CSS and comparison samples of large-scale radio sources is needed to confirm whether the host galaxies and clustering environments are similar in these objects.

5. Sensitive near-far-IR observations should be obtained to determine the bolometric luminosity and IR colors in order to constrain the stellar populations, the AGN, and its circumnuclear environment.

6. Searches for cold gas via CO and 21 cm H I are needed to determine the gas content of the host galaxies and determine whether some objects could be “frustrated.”

7. Sensitive high spatial resolution and high dispersion optical spectra are needed to study the kinematics of the emission-line gas and determine its relationship to the radio source. Combined with broadband colors and polarimetry, the spectra will also elucidate the nature of the aligned component in CSS sources.

8. X-ray observations of complete samples of sources should be obtained in order to determine the strength of the central AGN, the columns of any obscuring material, and the nature of the clustering environments.

Much theoretical work is needed on how radio sources should evolve including the evolution of the relativistic particles, magnetic fields, and efficiency.

I am grateful to many colleagues who provided reprints, preprints, and information in advance of publication; to my collaborators, especially Stefi Baum and Carlo Stanghellini; and to Wim de Vries for permission to present the results of work in progress. Thanks are due to Stefi Baum, Wim de Vries, Greg Taylor, Anton Koekemoer, Carla and Roberto Fanti, and Carlo Stanghellini for comments on the manuscript. Wim de Vries helped with the figures. I would like to thank Harvey Butcher and the Netherlands Foundation for Research in Astronomy for hospitality during which this review was begun. This research made use of (1) the NASA/IPAC Extragalactic Database (NED), which is operated by the Jet Propulsion Laboratory, California Institute of Technology, under contract with the National Aeronautics and Space Administration, and (2) NASA’s Astrophysics Data System Abstract Service.

REFERENCES

- Aizu, K., Inoue, M., Tabara, H., & Kato, T. 1990, in IAU Symp. 140, Galactic and Intergalactic Magnetic Fields, ed. R. Beck, P. P. Kronberg, & R. Wielebinski (Dordrecht: Kluwer), 472
- Akujor, C. E., & Garrington, S. T. 1995, A&AS, 112, 235
- Akujor, C. E., Porcas, R. W., & Smoker, J. V. 1996, A&A, 306, 391
- Akujor, C. E., Spencer, R. E., & Saikia, D. J. 1991a, A&A, 249, 337
- Akujor, C. E., Spencer, R. E., & Wilkinson, P. N. 1990, MNRAS, 244, 362
- Akujor, C. E., Spencer, R. E., Zhang, F. J., Davis, R. J., Browne, I. W. A., & Fanti, C. 1991b, MNRAS, 250, 215
- Akujor, C. E., Spencer, R. E., Zhang, F. J., Fanti, C., Lüdke, E., & Garrington, S. T. 1993, A&A, 274, 752
- Allen, L. R., Anderson, B., Conway, R. G., Palmer, H. P., Reddish, V. C., & Rowson, B. 1962, MNRAS, 124, 477
- Aller, M. F., Aller, H. D., & Hughes, P. A. 1992, ApJ, 399, 16
- Antonucci, R. R. J. 1984, ApJ, 278, 499

- Bååth, L. 1987, in *Superluminal Radio Sources*, ed. J. A. Zensus & T. J. Pearson (Cambridge: Cambridge Univ. Press), 206
- Baker, J. C., & Hunstead, R. W. 1995, *ApJ*, 452, L95; erratum 461, L59
- . 1996, in *Proc. Second Workshop on Gigahertz Peaked-Spectrum and Compact Steep-Spectrum Radio Sources*, ed. I. A. G. Snellen, R. T. Schilizzi, H. J. A. Röttgering, & M. N. Bremer (Leiden: Leiden Obs.), 166
- Baker, J. C., Hunstead, R. W., & Brinkmann, W. 1995, *MNRAS*, 277, 553
- Baldwin, J. E. 1982, in *IAU Symp. 97, Extragalactic Radio Sources*, ed. D. S. Heeschen & C. M. Wade (Dordrecht: Reidel), 21
- Balsara, D. S. 1991, Ph.D. thesis, Univ. Illinois
- Barnes, J. E., & Hernquist, L. E. 1991, *ApJ*, 370, L65
- Bartel, N., et al. 1984b, *ApJ*, 279, 116
- Bartel, N., Shapiro, I. I., Huchra, J. P., & Kühr, H. 1984a, *ApJ*, 279, 112
- Barthel, P. D. 1986, in *IAU Symp. 119, Quasars*, ed. G. Swarup & V. K. Kapahi (Dordrecht: Reidel), 181
- Barthel, P. D., Pearson, T. J., & Readhead, A. C. S. 1988, *ApJ*, 329, L51
- Baum, S. A., & Heckman, T. 1989, *ApJ*, 336, 702
- Baum, S. A., Heckman, T., Bridle, A., van Breugel, W., & Miley, G. 1988, *ApJS*, 68, 643
- Baum, S. A., O'Dea, C. P., Murphy, D. W., & de Bruyn, A. G. 1990, *A&A*, 232, 19
- Baum, S. A., Zirbel, E. L., & O'Dea, C. P. 1995, *ApJ*, 451, 88
- Baum, S. A., et al. 1998, in preparation
- Begelman, M. C. 1996, in *Cygnus A: Study of a Radio Galaxy*, ed. C. Carilli & D. Harris (Cambridge: Cambridge Univ. Press), 209
- Begelman, M. C., & Cioffi, D. F. 1989, *ApJ*, 345, L21
- Bekki, K., & Noguchi, M. 1994, *A&A*, 290, 7
- Bicknell, G., Dopita, M. A., & O'Dea, C. P. 1997, *ApJ*, 485, 112
- Biretta, J. A., Schneider, D. P., & Gunn, J. E. 1985, *AJ*, 90, 2508
- Blake, G. M. 1970, *Astrophys. Lett.*, 6, 201
- Bloom, S. D., & Marscher, A. P. 1991, *ApJ*, 366, 16
- Bolton, J. G., Gardner, F. F., & Mackey, M. B. 1963, *Nature*, 199, 682
- Bremer, M. N., Fabian, A. C., & Crawford, C. S. 1997, *MNRAS*, 284, 213
- Bremer, M. N., & Snellen, I. A. G. 1996, in *Proc. Second Workshop on Gigahertz Peaked-Spectrum and Compact Steep-Spectrum Radio Sources*, ed. I. A. G. Snellen, R. T. Schilizzi, H. J. A. Röttgering, & M. N. Bremer (Leiden: Leiden Obs.), 131
- Bridle, A. H., Fomalont, E. B., & Cornwell, T. J. 1981, *AJ*, 86, 1294
- Bruzual, G. A., & Charlot, S. 1993, *ApJ*, 405, 538
- Burns, J. O., Owen, F. N., & Rudnick, L. 1979, *AJ*, 84, 1683
- Carlberg, R. G. 1990, *ApJ*, 350, 505
- Carvalho, J. C. 1985, *MNRAS*, 215, 463
- . 1994, *A&A*, 292, 392
- . 1998, *A&A*, 329, 845
- Cawthorne, T. V., Wardle, J. F. C., Roberts, D. H., & Gabuzda, D. C. 1993a, *ApJ*, 416, 519
- Cawthorne, T. V., Wardle, J. F. C., Roberts, D. H., Gabuzda, D. C., & Brown, L. F. 1993b, *ApJ*, 416, 496
- Cersosimo, J. C., Santos, M. L., Cintrón, S. I., & Quiniento, Z. M. 1994, *ApJS*, 95, 157
- Chambers, K. C., Miley, G. K., & van Breugel, W. 1987, *Nature*, 329, 604
- Charlot, S., & Bruzual, G. A. 1991, *ApJ*, 367, 126
- Charlot, S., Worthey, G., & Bressan, A. 1996, *ApJ*, 457, 625
- Cohen, M. H., Vermeulen, R. C., Ogle, P. M., Tran, H. D., & Goodrich, R. W. 1997, *ApJ*, 484, 193
- Conway, J. E. 1996, in *Proc. Second Workshop on Gigahertz Peaked-Spectrum and Compact Steep-Spectrum Radio Sources*, ed. I. A. G. Snellen, R. T. Schilizzi, H. J. A. Röttgering, & M. N. Bremer (Leiden: Leiden Obs.), 198
- Conway, J. E., Myers, S. T., Pearson, T. J., Readhead, A. C. S., Unwin, S. C., & Xu, W. 1994, *ApJ*, 425, 568
- Conway, J. E., Pearson, T. J., Readhead, A. C. S., & Unwin, S. C. 1990a, in *Proc. NRAO Workshop on Parsec-Scale Radio Jets*, ed. J. A. Zensus & T. J. Pearson (Cambridge: Cambridge Univ. Press), 167
- Conway, J. E., Pearson, T. J., Readhead, A. C. S., Unwin, S. S., Xu, W., & Mutel, R. L. 1992, *ApJ*, 396, 62
- Conway, J. E., Unwin, S. C., Pearson, T. J., Readhead, A. C. S., & Xu, W. 1990b, in *Proc. Dwingeloo Workshop on Compact Steep-Spectrum and GHz Peaked-Spectrum Radio Sources*, ed. C. Fanti, R. Fanti, C. P. O'Dea, & R. T. Schilizzi (Bologna: Istituto di Radioastron.), 157
- Conway, R. G., Kellermann, K. I., & Long, R. J. 1963, *MNRAS*, 125, 313
- Cooray, A. R., Grego, L., Holzapfel, W. L., Joy, M., & Carlstrom, J. E. 1998, *AJ*, in press
- Cotton, W. D., Dallacasa, D., Fanti, C., Fanti, R., Foley, A. R., Schilizzi, R. T., & Spencer, R. E. 1997a, *A&A*, 325, 493
- Cotton, W. D., Fanti, C., Fanti, R., Dallacasa, D., Foley, A. R., Schilizzi, R. T., & Spencer, R. E. 1997b, *A&A*, 325, 479
- Cotton, W. D., Feretti, L., Giovannini, G., Venturi, T., Lara, L., Marcaide, J., & Wehrle, A. E. 1995, *ApJ*, 452, 605
- Cotton, W. D., Owen, F. N., & Mahoney, M. J. 1989, *ApJ*, 338, 37
- Crawford, C. S., & Fabian, A. C. 1996, *MNRAS*, 282, 1483
- Crawford, T., Marr, J., Partridge, B., & Strauss, M. A. 1996, *ApJ*, 460, 225
- Dahari, O. 1984, *AJ*, 89, 966
- . 1985a, *AJ*, 90, 1772
- . 1985b, *ApJS*, 57, 643
- Dallacasa, D., Fanti, C., & Fanti, R. 1993, in *Jets in Extragalactic Radio Sources*, ed. H.-J. Röser & K. Meisenheimer (Heidelberg: Springer), 27
- Dallacasa, D., Fanti, C., Fanti, R., Schilizzi, R. T., & Spencer, R. E. 1995, *A&A*, 295, 27
- Dallacasa, D., & Stanghellini, C. 1990, in *Proc. Dwingeloo Workshop on Compact Steep-Spectrum and GHz Peaked-Spectrum Radio Sources*, ed. C. Fanti, R. Fanti, C. P. O'Dea, & R. T. Schilizzi (Bologna: Istituto di Radioastron.), 224
- Daly, R. A. 1990, *ApJ*, 355, 416
- . 1992, *ApJ*, 386, L9
- de Bruyn, A. G. 1990, in *Proceedings of the Dwingeloo Workshop Compact Steep-Spectrum and GHz Peaked-Spectrum Radio Sources*, ed. C. Fanti, R. Fanti, C. P. O'Dea, & R. T. Schilizzi (Bologna: Istituto di Radioastron.), 206
- De Koff, S., Baum, S. A., Biretta, J., Golombek, D., Macchetto, F. D., McCarthy, P. J., Miley, G. K., & Sparks, W. B. 1996, *ApJS*, 107, 621
- de Vries, W. H. 1995, Masters thesis, Univ. Groningen
- de Vries, W. H., Barthel, P. D., & Hes, R. 1995, *A&AS*, 114, 259
- de Vries, W. H., Barthel, P. D., & O'Dea, C. P. 1997a, *A&A*, 321, 105
- de Vries, W. H., et al. 1997b, *ApJS*, 110, 191
- de Vries, W. H., O'Dea, C. P., Baum, S. A., & Barthel, P. D. 1998a, in preparation
- de Vries, W. H., O'Dea, C. P., Baum, S. A., Lehnert, M., Perlman, E., Stocke, J., Elston, R., & Rector, T. 1998b, *ApJ*, submitted
- de Vries, W. H., O'Dea, C. P., Baum, S. A., Perlman, E., Lehnert, M., & Barthel, P. D. 1998c, *ApJ*, submitted

- De Young, D. S. 1989, *ApJ*, 342, L59
 ———. 1991, *ApJ*, 371, 69
 ———. 1993, *ApJ*, 402, 95
 ———. 1996, in *Proc. Second Workshop on Gigahertz Peaked-Spectrum and Compact Steep-Spectrum Radio Sources*, ed. I. A. G. Snellen, R. T. Schilizzi, H. J. A. Röttgering, & M. N. Bremer (Leiden: Leiden Obs.), 275
 ———. 1997, *ApJ*, 490, L55
- Dey, A., & van Breugel, W. J. M. 1994, *AJ*, 107, 1977
- di Serego Alighieri, S., Danziger, I. J., Morganti, R., & Tadhunter, C. N. 1994, *MNRAS*, 269, 998
- Dickson, R., Tadhunter, C., Shaw, M., Clark, N., & Morganti, R. 1995, *MNRAS*, 273, L29
- Dickey, J. M., Planesas, P., Mirabel, I. F., & Kazes, I. 1990, *AJ*, 100, 1457
- Djorgovski, S. 1987, in *Nearly Normal Galaxies*, ed. S. Faber (New York: Springer), 290
- Dopita, M. A., & Sutherland, R. S. 1995, *ApJ*, 455, 468
 ———. 1996, *ApJS*, 102, 161
- Eales, S. A. 1985, *MNRAS*, 213, 899
- Edge, A. C., Jones, M., Saunders, R., Pooley, G., & Graings, K. 1996, in *Proc. Second Workshop on Gigahertz Peaked-Spectrum and Compact Steep-Spectrum Radio Sources*, ed. I. A. G. Snellen, R. T. Schilizzi, H. J. A. Röttgering, & M. N. Bremer (Leiden: Leiden Obs.), 43
- Eilek, J. A., & Shore, S. N. 1989, *ApJ*, 342, 187
- Elvis, M., Fiore, F., Wilkes, B., McDowell, J., & Bechtold, J. 1994, *ApJ*, 422, 60
- Eracleous, M., & Halpern, J. P. 1994, *ApJS*, 90, 1
- Evans, A. S., Sanders, D. B., Mazzarella, J. M., Solomon, P. M., Downes, D., Kramer, C., & Radford, S. J. E. 1996, *ApJ*, 457, 658
- Fabian, A. C. 1989, *MNRAS*, 238, 41P
- Fanaroff, B., & Riley, J. 1974, *MNRAS*, 167, 31P
- Fanti, C., & Fanti, R. 1994, in *ASP Conf. Ser. 54, The Physics of Active Galaxies*, ed. G. V. Bicknell, M. A. Dopita, & P. J. Quinn (San Francisco: ASP), 341
- Fanti, C., Fanti, R., Dallacasa, D., Schilizzi, R. T., Spencer, R. E., & Stanghellini, C. 1995, *A&A*, 302, 317
- Fanti, C., Fanti, R., O'Dea, C. P., & Schilizzi, R. T., eds. 1990a, *Proc. Dwingeloo Workshop on Compact Steep-Spectrum and GHz Peaked-Spectrum Radio Sources* (Bologna: Istituto di Radioastron.)
- Fanti, C., Fanti, R., Parma, P., Schilizzi, R. T., & van Breugel, W. J. M. 1985, *A&A*, 143, 292
- Fanti, C., et al. 1989, *A&A*, 217, 44
- Fanti, R., Fanti, C., Schilizzi, R. T., Spencer, R. E., Rendong, N., Parma, P., van Breugel, W. J. M., & Venturi, T. 1990b, *A&A*, 231, 333
- Fanti, C., Fanti, R., Schilizzi, R. T., Spencer, R. E., & van Breugel, W. J. M. 1986, *A&A*, 170, 10
- Fanti, R., & Spencer, R. E. 1995, in *IAU Symp. 175, Extragalactic Radio Sources*, ed. R. Ekers, C. Fanti, & L. Padrielli (Dordrecht: Kluwer), 63
- Fanti, C., Vigotti, M., & Di Paolo, C. 1996, in *Proc. Second Workshop on Gigahertz Peaked-Spectrum and Compact Steep-Spectrum Radio Sources*, ed. I. A. G. Snellen, R. T. Schilizzi, H. J. A. Röttgering, & M. N. Bremer (Leiden: Leiden Obs.), 38
- Fey, A. L., Spangler, S. R., Mutel, R. L., & Benson, J. M. 1985, *ApJ*, 295, 134
- Forbes, D. A., Crawford, C. S., Fabian, A. C., & Johnstone, R. M. 1990, *MNRAS*, 244, 680
- Forman, W., Jones, C., & Tucker, W. 1985, *ApJ*, 293, 102 (erratum 300, 836 [1986])
- Fosbury, R. 1990, in *Proc. Dwingeloo Workshop on Compact Steep-Spectrum and GHz Peaked-Spectrum Radio Sources*, ed. C. Fanti, R. Fanti, C. P. O'Dea, & R. T. Schilizzi (Bologna: Istituto di Radioastron.), 197
- Fosbury, R. A. E., Bird, M. C., Nicholson, W., & Wall, J. V. 1987, *MNRAS*, 225, 761
- Fosbury, R. A. E., Mebold, U., Goss, W. M., & van Woerden, H. 1977, *MNRAS*, 179, 89
- Fugmann, W., & Meisenheimer, K. 1988, *A&AS*, 76, 145
- Fugmann, W., Meisenheimer, K., & Röser, H.-J. 1988, *A&AS*, 75, 173
- Garrington, S. T., Leahy, J. P., Conway, R. G., & Laing, R. A. 1988, *Nature*, 133, 147
- Ge, J., & Owen, F. N. 1994, *AJ*, 108, 1523
- Gelderman, R. 1994, Ph.D. thesis, Univ. Virginia
 ———. 1996, in *Proc. Second Workshop on Gigahertz Peaked-Spectrum and Compact Steep-Spectrum Radio Sources*, ed. I. A. G. Snellen, R. T. Schilizzi, H. J. A. Röttgering, & M. N. Bremer (Leiden: Leiden Obs.), 208
- Gelderman, R., & Whittle, M. 1994, *ApJS*, 91, 491
- Gilmore, G., & Shaw, M. A. 1986, *Nature*, 321, 750
- Golombek, D., Miley, G. K., & Neugebauer, G. 1988, *AJ*, 95, 26
- Gopal-Krishna. 1995, *Publ. Nat. Acad. Sci.*, 92, 11399
- Gopal-Krishna, Patnaik, A. R., & Steppe, H. 1983, *A&A*, 123, 107
- Gopal-Krishna, Preuss, E., & Schilizzi, R. T. 1980, *Nature*, 288, 344
- Gopal-Krishna, & Spoelstra, T. A. Th. 1993, *A&A*, 271, 101
- Gopal-Krishna, Steppe, H., & Witzel, A. 1980, *A&A*, 89, 169
- Gopal-Krishna & Wiita, P. J. 1991, *ApJ*, 373, 325
- Güijosa, A., & Daly, R. A. 1996, *ApJ*, 461, 600
- Gurvits, L. I., Kardashev, N. S., Popov, M. V., Schilizzi, R. T., Barthel, P. D., Pauliny-Toth, I. I. K., & Kellermann, K. I. 1992, *A&A*, 260, 82
- Gurvits, L. I., Schilizzi, R. T., Barthel, P. D., Kardashev, N. S., Kellermann, K. I., Lobanov, A. P., Pauliny-Toth, I. I. K., & Popov, M. V. 1994, *A&A*, 291, 737
- Heckman, T. M., Armus, L., & Miley, G. K. 1990, *ApJS*, 74, 833
- Heckman, T. M., Miley, G. K., Balick, B., van Breugel, W. J. M., & Butcher, H. R. 1982, *ApJ*, 262, 529
- Heckman, T. M., O'Dea, C. P., Baum, S. A., & Laurikainen, E. 1994, *ApJ*, 428, 65
- Heckman, T. M., Smith, E. P., Baum, S. A., van Breugel, W. J. M., Miley, G. K., Illingworth, G. D., Bothun, G. D., & Balick, B. 1986, *ApJ*, 311, 526
- Hernquist, L. E. 1989, *Nature*, 340, 687
- Hernquist, L., & Mihos, J. C. 1995, *ApJ*, 448, 41
- Hes, R., Barthel, P. D., & Hoekstra, H. 1995, *A&A*, 303, 8
- Hill, G. J., & Lilly, S. J. 1991, *ApJ*, 367, 1
- Hirst, P., Jackson, N., & Rawlings, S. 1996, in *Proc. Second Workshop on Gigahertz Peaked-Spectrum and Compact Steep-Spectrum Radio Sources*, ed. I. A. G. Snellen, R. T. Schilizzi, H. J. A. Röttgering, & M. N. Bremer (Leiden: Leiden Obs.), 222
- Hodges, M. W., & Mutel, R. L. 1987, in *Superluminal Radio Sources*, ed. J. A. Zensus & T. J. Pearson (Cambridge: Cambridge Univ. Press), 168
- Hodges, M. W., Mutel, R. L., & Phillips, R. B. 1984, *AJ*, 89, 1327
- Hummel, C. A., Schalinski, C. J., Krichbaum, T. P., Witzel, A., & Johnston, K. J. 1988, *A&A*, 204, 68
- Hutchings, J. B., Johnson, I., & Pyke, R. 1988, *ApJS*, 66, 361
- Impey, C. D., Lawrence, C. R., & Tapia, S. 1991, *ApJ*, 375, 46
- Impey, C. D., & Tapia, S. 1990, *ApJ*, 354, 124
- Inoue, M., Tabara, H., Kato, T., & Aizu, K. 1995, *PASJ*, 47, 725
- Jiménez, E. P. 1987, Ph.D. thesis, Univ. Sussex
- Jones, D. L. 1984, *ApJ*, 276, L5
- Kameno, S., et al. 1995, *PASJ*, 47, 711

- Kapahi, V. K. 1981, *A&AS*, 43, 381
- Kardashev, N. S. 1962, *Soviet Astron.—AJ*, 6, 317
- Kato, T., Tabara, H., Inoue, M., & Fukue, J. 1987, *Nature*, 329, 223
- Katz-Stone, D. M., & Rudnick, L. 1997, *ApJ*, 479, 258
- Kellermann, K. I. 1966a, *Australian J. Phys.* 19, 195
- . 1966b, *ApJ*, 146, 621
- Kellermann, K. I., & Pauliny-Toth, I. I. K. 1981, *ARA&A*, 19, 373
- King, E. A., et al. 1996, in *Proc. Second Workshop on Gigahertz Peaked-Spectrum and Compact Steep-Spectrum Radio Sources*, ed. I. A. G. Snellen, R. T. Schilizzi, H. J. A. Röttgering, & M. N. Bremer (Leiden: Leiden Obs.), 17
- Knapp, G. R., Bies, W. E., & van Gorkom, J. H. 1990, *AJ*, 99, 476
- Knapp, G. R., & Patten, B. M. 1991, *AJ*, 101, 1609
- Kollgaard, R. I., Feigelson, E. D., Laurent-Muehleisen, S. A., Spinrad, H., Dey, A., & Brinkmann, W. 1995, *ApJ*, 449, 61
- Kriss, G. A., Cioffi, D. F., & Canizares, C. R. 1983, *ApJ*, 272, 439
- Kühr, H., Johnston, K. J., Odenwald, S., & Adlhoch, J. 1987, *A&AS*, 71, 493
- Kühr, H., Nauber, U., Pauliny-Toth, I. I. K., & Witzel, A. 1981a, *Max-Planck-Institut für Radioastronomie preprint* 55
- Kühr, H., Witzel, A., Pauliny-Toth, I. I. K., & Nauber, U. 1981b, *A&AS*, 45, 367
- Kulkarni, V. K., & Romney, J. D. 1988, in *Proc. IAU Symp. 129, The Impact of VLBI on Astrophysics and Geophysics*, ed. M. J. Reid & J. M. Moran (Dordrecht: Kluwer), 123
- . 1990, in *Proc. Dwingeloo Workshop on Compact Steep-Spectrum and GHz Peaked-Spectrum Radio Sources*, ed. C. Fanti, R. Fanti, C. P. O’Dea, & R. T. Schilizzi (Bologna: Istituto di Radioastron.), 85
- Kuncic, Z., Bicknell, G. V., & Dopita, M. A. 1998, *ApJ*, 495, L35
- Laing, R. A. 1988, *Nature*, 331, 149
- Laing, R. A., Riley, J. M., & Longair, M. S. 1983, *MNRAS*, 204, 151
- Lawrence, C. R., Pearson, T. J., Readhead, A. C. S., & Unwin, S. C. 1986, *AJ*, 91, 494
- Lawrence, C. R., Readhead, A. C. S., Pearson, T. J., & Unwin, S. C. 1987, in *Superluminal Radio Sources*, ed. J. A. Zensus & T. J. Pearson (Cambridge: Cambridge Univ. Press), 260
- Lawrence, C. R., Zucker, J. R., Readhead, A. C. S., Unwin, S. C., Pearson, T. J., & Xu, W. 1996, *ApJS*, 107, 541
- Leahy, J. P., & Williams, A. G. 1984, *MNRAS*, 210, 929
- Ledlow, M. J., & Owen, F. N. 1995, *AJ*, 110, 1959
- Lees, J. F., Knapp, G. R., Rupen, M. P., & Phillips, T. G. 1991, *ApJ*, 379, 177
- Lehnert, M. D. 1996, in *Proc. Second Workshop on Gigahertz Peaked-Spectrum and Compact Steep-Spectrum Radio Sources*, ed. I. A. G. Snellen, R. T. Schilizzi, H. J. A. Röttgering, & M. N. Bremer (Leiden: Leiden Obs.), 119
- Lüdke, E., Sanghera, H. S., Dallacasa, D., & Cotton, W. D. 1996, in *Proc. Second Workshop on Gigahertz Peaked-Spectrum and Compact Steep-Spectrum Radio Sources*, ed. I. A. G. Snellen, R. T. Schilizzi, H. J. A. Röttgering, & M. N. Bremer (Leiden: Leiden Obs.), 100
- Maloney, P. R., Begelman, M. C., & Rees, M. J. 1994, *ApJ*, 432, 606
- Mamon, G. A. 1987, *ApJ*, 321, 622
- Mantovani, F., Junor, W., Fanti, R., Padrielli, L., Browne, I. W. A., & Muxlow, T. W. B. 1992, *A&A*, 257, 353
- Mantovani, F., Junor, W., Fanti, R., Padrielli, L., & Saikia, D. J. 1994, *A&A*, 292, 59
- Marchã, M. J. M., Browne, I. W. A., Impey, C. D., & Smith, P. S. 1996, *MNRAS*, 281, 425
- Marecki, A., Niezgodza, J., Falcke, H., Garrington, S. T., & Patnaik, A. R. 1996, in *Proc. Second Workshop on Gigahertz Peaked-Spectrum and Compact Steep-Spectrum Radio Sources*, ed. I. A. G. Snellen, R. T. Schilizzi, H. J. A. Röttgering, & M. N. Bremer (Leiden: Leiden Obs.), 14
- Mazzarella, J. M., Graham, J. R., Sanders, D. B., & Djorgovski, S. 1993, *ApJ*, 409, 170
- McCarthy, P. J. 1993, *ARA&A*, 31, 639
- McCarthy, P. J., van Breugel, W., Spinrad, H., & Djorgovski, S. 1987, *ApJ*, 321, L29
- Menon, T. K. 1983, *AJ*, 88, 598
- . 1984, in *IAU Symp. 110 VLBI and Compact Radio Sources*, ed. R. Fanti, K. Kellermann, & G. Setti (Dordrecht: Reidel), 45
- Mihos, C. J., & Hernquist, L. 1994, *ApJ*, 431, L9
- Miley, G. K., & Chambers, K. 1989, in *Proc. ESO Workshop 32, Extranuclear Activity in Galaxies*, ed. E. J. A. Meurs & R. A. E. Fosbury (Garching: ESO), 43
- Mirabel, I. F. 1989, *ApJ*, 340, L13
- . 1990, *ApJ*, 352, L37
- Mirabel, I. F., Sanders, D. B., & Kazès, I. 1989, *ApJ*, 340, L9
- Morganti, R., Tadhunter, C. N., Dickson, R., & Shaw, M. 1997, *A&A*, 326, 130
- Murphy, D. W., Browne, I. W. A., & Perley, R. A. 1993, *MNRAS*, 264, 298
- Mutel, R. L., & Hodges, M. W. 1986, *ApJ*, 307, 472
- Mutel, R. L., Hodges, M. W., & Phillips, R. B. 1985, *ApJ*, 290, 86
- Mutel, R. L., & Phillips, R. B. 1988, in *Proc. IAU Symp. 129, The Impact of VLBI on Astrophysics and Geophysics*, ed. M. J. Reid & J. M. Moran (Dordrecht: Kluwer), 73
- Mutel, R. L., Phillips, R. B., & Skuppin, R. 1981, *AJ*, 86, 1600
- Mutel, R. L., Su, B., & Song, S. 1990, in *Proc. Dwingeloo Workshop on Compact Steep-Spectrum and GHz Peaked-Spectrum Radio Sources*, ed. C. Fanti, R. Fanti, C. P. O’Dea, & R. T. Schilizzi (Bologna: Istituto di Radioastron.), 209
- Muxlow, T. W. B., & Garrington, S. T. 1991, in *Beams and Jets in Astrophysics*, ed. P. A. Hughes (Cambridge: Cambridge Univ. Press), 52
- Nan, R., Schilizzi, R. T., Fanti, C., & Fanti, R. 1991a, *A&A*, 252, 513
- Nan, R., Schilizzi, R. T., van Breugel, W. J. M., Fanti, C., Fanti, R., Muxlow, T. W. B., & Spencer, R. E. 1991b, *A&A*, 245, 449
- Nan, R., Cai, Z., Inoue, M., Kameno, S., Schilizzi, R. T., Fanti, C., & Fanti, R. 1992, *PASJ*, 44, 273
- Neeser, M. J., Eales, S. A., Duncan Law-Green, J., Leahy, J. P., & Rawlings, S. 1995, *ApJ*, 451, 76
- Nilsson, K., Valtonen, M. J., Kotilainen, J., & Jaakkola, T. 1993, *ApJ*, 413, 453
- Norman, C., & Scoville, N. 1988, *ApJ*, 332, 124
- O’Dea, C. P. 1990, *MNRAS*, 245, 20P
- O’Dea, C. P., & Baum, S. A. 1997, *AJ*, 113, 148
- O’Dea, C. P., Baum, S. A., & Gallimore, J. F. 1994a, *ApJ*, 436, 669
- O’Dea, C. P., Baum, S. A., Maloney, P. R., Tacconi, L. J., & Sparks, W. B. 1994b, *ApJ*, 422, 467
- O’Dea, C. P., Baum, S. A., & Morris, G. B. 1990a, *A&AS*, 82, 261
- O’Dea, C. P., Baum, S. A., & Stanghellini, C. 1991, *ApJ*, 380, 66
- O’Dea, C. P., Baum, S. A., Stanghellini, C., Dey, A., van Breugel, W., Deustua, S., & Smith, E. P. 1992, *AJ*, 104, 1320
- O’Dea, C. P., Baum, S. A., Stanghellini, C., Morris, G. B., Patnaik, A. R., & Gopal-Krishna. 1990b, *A&AS*, 84, 549
- O’Dea, C. P., Davies, J. K., Stanghellini, C., Baum, S. A., & Laurikainen, E. 1992, in *AIP Conf. Proc. 254, Testing the AGN Paradigm*, ed. S. S. Holt, S. G. Neff, & C. M. Urry (New York: AIP), 435
- O’Dea, C. P., Stanghellini, C., Baum, S. A., & Charlot, S. 1996a, *ApJ*, 470, 806

- O'Dea, C. P., Worrall, D. M., Baum, S. A., & Stanghellini, C. 1996b, *AJ*, 111, 92
- Osterbrock, D. E. 1989, *Astrophysics of Gaseous Nebulae and Active Galactic Nuclei* (Mill Valley: University Science Books)
- Owen, F. N., & Laing, R. A. 1989, *MNRAS*, 238, 357
- Owen, F. N., & White, R. A. 1991, *MNRAS*, 249, 164
- Pauliny-Toth, I. I. K., Porcas, R. W., Zensus, A., & Kellermann, K. I. 1984, in *IAU Symp. 110, VLBI and Compact Radio Sources*, ed. R. Fanti, K. Kellermann, & G. Setti (Dordrecht: Reidel), 149
- Pauliny-Toth, I. I. K., Witzel, A., Preuss, E., Kühr, H., Kellermann, K. I., Fomalont, E. B., & Davis, M. M. 1978, *AJ*, 83, 451
- Peacock, J. A., & Wall, J. V. 1982, *MNRAS*, 198, 843
- Pearson, T. J., Perley, R. A., & Readhead, A. C. S. 1985, *AJ*, 90, 738
- Pearson, T. J., & Readhead, A. C. S. 1984, in *IAU Symp. 110, VLBI and Compact Radio Sources*, ed. R. Fanti, K. Kellermann, & G. Setti (Dordrecht: Reidel), 15
- . 1988, *ApJ*, 328, 114
- Pearson, T. J., Readhead, A. C. S., & Barthel, P. D. 1987, in *Superluminal Radio Sources*, ed. J. A. Zensus & T. J. Pearson (Cambridge: Cambridge Univ. Press), 94
- Perley, R. A. 1990, in *IAU Symp. 140, Galactic and Intergalactic Magnetic Fields*, ed. R. Beck, P. P. Kronberg, & R. Wielebinski (Dordrecht: Kluwer), 463
- Perlman, E. S., Carilli, C. L., Stocke, J. T., & Conway, J. 1996, *AJ*, 111, 1839
- Peterson, B. A., Savage, A., Jauncey, D. L., & Wright, A. E. 1982, *ApJ*, 260, L27
- Phillips, R. B., & Mutel, R. L. 1980, *ApJ*, 236, 89
- . 1981, *ApJ*, 244, 19
- . 1982, *A&A*, 106, 21
- Phillips, R. B., & Shaffer, D. B. 1983, *ApJ*, 271, 32
- Phinney, E. S. 1985, in *Astrophysics of Active Galaxies and Quasistellar Objects*, ed. J. S. Miller (Mill Valley: University Science Books), 453
- Polatidis, A. G., Wilkinson, P. N., Xu, W., Readhead, A. C. S., Pearson, T. J., Taylor, G. B., & Vermeulen, R. C. 1995, *ApJS*, 98, 1
- Porcas, R. W. 1990, in *Proc. Dwingeloo Workshop on Compact Steep-Spectrum and GHz Peaked-Spectrum Radio Sources*, ed. C. Fanti, R. Fanti, C. P. O'Dea, & R. T. Schilizzi (Bologna: Istituto di Radioastron.), 167
- Postman, M., & Lauer, T. R. 1995, *ApJ*, 440, 28
- Prieto, M. A. 1996, *MNRAS*, 282, 421
- Rawlings, S., & Saunders, R. 1991, *Nature*, 349, 138
- Readhead, A. C. S. 1994, *ApJ*, 426, 51
- . 1995, *Publ. Nat. Acad. Sci.*, 92, 11447
- Readhead, A. C. S., & Hewish, A. 1976, *MNRAS*, 176, 571
- Readhead, A. C. S., Taylor, G. B., Pearson, T. J., & Wilkinson, P. N. 1996a, *ApJ*, 460, 634
- Readhead, A. C. S., Taylor, G. B., Xu, W., Pearson, T. J., Wilkinson, P. N., & Polatidis, A. G. 1996b, *ApJ*, 460, 612
- Readhead, A. C. S., Xu, W., Pearson, T. J., Wilkinson, P. N., & Polatidis, A. G. 1994, in *Proc. NRAO Workshop 23, Compact Extragalactic Radio Sources*, ed. J. A. Zensus & K. I. Kellermann (Greenbank: NRAO), 17
- Rees, M. J. 1989, *MNRAS*, 239, 1P
- Reynolds, C. S., & Begelman, M. C. 1997, *ApJ*, 487, L135
- Rieke, G. H., Lebofsky, M. J., & Kinman, T. D. 1979, *ApJ*, 232, L151
- Rieke, G. H., Wisniewski, W. Z., & Lebofsky, M. J. 1982, *ApJ*, 263, 73
- Roos, N. 1985, *ApJ*, 294, 486
- Röttgering, H. J. A., Best, P., Carilli, C., & Longair, M. 1996, in *Proc. Second Workshop on Gigahertz Peaked-Spectrum and Compact Steep-Spectrum Radio Sources*, ed. I. A. G. Snellen, R. T. Schilizzi, H. J. A. Röttgering, & M. N. Bremer (Leiden: Leiden Obs.), 48
- Röttgering, H. J. A., Lacy, M., Miley, G. K., Chambers, K. C., & Saunders, R. 1994, *A&AS*, 108, 79
- Rudnick, L., & Jones, T. W. 1982, *ApJ*, 255, 39
- Rudnick, L., & Jones, T. W. 1983, *AJ*, 88, 518
- Rudnick, L., Zukowski, E., & Kronberg, P. P. 1983, *A&AS*, 52, 317
- Rusk, R. E. 1988, Ph.D. thesis, Univ. Toronto
- Saikia, D. J. 1988, in *Active Galactic Nuclei*, ed. H. R. Miller & P. J. Wiita (Berlin: Springer), 317
- . 1995, in *Publ. Nat. Acad. Sci.*, 92, 11417
- Saikia, D. J., Jeyakumar, S., Wiita, P. J., & Hooda, J. S. 1996, *Proc. Second Workshop on Gigahertz Peaked-Spectrum and Compact Steep-Spectrum Radio Sources*, ed. I. A. G. Snellen, R. T. Schilizzi, H. J. A. Röttgering, & M. N. Bremer (Leiden: Leiden Obs.), 252
- Saikia, D. J., Jeyakumar, S., Wiita, P. J., Sanghera, H. S., & Spencer, R. E. 1995, *MNRAS*, 276, 1215
- Saikia, D. J., Singal, A. K., & Cornwell, T. J. 1987, *MNRAS*, 224, 379
- Saikia, D. J., Swarup, G., & Kodali, P. D. 1985, *MNRAS*, 216, 385
- Sanders, D. B., Soifer, B. T., Elias, J. H., Madore, B. F., Matthews, K., Neugebauer, G., & Scoville, N. Z. 1988, *ApJ*, 325, 74
- Sanghera, H. S., Saikia, D. J., Lüdke, E., Spencer, R. E., Foulsham, P. A., Akujor, C. E., & Tzioumis, A. K. 1995, *A&A*, 295, 629
- Sanders, D. B., Scoville, N. Z., & Soifer, B. T. 1991, *ApJ*, 370, 158
- Savage, A., Jauncey, D. L., White, G. L., Peterson, B. A., Peters, W. L., Gulkis, S., & Condon, J. J. 1990, *Australian J. Phys.*, 43, 241
- Savage, A., & Peterson, B. A. 1983, in *IAU Symp. 104, Early Evolution of the Universe and its Present Structure*, ed. G. O. Abell & C. Chincarini (Dordrecht: Reidel), 57
- Scheuer, P. A. G. 1974, *MNRAS*, 166, 513
- Schilizzi, R. T., Inoue, M., Nan Rendong, Fanti, C., Fanti, R., & Wu Shengyin. 1990, in *Proc. Dwingeloo Workshop on Compact Steep-Spectrum and GHz Peaked-Spectrum Radio Sources*, ed. C. Fanti, R. Fanti, C. P. O'Dea, & R. T. Schilizzi (Bologna: Istituto di Radioastron.), 42
- Schilizzi, R. T., & Shaver, P. A. 1981, *A&A*, 96, 365
- Schilizzi, R. T., et al. 1988, in *IAU Symp. 129, The Impact of VLBI on Astrophysics and Geophysics*, ed. M. J. Reid & J. M. Moran (Dordrecht: Kluwer), 127
- Scoville, N. Z., Hibbard, J. E., Yun, M. S., & van Gorkom, J. H. 1994, in *Mass-Transfer Induced Activity in Galaxies*, ed. I. Shlosman (Cambridge: Cambridge Univ. Press), 191
- Scoville, N. Z., Padin, S., Sanders, D. B., Soifer, B. T., & Yun, M. S. 1993, *ApJ*, 415, L75
- Seielstad, G. A., Pearson, T. J., & Readhead, A. C. S. 1983, *PASP*, 95, 842
- Shaw, M. A., Tadhunter, C., Dickson, R., & Morganti, R. 1995, *MNRAS*, 275, 703
- Shaw, M. A., Tzioumis, A. K., & Pedlar, A. 1992, *MNRAS*, 256, 6P
- Shklovsky, I. S. 1965, *Nature*, 206, 176
- Siebert, J., Brinkmann, W., Morganti, R., Tadhunter, C. N., Danziger, I. J., Fosbury, R. A. E., & di Serego Alighieri, S. 1996, *MNRAS*, 279, 1331
- Simard-Normandin, M., Kronberg, P. P., & Button, S. 1981, *ApJS*, 45, 97
- Simon, R. S., Readhead, A. C. S., Moffet, A. T., Wilkinson, P. N., Booth, R., Allen, B., & Burke, B. F. 1990, *ApJ*, 354, 140
- Singal, A. K., & Gopal-Krishna, 1985, *MNRAS*, 215, 383
- Sligh, V. I. 1963, *Nature*, 199, 682
- Smith, E. P., & Heckman, T. M. 1989a, *ApJS*, 69, 365
- . 1989b, *ApJ*, 341, 658
- Smith, E. P., O'Dea, C. P., & Baum, S. A. 1995, *ApJ*, 441, 113
- Snellen, I. A. G., Bremer, M. N., Schilizzi, R. T., & Miley, G. K. 1996a, *MNRAS*, 283, L123

- Snellen, I. A. G., Bremer, M. N., Schilizzi, R. T., Miley, G. K., & van Ojik, R. 1996b, *MNRAS*, 279, 1294
- Snellen, I. A. G., Schilizzi, R. T., De Bruyn, A. G., & Miley, G. K. 1998, *A&A*, 333, 70
- Snellen, I. A. G., Schilizzi, R. T., De Bruyn, A. G., Miley, G. K., Bremer, M. N., & Röttgering, H. 1996c, in *Proc. Second Workshop on Gigahertz Peaked-Spectrum and Compact Steep-Spectrum Radio Sources*, ed. I. A. G. Snellen, R. T. Schilizzi, H. J. A. Röttgering, & M. N. Bremer (Leiden: Leiden Obs.), 28
- Snellen, I. A. G., Schilizzi, R. T., Röttgering, H. J. A., & Bremer, M. N., eds. 1996d, *Proc. Second Workshop on Gigahertz Peaked-Spectrum and Compact Steep-Spectrum Radio Sources* (Leiden: Leiden Obs.)
- Snellen, I. A. G., Zhang, M., Schilizzi, R. T., Röttgering, H. J. A., de Bruyn, A. G., & Miley, G. K. 1995, *A&A*, 300, 359
- Soker, N., & Sarazin, C. L. 1990, *ApJ*, 348, 73
- Spangler, S. R., Benson, J. M., Cordes, J. M., Hall, R. B., Jones, T. W., & Johnston, K. J. 1981, *AJ*, 86, 1155
- Spangler, S. R., Mutel, R. L., & Benson, J. M. 1983, *ApJ*, 271, 44
- Spencer, R. E., McDowell, J. C., Charlesworth, M., Fanti, C., Parma, P., & Peacock, J. A. 1989, *MNRAS*, 240, 657
- Spencer, R. E., et al. 1991, *MNRAS*, 250, 225
- Spinrad, H. 1986, *PASP*, 98, 269
- Spinrad, H., & Djorgovski, S. 1987, in *IAU Symp. 124, Observational Cosmology*, ed. A. Hewitt, G. Burbidge, & Zh.-F. Li (Dordrecht: Reidel), 129
- Spoelstra, T. A. T., Patnaik, A. R., & Gopal-Krishna. 1985, *A&A*, 152, 38
- Stanghellini, C. 1992, Ph.D. thesis, Univ. Bologna
- Stanghellini, C., Baum, S. A., O'Dea, C. P., & Morris, G. B. 1990a, *A&A*, 233, 379
- . 1990b, in *Proc. Dwingeloo Workshop on Compact Steep-Spectrum and GHz Peaked-Spectrum Radio Sources*, ed. C. Fanti, R. Fanti, C. P. O'Dea, & R. T. Schilizzi (Bologna: Istituto di Radioastron.), 55
- Stanghellini, C., Bondi, M., Dallacasa, D., O'Dea, C. P., Baum, S. A., Fanti, R., & Fanti, C. 1997a, *A&A*, 318, 376
- Stanghellini, C., Dallacasa, D., O'Dea, C. P., Baum, S. A., Fanti, R., & Fanti, C. 1996, in *Proc. Second Workshop on Gigahertz Peaked-Spectrum and Compact Steep-Spectrum Radio Sources*, ed. I. A. G. Snellen, R. T. Schilizzi, H. J. A. Röttgering, & M. N. Bremer (Leiden: Leiden Obs.), 4
- Stanghellini, C., Dallacasa, D., O'Dea, C. P., Baum, S. A., Fanti, C., & Fanti, R. 1998a, in *IAU Symp. 164, Compact Radio Sources*, in press
- Stanghellini, C., O'Dea, C. P., Baum, S. A., Dallacasa, D., Fanti, R., & Fanti, C. 1997b, *A&A*, 325, 943
- Stanghellini, C., O'Dea, C. P., Baum, S. A., & Fanti, R. 1990c, in *Proc. Dwingeloo Workshop on Compact Steep-Spectrum and GHz Peaked-Spectrum Radio Sources*, ed. C. Fanti, R. Fanti, C. P. O'Dea, & R. T. Schilizzi (Bologna: Istituto di Radioastron.), 17
- Stanghellini, C., O'Dea, C. P., Dallacasa, D., Baum, S. A., & Fanti, R. 1998b, *A&AS*, in press
- Stanghellini, C., O'Dea, C. P., Baum, S. A., & Laurikainen, E. 1993, *ApJS*, 88, 1
- Steppe, H., Jayakumar, S., Saikia, D. J., & Salter, C. J. 1995, *A&AS*, 113, 409
- Steppe, H., Salter, C. J., & Saikia, D. J. 1990, in *Proc. Dwingeloo workshop on Compact Steep-Spectrum and GHz Peaked-Spectrum Radio Sources*, ed. C. Fanti, R. Fanti, C. P. O'Dea, & R. T. Schilizzi (Bologna: Istituto di Radioastron.), 44
- Stickel, M., & Kühr, H. 1993, *A&AS*, 100, 395
- Stickel, M., Meisenheimer, K., & Kühr, H. 1994, *A&AS*, 105, 211
- Stickel, M., Rieke, G. H., Kühr, H., & Rieke, M. J. 1996a, *ApJ*, 468, 556
- Stickel, M., Rieke, M. J., Rieke, G. H., & Kühr, H. 1996b, *A&A*, 306, 49
- Tadhunter, C. N., Fosbury, R. A. E., & di Serego Alighieri, S. 1988, in *BL Lac Objects: Proceedings of the Como Conf.*, ed. L. Maraschi, T. Maccacaro, & M.-H. Ulrich (Heidelberg: Springer), 79
- Tadhunter, C. N., Scarrott, S. M., Draper, P., & Rolph, C. 1992, *MNRAS*, 256, L53
- Tadhunter, C. N., Shaw, M. A., & Morganti, R. 1994, *MNRAS*, 271, 807
- Taylor, G. B., Ge, J. P., & O'Dea, C. P. 1995, *AJ*, 110, 522
- Taylor, G. B., Inoue, M., & Tabara, H. 1992, *A&A*, 264, 421
- Taylor, G. B., Readhead, A. C., & Pearson, T. J. 1996a, *ApJ*, 463, 95
- Taylor, G. B., & Vermeulen, R. C. 1997, *ApJ*, 485, L9
- Taylor, G. B., Vermeulen, R. C., Pearson, T. J., Readhead, A. C. S., Henstock, D. R., Browne, I. W. A., Wilkinson, P. N. 1994, *ApJS*, 95, 345
- Taylor, G. B., Vermeulen, R. C., Pearson, T. J., Readhead, A. C. S., Henstock, D. R., & Wilkinson, P. N. 1996c, in *Proc. Second Workshop on Gigahertz Peaked-Spectrum and Compact Steep-Spectrum Radio Sources*, ed. I. A. G. Snellen, R. T. Schilizzi, H. J. A. Röttgering, & M. N. Bremer (Leiden: Leiden Obs.), 263
- Taylor, G. B., Udomprasert, P., Pearson, T. J., & Roberts, D. H. 1996b, in *Proc. Second Workshop on Gigahertz Peaked-Spectrum and Compact Steep-Spectrum Radio Sources*, ed. I. A. G. Snellen, R. T. Schilizzi, H. J. A. Röttgering, & M. N. Bremer (Leiden: Leiden Obs.), 92
- Thakkar, D. D., Xu, W., Readhead, A. C. S., Pearson, T. J., Taylor, G. B., Vermeulen, R. C., Polatidis, A. G., & Wilkinson, P. N. 1995, *ApJS*, 98, 33
- Tingay, S. J., et al. 1997, *AJ*, 113, 2025
- Tzioumis, A. K., et al. 1989, *AJ*, 98, 36
- Udomprasert, P. S., Taylor, G. B., Pearson, T. J., & Roberts, D. H. 1997, *ApJ*, 483, L9
- Vader, J. P., Frogel, J. A., Terndrup, D. A., & Heisler, C. A. 1993, *AJ*, 106, 1743
- van Breugel, W., Heckman, T., & Miley, G. 1984a, *ApJ*, 276, 79
- van Breugel, W., Miley, G., & Heckman, T. 1984b, *AJ*, 89, 5
- van Breugel, W., Rendong, N., Schilizzi, R. T., Fanti, C., & Fanti, R. 1988, in *IAU Symp. 129, The Impact of VLBI on Astrophysics and Geophysics*, ed. M. J. Reid & J. M. Moran (Dordrecht: Kluwer), 115
- van Breugel, W. J. M., Fanti, C., Fanti, R., Stanghellini, C., Schilizzi, R. T., & Spencer, R. E. 1992, *A&A*, 256, 56
- van der Laan, H., & Perola, G. C. 1969, *A&A*, 3, 468
- van Gorkom, J. H., Knapp, G. R., Ekers, R. D., Ekers, D. D., Laing, R. A., & Polk, K. S. 1989, *AJ*, 97, 708
- Véron-Cetty, M.-P., Woltjer, L., Ekers, R. D., & Staveley-Smith, L. 1995, *A&A*, 297, L79
- Wall, J. V., & Peacock, J. A. 1985, *MNRAS*, 216, 173
- Waltman, E. B., Fiedler, R. L., Johnston, K. J., Spencer, J. H., Florkowski, D. R., Josties, F. J., McCarthy, D. D., & Matsakis, D. N. 1991, *ApJS*, 77, 379
- Wehrle, A. E., & Cohen, M. 1989, *ApJ*, 346, L69
- Wehrle, A. E., Cohen, M., H., Unwin, S. C., Aller, H. D., Aller, M. F., & Nicolson, G. 1992, *ApJ*, 391, 589
- Wilkes, B. J., Tananbaum, H., Worrall, D. M., Avni, Y., Oey, M. S., & Flanagan, J. 1994, *ApJS*, 92, 53
- Wilkinson, P. N., Akujor, C. E., Cornwell, T. J., & Saikia, D. J. 1991a, *MNRAS*, 248, 86
- Wilkinson, P. N., Booth, R. S., Cornwell, T. J., & Clark, R. R. 1984a, *Nature*, 308, 619

- Wilkinson, P. N., Cornwell, T. J., Kus, A. J., Readhead, A. C. S., & Pearson, T. J. 1985, in NRAO Workshop 9, Physics of Energy Transport in Extragalactic Radio Sources, ed. A. H. Bridle & J. A. Eilek (Greenbank: NRAO), 76
- Wilkinson, P. N., Polatidis, A. G., Readhead, A. C. S., Xu, W., & Pearson, T. J. 1994, *ApJ*, 432, L87
- Wilkinson, P. N., Readhead, A. C. S., Anderson, B., & Purcell, G. H. 1979, *ApJ*, 232, 365
- Wilkinson, P. N., Spencer, R. E., Readhead, A. C. S., Pearson, T. J., & Simon, R. S. 1984b, in IAU Symp. 110, VLBI and Compact Radio Sources, ed. R. Fanti, K. Kellermann, & G. Setti (Dordrecht: Reidel), 25
- Wilkinson, P. N., Tzioumis, A. K., Benson, J. M., Walker, R. C., Simon, R. S., & Kahn, F. D. 1991b, *Nature*, 352, 313
- Williams, P. J. S. 1963, *Nature*, 200, 56
- Wills, B. J., Wills, D., Breger, M., Antonucci, R. R. J., & Barvainis, R. 1992, *ApJ*, 398, 454
- Wink, J. E., Guilloteau, S., & Wilson, T. L. 1997, *A&A*, 322, 427
- Witzel, A. 1987, in Superluminal Radio Sources, ed. J. A. Zensus & T. J. Pearson (Cambridge: Cambridge Univ. Press), 83
- Young, S., Hough, J. H., Efstathiou, A., Wills, B. J., Bailey, J. A., Ward, M. J., & Axon, D. J. 1996, *MNRAS*, 281, 1206
- Zepf, S. E., & Koo, D. C. 1989, *ApJ*, 337, 34
- Zhang, F. J., et al. 1991, *MNRAS*, 250, 650
- Zhang, F. J., Spencer, R. E., Schilizzi, R. T., Fanti, C., Baath, L. B., & Su, B. M. 1994, *A&A*, 287, 32
- Zhang, Y. F., & Marscher, A. P. 1994, in Proc. 1993 *ROSAT* Science Symp., ed. E. Schlegel & R. Petre (New York: AIP), 406
- Zirbel, E. L., & Baum, S. A. 1995, *ApJ*, 448, 521